GEOLOGY OF THE SKLODOWSKA REGION

LUNAR FARSIDE

A Thesis

Presented in Partial Fulfillment of the Requirement for the

DEGREE OF MASTER OF SCIENCE

Major in Geology

in the

UNIVERSITY OF IDAHO GRADUATE SCHOOL

by

JOHN DAVID KAUFFMAN

November 1974

FINAL REPORT

NASA Grant NGR 13-001-014

ACKNOWLEDGEMENTS

I gratefully acknowledge the financial assistance provided by both the National Aeronautics and Space Administration under NASA grant NGR-13-001-014, and the Idaho Bureau of Mines and Geology. Helpful suggestions and moral support provided by Dr. Donald E. Wilhelms (U.S. Geologic Survey Astrogeologic Branch, Menlo Park, California) greatly encouraged the the writer throughout this project. Conversations with other Geologic Survey personnel at both Menlo Park and Flagstaff were also beneficial. Photographs used for mapping and interpretation were supplied by the National Space Science Data Center (NSSDC), Greenbelt, Maryland.

I also wish to thank my faculty advisors, Dr. John G. Bond, Dr. Dale O. Everson, Dr. William B. Hall, and the late Dr. Roald Fryxell for continued encouragement and assistance in preparing and reviewing the original proposal, the geologic map, and the final manuscript.

Others deserving special mention are: my wife, Marj, for constant support throughout the years of my graduate work; fellow graduate students at the University of Idaho, in particular Jim Fitzgerald, Rick Standish, Dwight Juras, Norm Day, and Frank Fenne for making the ordeal bearable; and Jan Juras, for typing the final manuscript. To all others who have assisted in this project, I extend my appreciation.

CONTENTS

LIST OF FIGURES

LIST OF TABLES

LIST OF PLATES

ABSTRACT

Investigation of an area on the lunar farside has resulted in a geologic map, development of a regional stratigraphic sequence, and interpretation of surface materials.

Apollo 15 metric photographs were used in conjunction with photogrammetric techniques to produce a base map to which geologic units were later added. Geologic units were first delineated on the metric photographs and then transferred to the base map. Materials were defined and described from selected Lunar Orbiter and Apollo 15 metric, panoramic, and Hasselblad photographs on the basis of distinctive morphologic characteristics.

Regional topography in the Sklodowska Region is dominated by the large Late Imbrian crater Sklodowska and its asymmetrical ejecta blanket. The remaining surface area consists of other crater materials, and terrae and plains materials.

Large and small craters occur throughout the region and range from fresh to totally subdued. From morphologic considerations and correlation to both nearside and farside interpretations, most crater, terrae, and plains materials are believed to have formed by or been modified by impact and subsequent ejecta deposition rather than by volcanic processes.

An exception occurs southeast of Sklodowska where the floor

of an irregularly-shaped Nectarian crater and a broad topographic trough have been covered by dark mare material. The mare and some associated lighter colored materials were extruded along a linear fissure. Collapse pits, flow fronts, narrow troughs, and a subsidence bench are associated volcanic structures.

No conclusive evidence was found to support a lunar structural grid. Most lineations are radial or subradial to large craters, indicating an origin by ejecta gouging or settling of material along fractures related to the impact event.

The geologic history of this region is interpreted to be similar to the history of other cratered highland surfaces on the moon.

INTRODUCTION

Purpose and Scope

The lunar farside has until recently been largely ignored by lunar stratigraphers because detailed nearside studies were necessary for the successful completion of the Apollo manned-landing missions. With the end of Apollo, attention is now shifting to interesting farside features. With the exception of farside mapping at a scale of 1:5,000,000 currently in progress by the U.S. Geological Survey, little or no regional mapping has been attempted to determine the history and morphologic evolution of large farside areas.

The purposes of this study are to produce a geologic map of a large area on the lunar farside, to determine the stratigraphic sequence, and to determine the origin and morphologic evolution of the materials present; all are based on interpretations from Apollo 15 metric and panoramic sterophotographs. The scope is limited to the above purposes and to the geographic area described below.

Location and General Description of Area

The study area (Fig. 1) centers at approximately 18° S and 96° E on the western limb of the lunar farside. It encompasses about 330,000 square kilometers and contains a variety of surface materials.

Occupying the central portion of the map area is the large terraced crater Sklodowska and its ejecta deposits. The ejecta partially

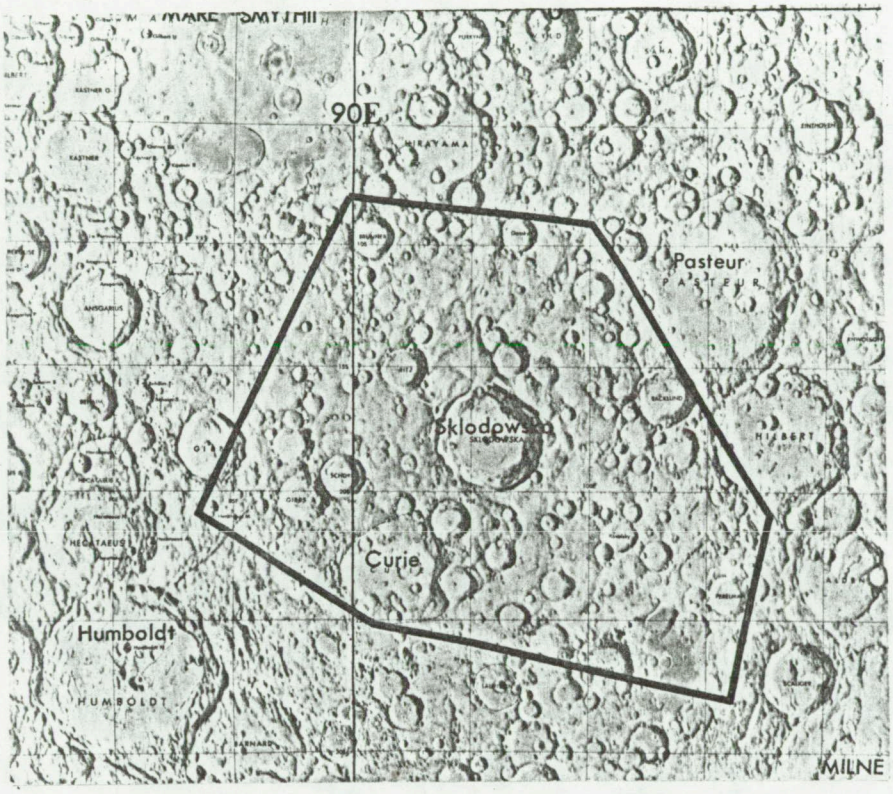

Figure 1. Location of study area showing major features (after Lunar Planning Chart, LOC-3, ACIC).

to totally fills large, older craters near the rim crest, and thins outward into a discontinuous deposit at roughly one crater diameter from the rim crest. The ejecta is deposited asymmetrically around Sklodowska and is marked by radial and subradial lineations, gouges, and secondary craters.

Plains and terrae materials of several ages are common throughout much of the area. Plains material tends to occupy the lower elevation features, such as broad depressions and the floors of large craters; terrae materials occur at higher elevations and have a more rugged surface topography.

A small surface of mare material, located southeast of Sklodowska, partially fills an irregular crater and covers a broad topographic depression. The surface of the mare material is pitted with many small craters but is otherwise nearly level. Collapse pits, troughs, flow-fronts, and pressure ridges are also present; as subsequently described these indicate that the mare and associated materials are of endogenic origin.

The area as a whole is characteristic of lunar highland or continental regions. Craters of all size and age categories are represented and are responsible for most of the surface topography. Crater characteristics with respect to size and age are discussed in later sections and in Appendix B.

Prior Work

This section presents a brief history of lunar geology and stratigraphy and is intended to acquaint the reader with some of the major works in various aspects of lunar research.

General

A considerable number of articles have been published since man first developed an interest in the moon; the overwhelming majority of publications appeared since 1960. The obvious reason for this recent voluminous outpouring was the advent of the "space age" and the United States - U.S.S.R. race to land the first man on the lunar surface. Most studies in the early 1960's dealt with specific geologic problems, such as the origin of craters, origin of mare ridges and rilles, and the nature and thickness of the regolith (lunar "soil"). Early lunar science conferences often became battlegrounds for the impact-volcanic controversy with respect to the origin of lunar surface features. Symposia volumes from these conferences (for example Whipple, 1965) offer an interesting insight to the divergent concepts.

A stratigraphic approach to lunar mapping was not envisioned until the early 1960's when a photogeologist with the U.S. Geological Survey, Robert J. Hackman, mapped three stratigraphic units on the nearside -- pre-mare, mare, and post-mare (Hackman and

Mason, 1961). Meanwhile, Eugene Shoemaker was mapping the Copernicus area at a scale of 1:1,000,000. In a joint publication, Shoemaker and Hackman (1962) developed the principles of systematic lunar mapping. Although minor changes have been made, their system for distinguishing stratigraphic sequence is still in use. A comparison of the stratigraphic column of Shoemaker and Hackman and the revised column presently accepted is shown below.

LUNAR STRATIGRAPHIC COLUMN

Shoemaker and Hackman	Revised
Copernican period	Copernican System
Eratosthenian period	Eratosthenian System
Procellarian period	
Imbrian period	Imbrian System
pre-Imbrian time	pre-Imbrian: Nectarian System; pre-Nectarian time

Prior to the Ranger, Surveyor, and Lunar Orbiter missions of the middle 1960's lunar mapping was based on telescopic observations, as well as considerable imagination, with remarkably accurate results. The U.S. Geological Survey publication, "Summary of Lunar Stratigraphy -- Telescopic Observations", (Wilhelms, 1970) is an excellent guide to the fundamentals and principles of lunar stratigraphy.

Nearly all of the nearside has been mapped by the personnel of the Astrogeologic Branch of the U.S. Geologic Survey. Quadrangle maps at a scale of 1:1,000,000 are most common, although selected areas have been mapped at various larger scales. A geologic map of the nearside at a scale of 1:5,000,000 has also been published (Wilhelms and McCauley, 1971).

For further information regarding lunar geology and related subjects, the readers attention is directed to the U. S. Department of Interior publication, "Bibliography of the Lunar Surface", (Freeberg, 1970). It contains over 4500 references to research prior to 1970 pertaining to the nature of the lunar surface. A great number of articles have also been published since 1970 in the various scientific journals and in the Apollo Preliminary Science Reports published by the National Aeronautics and Space Administration.

Several books are also recommended as sources of basic information regarding the study of the moon. These are: R.B. Baldwin's "The Face of the Moon" (1949) and "The Measure of the Moon" (1963); G. Fielder's "Structure of the Moon's Surface" (1961) and "Lunar Geology" (1965); and T.A. Mutch's "Geology of the Moon -- A Stratigraphic View" (1970).

Farside

As previously stated, farside mapping has generally been

limited to selected craters and other specific features. For example, Hixon (1968) examined a farside crater south of Tsiolkovsky that had some associated volcanic landforms; El-Baz (1970) interpreted certain features in King crater as probably dikes.

Guest and Murray (1969) conducted a detailed investigation of Tsiolkovsky, a large farside crater that is similar in many respects to Sklodowska. They concluded that Tsiolkovsky and most of its associated features were formed by a single impact event. Erlich and others(1970), however, interpret many of the same features as endogenic, although their supporting evidence is somewhat weaker than that of Guest and Murray.

Following Apollo 15 and Apollo 16, selected farside features became targets for study because of the excellent photographic imagery returned by these missions. One such feature is King Crater, a 75 km crater having many fresh (young) characteristics while lacking other features typical of young craters. Both Howard (1972) and El-Baz (1972) examine the morphology of King Crater and its ejecta deposits in detail. Howard interprets the ejecta blanket as material deposited following impact; El-Baz, while accepting that some features are characteristic of impact, feels that other features and the lack of some typical impact features can be explained only by volcanism.

Relative Age Determination

Crater size/density relationships are commonly used for relative age determination and are reasonably reliable indicators for different stratigraphic units, provided the limits of the method are recognized. Several investigators have attempted age dating using this technique with various degrees of success (Opik, 1960, Palm and Strom, 1963).

Dodd, Salisbury, and Smalley (1963) used crater frequency on various mare surfaces to interpret lunar history, but recognized that crater counts may be complicated by the presence of secondary and volcanic craters. Hartmann (1964) recognized that mare formation occurred after most of the large craters had formed; that smaller craters are preferentially destroyed by the formation of larger craters; and that the technique of determining crater densities appeared to be a valid indicator of relative age. Further crater counts by Hartmann (1967; 1968) and Hartmann and Yale (1968) produced similar results. Regardless of their accuracy in determining relative age, crater counts are time consuming and often contain considerable bias on the part of the investigator.

Soderblom (1970) developed a technique for rapid age determination of a lunar surface using interior crater slope angle versus crater diameter. Further development of the technique (Soderblom and

Lebofsky, 1972) and comparison of ages determined by this method to those established by stratigraphic methods, along with comparison to absolute dates from returned rock samples (Soderblom and Boyce, 1972), have proven the validity of the technique.

Crater morphology has been used to determine the relative age of craters, and to some extent, the units on which the craters are superposed. Ages are based on the degree to which a crater has been subdued; the basic assumption is that as a crater ages, it becomes continually more subdued by younger impacts, ejecta deposition, and mass wasting processes. Crustal vibrations and volcanic processes may also contribute to the aging process. Trask (1971) assigned relative ages to mare surfaces on the basis of the oldest craters developed on them. He found that newly formed craters are sharp and fresh in appearance; that all craters undergo modification; that smaller craters disappear before larger ones; and that for any surface there is a critical crater diameter below which craters display all degrees of aging, and above which craters range from fresh to only partly destroyed. Several authors have demonstrated that the limiting diameter increases with time for any given surface (Morris and Shoemaker, 1968; Ross 1968; Soderblom, 1970).

A relative age sequence for craters has been developed which separates craters into three size classifications as well as into numerical morphologic age designations ranging from 0.0 (oldest)

to 7.0 (youngest) (Pohn and Offield, 1970; Offield and Pohn, 1970). They describe the morphologic changes that occur as craters age and show that for each size class these changes will vary overall; that is the larger craters will take longer to age than the small craters.

Crater Origin

The origin of lunar craters has long been a controversial subject with speculations polarizing either about endogenic or exogenic processes. Most European scientists tend to favor an endogenic origin for craters, basins, and most other lunar materials; that is -- a volcanic origin. American scientists favor an exogenic or impact model tempered with a certain amount of volcanism.

Before systematic mapping was begun, most proponents for either hypothesis based their arguments on studies of terrestrial analogs, selecting those features that best supported their personal views. While this is still practiced to some extent, greater emphasis is now placed on a less subjective approach to determine crater origin; this generally uses a stratistical comparison of lunar and terrestrial craters.

One statistical approach applies height-depth ratios to compare lunar and terrestrial craters (Pike, 1971b). With few exceptions, terrestrial volcanic craters and calderas fall in a separate field from normal lunar craters, whereas terrestrial impact and explo-

sion craters fall within the same limits as normal lunar craters. Summit craters on lunar domes were found to have trends similar to terrestrial volcanic crater ratios. Depth-diameter relationships (Pike, 1971a), rim width-diameter relationships (Pike, 1972), and circularity index analyses (Ronca and Salisbury, 1966; Alder and Salisbury, 1969) have shown similar results; conclusions generally are that most lunar craters were formed as a result of impact explosions rather than by volcanism.

METHODS

Mechanical

Base Map Construction

Construction of a base map was necessary because no farside base maps of the area were available. A workable map was produced by means of the radial line plotting technique using slotted templets (Spurr, 1948) on Apollo 15 metric camera stereophotographs along five adjacent flight lines.

Principal points, conjugate points, and pass points were marked on photographs along each flight line. Slotted metal templets were then constructed over each photograph and labeled according to flight lines. After all the templets were similarly constructed, they were arranged on a sheet of paper and positioned so that matching points overlapped. When the entire set was arranged, the points were marked on the underlying paper (Figure 2). Using a Ryker Model L-1 vertical sketchmaster, points on the photograph were projected so they were superimposed on corresponding points on the paper and the outline of the surface features were traced on the base sheet (Figure 3).

The resulting constructed base map has an approximate scale of 1:800,000 (Plate 2 is a reduced version of the base map) slightly larger than the desired scale of 1:1,000,000. This enlargement is

the result of two main factors: 1) a photo scale slightly larger than 1:1,000,000 and 2) a slight enlargement during the transfer process. Other error factors affect the geographic positioning of features. These factors include lack of ground control necessary to establish accurate control points; inconsistancy of the photo scale; curvature of the flightlines; distortion toward the edges of the photographs; and error inherent in the technique itself.

In spite of these error factors, the resulting map is reasonably accurate and shows the relative positioning of major features and lineations; few discrepancies were found when compared to a portion of the Lunar Planning Chart LOC-3 (ACIC, 1971). Enlarged to 1:1,000,000 this map was generously provided by the U.S. Geological Survey Astrogeologic Branch in Flagstaff.

Geologic Map Construction

Geologic units were delineated on Apollo 15 metric photographs and transferred to a base map overlay. Units were divided on the basis of morphologic dissimilarities of materials, stratigraphic position, overlap and embayment relationships, albedo differences, and visual crater density estimations. Several Lunar Orbiter photographs and two sets of Apollo 15 panoramic stereophotographs were also used to assist in geologic mapping and interpretation.

As nearly as possible, standard U.S. Geological Survey Lunar

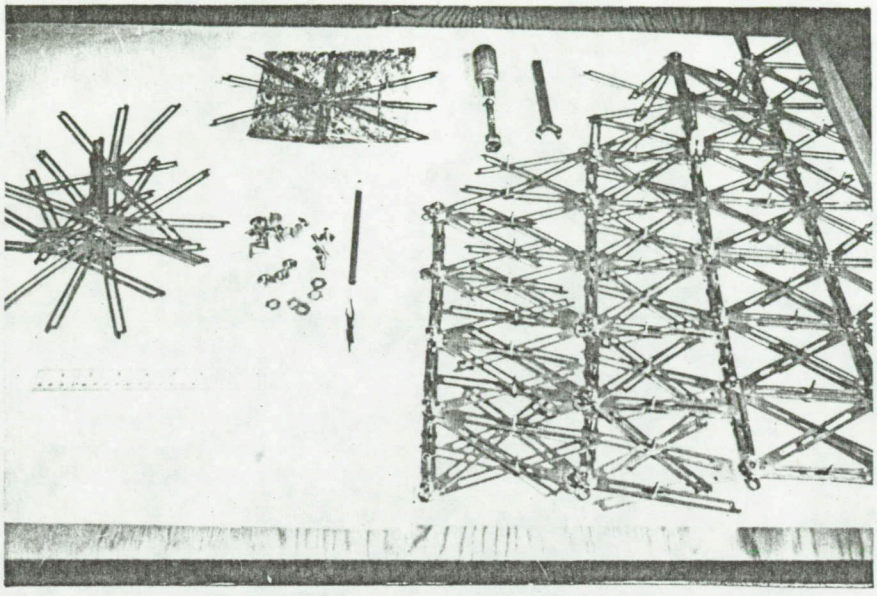

Figure 2. Slotted metal templets used to construct the base map.

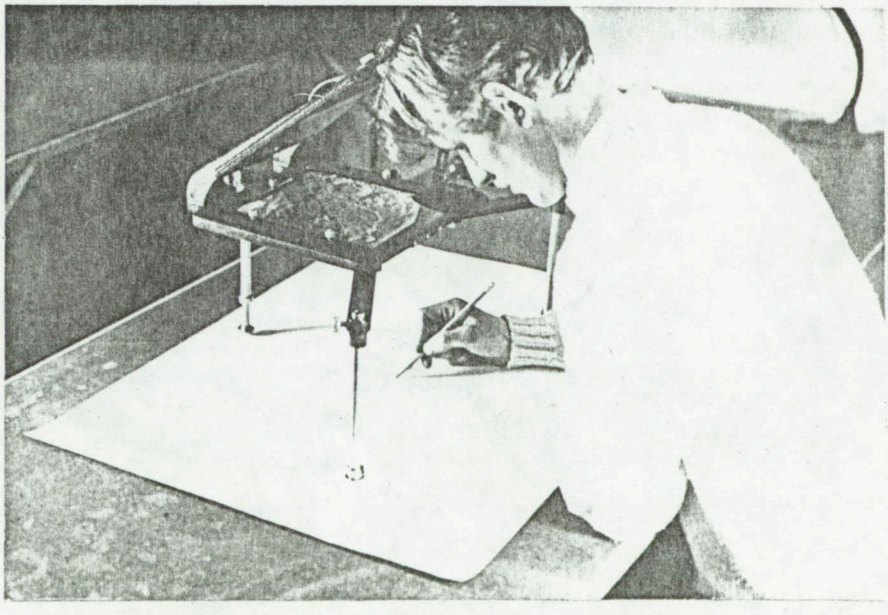

Figure 3. Sketching lunar features with the Ryker Model L-1 Vertical Sketchmaster.

mapping symbology was followed, with most symbols, colors, and unit names taken from existing nearside lunar geologic maps (for example: Wilhelms and McCauley, 1971; Scott, 1972; Scott and Pohn, 1972; and Hodges, 1973).

Major structural features are included on the geologic map (Phate 1); minor lineations, however, are shown on both the base map (Plate 2) and the lineation map (Plate 3).

Construction of Cross-Sections

Topographic profiles across Sklodowska and several smaller craters were provided by Richard J. Pike of the U. S. Geological Survey Astrogeologic Branch at Menlo Park, California. The profiles were originally produced on the U.S. Geological Survey AP/C analytical steroplotter in Flagstaff, Arizona from Apollo 15 metric camera photographs (R. J. Pike, written comm.). Extensions of the Sklodowska profiles were constructed by the writer using a floating-dot parallex bar with an Abrams Model CB-1 steroscope. This technique is described in U.S. Geological Survey Professional Paper "Aerial Photographs in Geologic Interpretation and Mapping" (Ray, 1960, p. 50-55). The resulting profiles have been used for geologic cross-sections (Plate 1).

Statistical

Crater diameters were measured and relative morphologic ages were assigned to all craters equal to or larger than 8 km in diameter in order to calculate the crater size/frequency relationship within the area (i.e., the cumulative number of craters of a given diameter per 10^6 km^2) and to evaluate the relative rate of cratering through time. A total of 223 craters were measured and assigned a relative age (see Appendix C). Craters were also numbered for identification purposes.

Crater Size/Frequency Determination

Maximum and minimum diameters of each crater were measured on Apollo 15 metric (mapping) stereophotographs and averaged to obtain an average diameter value for each crater. The purpose of this procedure was to determine the relationship between the cumulative crater frequency and crater size (diameter), and to compare the relationship to similar relationships derived for other lunar areas, specifically for several nearside areas examined by Dodd, Salisbury, and Smalley (1963).

The cumulative frequency/diameter data were subjected to a least-squares treatment on an IBM 370/145 computer. The relationship is best approximated by the equation:

$$F = AD^B$$

where F is the cumulative frequency, D is the crater diameter in kilometers and A and B are constants representing the Y-intercept and the slope of the regression line respectively. For the Sklodowska Region, A=4.628 and B=-1.678. These values are from least squares equation estimates obtained by $\log_{10} F = A + B \log_{10} D$.

Data are listed in Appendix C; results and interpretations are given in the section "Correlation of Statistical Results".

Relative Age/Rate of Cratering Determination

Crater ages were assigned on the basis of morphologic criteria as outlined by Pohn and Offield (1970). The classification follows a decimal system where 0.0 represents a totally subdued crater and 7.0 represents a newly formed crater. Morphologic ages were divided into seven classes and the number of craters per relative age class was determined 1) for all crater sizes and 2) for craters in three size categories. The data are located in Appendix C; discussion and interpretations are found in the section "Correlation of Statistical Results".

A chi-square test was also performed to test the hypothesis (considered the null hypothesis, H_o) that "the proportion of craters in each relative age class is the same for each crater size class". Since visual observations and frequency results indicate that the proportions are not equal, the chi-square value should be large and H_o should be rejected.

STRATIGRAPHY

Stratigraphic Implications

Lunar stratigraphy is an adaptation of principles established for terrestrial stratigraphy. The lunar surface can be thought of as a layered sequence of rock units with younger units overlying or truncating older units. Although the units are not necessarily composed of lithified material, they are composed of rock material and therefore are considered rock units. Principles of uniformitarianism, superposition and lateral continuity are as applicable and essential to lunar geology as they are to terrestrial geology.

Age sequences are determined mainly by crater overlap and morphologic differences. As previously observed, younger craters are superposed on older craters or other materials, and younger craters are fresh and distinct whereas older craters are more subdued. Additional information regarding relative age differences may sometimes be obtained by crater density studies.

In addition to the systematic treatment, lunar stratigraphic units are given descriptive names having no genetic implications (for example: crater rim material; terra material; plains material). Interpretations are separated from descriptions permitting a more uniform system of nomenclature to develop regardless of individual bias to the origin of the materials.

Correlation to Nearside Stratigraphy

The stratigraphic sequence developed for the nearside is also applicable to the farside. One formal change has recently been adopted, however: the pre-Imbrian has been divided into pre-Nectarian age (older) and the Nectarian System (younger) (D. E. Wilhelms, oral comm.) based on features that pre-date or post-date the Nectaris basin-forming event. An outline of the lunar stratigraphic column utilized in this report is shown below, and a brief discussion from oldest to youngest about each division follows.

LUNAR STRATIGRAPHIC COLUMN

Time-Stratigraphic Sequence		Relative Age
Copernican System		youngest
Eratosthenian System		
Imbrian System		
Nectarian System	pre-Imbrian	
pre-Nectarian time		oldest

Pre-Nectarian craters are extremely subdued and often nearly destroyed. They retain few, if any, original characteristics and are generally in the form of large circular depressions or basins, such as that formed by the crater Curie (Fig. 4). Nectarian craters (those younger than the Nectaris basin-forming event but older than

the Imbrium basin-forming event) are highly subdued but retain a partial rim deposit. The crater Backlund exemplifies Nectarian craters (Fig. 5).

The event that formed the Imbrium basin is the marker for the beginning of the Imbrian System, and on the nearside, the base of the Imbrian is defined as the base of the Fra Mauro Formation (Wilhelms, 1970). In this study, Imbrian materials are identified by comparative morphology and stratigraphic relationships. Imbrian craters are moderately subdued and are not greatly modified by younger craters. Early Imbrian craters are typified by the crater Brunner (Fig. 6); Late Imbrian craters by Sklodowska (Fig. 7).

The top of the Imbrian System, and therefore the base of the Eratosthenian System, is considered to be the time of completion of major mare filling of nearside basins; this process is believed to have extended over a period of at least several million years and perhaps as long as one billion years (Hartmann, 1967; Ronca, 1971).

Units in the Eratosthenian System consist mainly of crater materials and some localized occurrences of mare material. Eratosthenian craters are slightly subdued and retain many of their original characteristics. The rim deposits of the crater Eratosthenes comprise the type area on the nearside for crater materials of the Eratosthenian System. In the research area, Eratosthenian

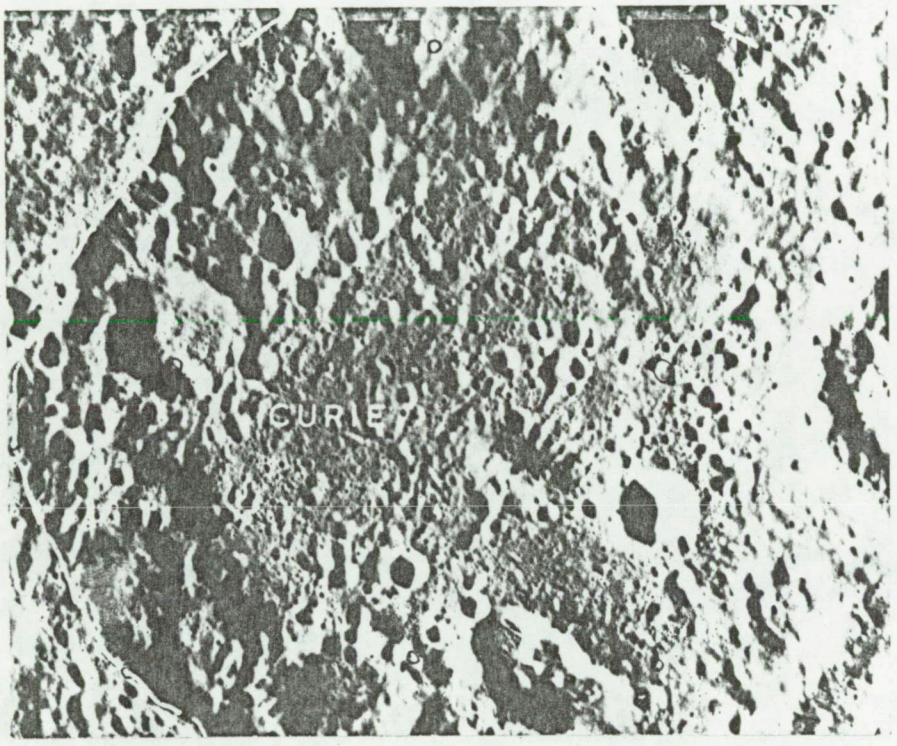

Figure 4. Pre-Nectarian crater Curie. Dashed line outlines the crater rim crest. Note the subdued, heavily cratered inner slopes and outer rim. Curie has a diameter of about 150 km (after Apollo 15 metric camera frame AS-15-2636).

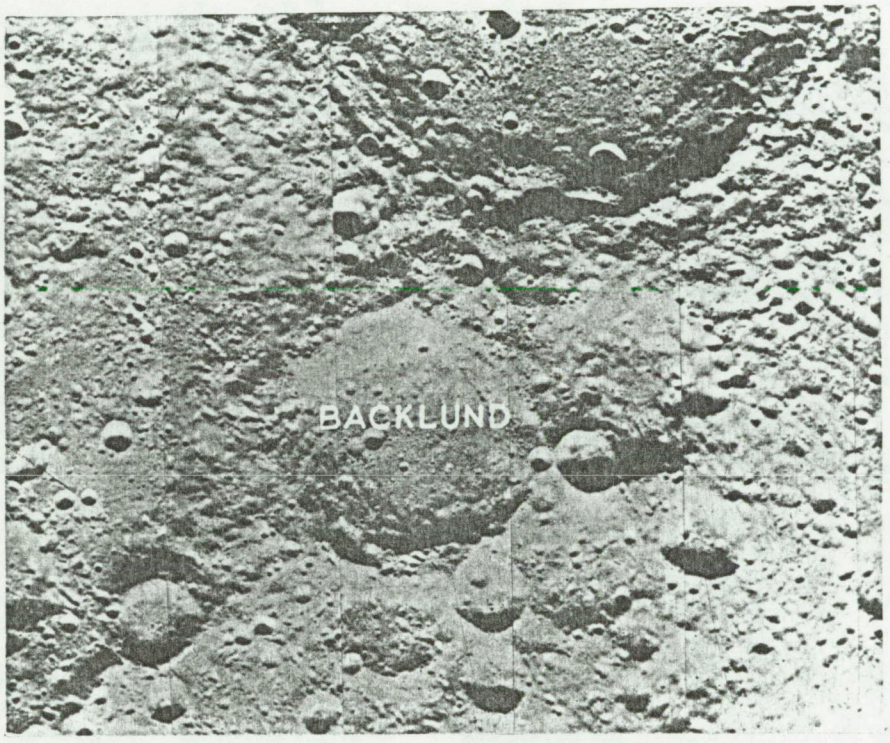

Figure 5. Nectarian crater Backlund. Inner slopes and rim are less cratered than for Curie. Backlund has a diameter of 76 km (after Lunar Orbiter II frame 196M).

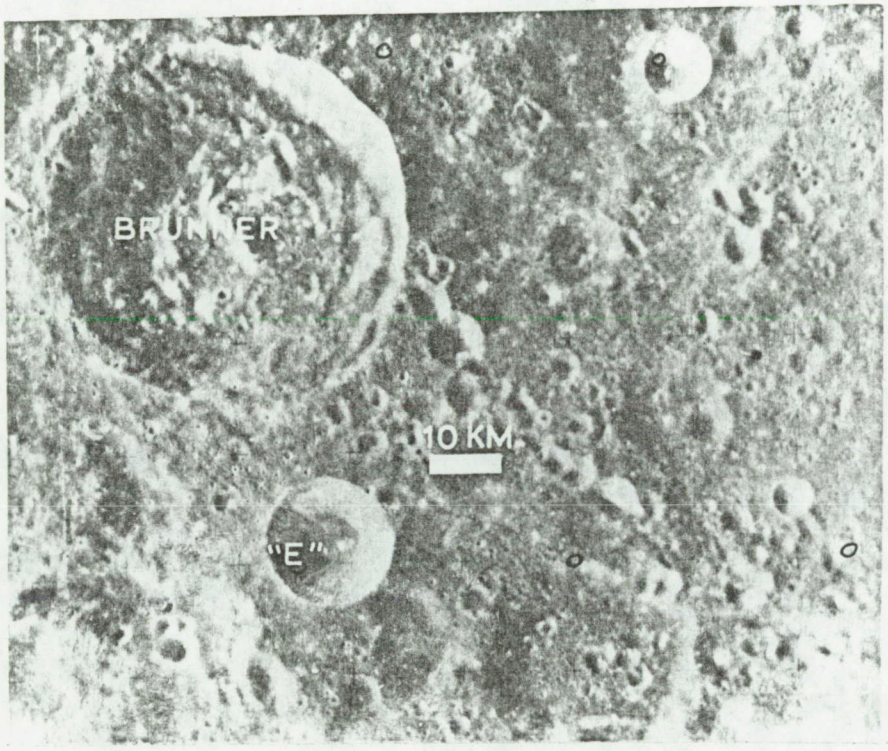

Figure 6. Lower Imbrian crater Brunner. Note the relatively uncratered eastern wall and distinct rim crest (after Apollo 15 metric camera frame AS-15-1744).

Figure 7. Upper Imbrian crater Sklodowska. Note the terraces on the inner slopes and the multiple peaks. Sklodowska is about 130 km in diameter (after Apollo 15 metric camera frame AS-15-1874).

craters are typified by Crater E (unofficial name) (Fig. 8).

The division between the Copernican System-Eratosthenian System is somewhat arbitrary but is generally based on the presence or absence of bright ray material around fresh craters. Copernican craters are normally fresh or very slightly subdued, but in rugged, highlands regions they become slightly subdued and often lose the bright ray material. When ray material is absent, age is determined by the presence or absence of boulders, ejecta flow scarps, "dunes" or other features generally associated with Copernican craters. Materials of the Copernican System are typified by deposits of the nearside crater Copernicus, for which the system was named (Shoemaker and Hackmann, 1962). Craters C and D (unofficial names) in the research area exemplify Early and Late Copernican craters respectively (Fig. 9 and 10).

On the accompanying geologic map (Plate 1) the complete stratigraphic sequence of the research area is correlated by relative age and units are briefly identified. More complete descriptions and interpretations of the units are given in Appendix B.

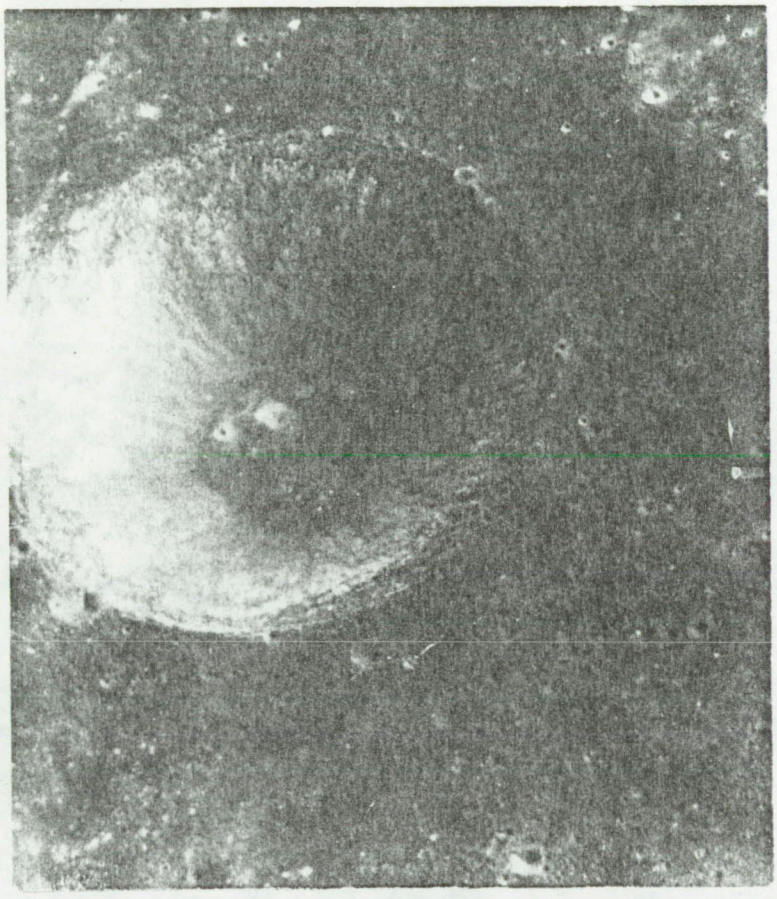

Figure 8. Eratosthenian crater "E" (unofficial name). Note the subdued floor material. The crater is approximately 17 km in diameter (after Apollo 15 panoramic camera frame AS-15-9720).

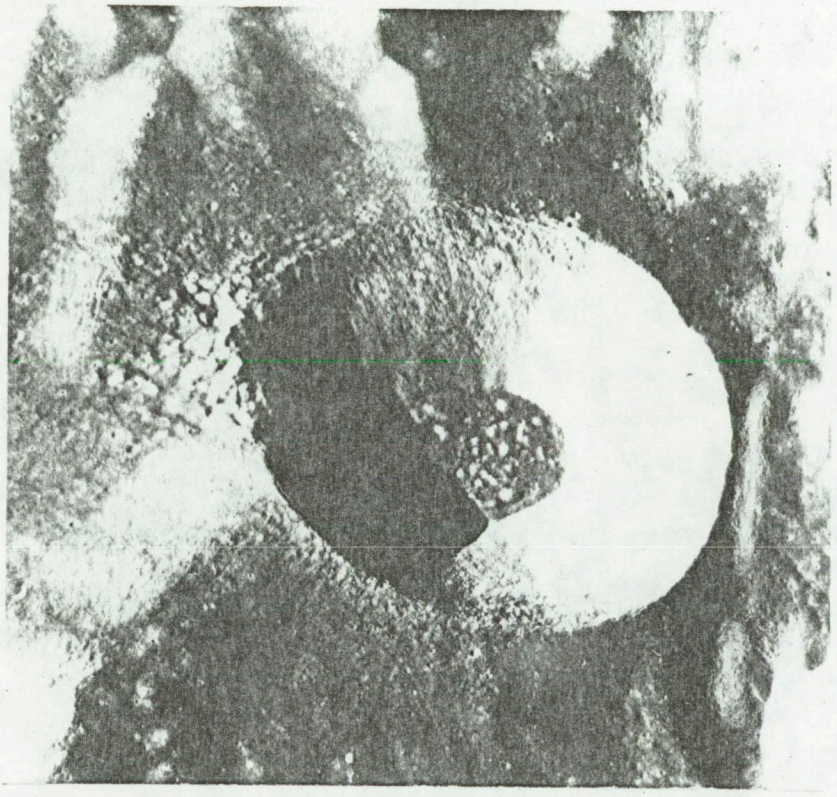

Figure 9. Lower Copernican crater "C" (unofficial name). Note the distinct mounds on the floor material. The crater is approximately 16 km in diameter. The rim crest of Sklodowska runs from the lower left of the photograph to the upper center (after Apollo 15 panoramic camera frame AS-15-9985).

Figure 10. Upper Copernican crater "D" (unofficial name). Note the ejecta material draped over the rim of Sklodowska at the lower right. The crater is 11 km in diameter (after Apollo 15 Hasselblad frame AS-15-13190).

DISCUSSION AND INTERPRETATION OF LUNAR MATERIALS

Based on crater morphology and correlation to findings of previous investigations, most of the mapped materials, with the exception of mare and associated materials, are interpreted as having formed by impact explosion and subsequent ejecta deposition. All materials are modified to varying degrees by mass wasting and other aging processes. To explain the basis for these interpretations, crater materials, terrae materials and plains materials, and mare material in the vicinity of the study area are discussed in some detail. The reader's attention is directed to Plate 1 (Geologic Map) for inspection during the following discussion. The reader is also reminded that the following discussion concentrates on mapped materials and as such irregularly crosses time or stratigraphic units.

Crater Materials

Most craters in the Sklodowska vicinity have features generally considered to be characteristic of impact explosion structures. Craters of differing sizes and ages possess different morphologic characteristics ranging from fresh and distinct for young craters to highly subuded for old craters. Distinct units can no longer be recognized on old craters; therefore they retain little evidence in support of either impact or volcanic origin. Small craters of younger ages like-wise do not have distinct deposits, except for extremely fresh

Copernican craters. On large craters of late Imbrian and younger ages, however, these units are usually well preserved.

Sklodowska and Related Materials

The Imbrian crater Sklodowska and its ejecta deposits serve as an example of the morphology characteristic of large lunar craters. Its morphology is similar to, although more subdued than, that of Copernicus on the lunar nearside. Various crater dimensions and other morphometric properties of Sklodowska and other farside craters are shown in Table 1.

Sklodowska and its deposits are divided into six morphologic units: 1) crater peak material; 2) floor-covering material (subdivided into two units of plains material and one unit of terra-like material); 3) wall material or inner slope material; 4) hummocky rim material; 5) radial rim material; and 6) material of the continuous secondary crater field.

Central Peak Material. Sklodowska has two major peaks and several small conical mounds in the same general vicinity (see Fig. 7). The largest peak is located slightly northeast of the crater center and rises about 2 km above the floor-covering material. The smaller of the two large peaks is located at the geometric center of the crater and stands 1 km above the floor. Neither peak has a visible

summit crater that would indicate a volcanic origin.

Crater peaks are common in craters larger than 20 to 30 km in diameter (Wood, 1968). All fresh-appearing craters with a crater diameter of 60 km that Wood examined had single or multiple peaks. Smith and Sanchez (1973) obtained similar results for 120 fresh lunar craters. Although peaks are common, their origin is controversial. Theories include origin by volcanic processes, isostatic rebound of the floor, megashatter cone development following impact, and some combination of two or more of these processes. Steinberg (1968) and Miyamoto (1968) explain most lunar craters and crater peaks as volcanoes and related extrusive features. Erlich and others (1970) proposed a similar origin for the crater Tsiolkovsky and concluded that its central peak was possibly a large extrusive dome. Guest and Murray (1969) also did not rule out the possibility that Tsiolkovksy's peak was volcanic, even though they concluded that the crater was of impact origin. Cohen (1961) suggested that central peaks may form as megashatter cones develop at the point of impact. Terrestrial cryptoexplosion structures (generally considered impact) often have an uplifted central area. Wilshire and Howard (1968) believe that the central uplift in the Sierra Madera structure in Texas was formed by material moving inward and upward following a meteorite impact. Shatter cones found in the cen-

Name or location	Rim diameter, km	Outer-rim width, km	Floor diameter, km	Inner-rim width, km	Depth, m	Outer-rim height, m	Inner-rim slope, deg	Outer-rim slope, deg	Circularity[a]
In Sklodowska	1.6	0.4	–	0.8	300	95	20.6	13.4	0.90
In Sklodowska	2.8	.5	–	1.4	550	125	21.5	14.0	.88
In Hirayama	3.5	1.0	–	1.7	500	175	16.2	9.9	.84
In Curie	4.3	.9	–	2.1	600	175	15.8	11.0	.64
In Tsiolkovsky	4.9	1.0	–	2.4	950	100	21.3	5.7	.73
In Hilbert	6.0	1.0	–	3.0	950	150	17.6	8.5	.79
In Pasteur[b]	9.9	1.8	2.8	3.6	1100	105	17.2	3.3	.79
In Saha[b]	15.7	3.6	9.0	3.4	880	280	14.7	4.4	.80
In Gagarin	16.0	3.5	10.0	3.0	1350	650	24.2	10.5	.90
In Gagarin	17.0	4.5	6.0	5.5	1700	450	17.2	5.7	.89
In Hilbert	17.0	3.0	5.0	6.0	1800	400	16.7	7.6	.79
On western rim of Gagarin	26.0	6.0	13.0	6.5	2600	725	21.8	6.9	.86
Izsak	33.2	7.7	13.0	10.1	3400	1025	18.6	7.6	.86
Gilbert M	34.0	5.5	18.0	8.0	3100	850	21.2	8.8	.84
Gansky	44.0	12.0	22.0	11.0	3550	950	17.9	4.5	.78
South of Saha	50.5	13.3	24.0	13.3	3640	1380	15.4	5.9	.83
Schorr	53.5	13.0	26.0	13.8	3700	730	15.1	3.2	.77
Ritz	59.0	15.5	24.0	17.5	3750	1800	12.1	6.6	.71
King	71.0	17.0	40.0	15.5	3830	1690	13.9	5.7	.80
Langemak[b]	110.0	17.0	60.0	25.0	4370	880	9.9	3.0	.68
Sklodowska	128.0	18.0	83.0	22.5	4500	1850	11.3	5.9	.78
Curie[b]	158.0	29.0	100.0	29.0	3850	1500	7.5	2.9	.73
Hilbert	178.0	35.0	125.0	26.5	4100	1500	8.8	2.5	.80
Tsiolkovsky	190.0	40.0	140.0	25.0	4700	1750	10.7	2.5	.83
Gagarin[b]	275.0	43.0	200.0	37.5	5375	(3350?)	8.2	(4.5?)	.79

[a]Ratio of areas of circles inscribed and circumscribed on rim-crest outline.
[b]Older appearing craters.

Table 1. Morphometric properties of farside craters (after Pike, 1973). Craters marked with a dot are present in the Sklodowska Region.

tral uplift at Sierra Madera add support to this conslusion (Howard and Offield, 1968). A similar process of central deformation could be expected to occur in lunar impact craters.

Sklodowska's peaks, although somewhat degraded, have no visible dikes, flow scarps, summit craters or other features indicative of volcanism. Although some crater peaks may well be volcanic, the peaks in Sklodowska, because of their conical shape, central location, and lack of volcanic features that conform to the general exogenic pattern typically found in this study, they are believed to represent central uplifts and/or megashatter cones that formed upon impact of a large extra-lunar mass, or as the immediate reaction following such an impact.

Floor-Covering Material. Two types of plains material and a more rugged unit of hilly and pitted material form the floor of Sklodowska. The plains material is divided into a "dark" unit and a "light" unit because of a slight albedo change. The dark plains material is less pitted and smoother than the light plains material and occurs around the central peaks as well as in small patches around the edge of the floor. The light plains material is similar to the terra-plains material of the nearside described by several authors (for example: Eggleton, 1965; Wilhelms and McCauley, 1971; Eggleton and Schaber, 1972) who interpret such material as basin and other large impact

ejecta deposits. Assuming the ejecta was in a fluid or semi-fluid state, it would tend to fill depressions to a nearly uniform surface elevation with little material deposited on slopes and topographic highs. Stuart-Alexander and Tabor (1972), however, attribute the wide dispersion of plains material to a large number of volcanic source areas, the plains material being interpreted as ash and other pyroclastic ejecta.

The light plains material within Sklodowska has no related structures, such as rilles or fracture systems, that indicate a volcanic origin; however, the dark plains material, because of its location around the peaks and around the floor margin where faulting and fracturing would most likely occur, and because of its similarity to mare material, may represent a stage of volcanism. The possibility remains that both plains units are mare material, the light plains material being slightly older and slightly subdued by a thin coating of ejecta material.

The remainder of the floor is characterized by low conical hills, mounds, and shallow, bowl-shaped craters. This material is believed to be part of the original flor material that has been modified by secondary cratering, mass wasting, and ejecta blanketing. Ejecta blanketing is indicated by the shallow form of many small, fairly sharp-rimmed craters, this lends support to the above hypo-

thesis that the light plains are the result of ejecta deposition.

The floor of Sklodowska has apparently subsided, perhaps several times, since the formation of the crater as evidenced by dark plains material mantling several terrace platforms on the inner slopes of the crater (Fig. 11). This suggests at least a moderate time interval between crater formation and the formation of the dark plains material followed by final subsidence of the crater floor. The subsidence process possibly was similar to previous terrace development by slump faulting as shown on the geologic cross-sections (Plate 1).

Crater Wall Material. The inner slopes of Sklodowska have numerous terraces and corresponding scarps on the eastern and western slopes that grade into radially channeled northern and southern slopes. The uppermost terrace scarp, occupying the upper one-third of the crater wall and completely encircling the crater, is only slightly subdued and has a moderate to high albedo indicating a relatively steep slope. The remaining terraces progressively coalesce downslope until the slopes become a mass of rubble at the edge of the crater floor.

Terraces are common in craters larger than 10 to 20 km diameter (Quaide and others, 1965; Smith and Sanchez, 1973) and are a function of crater size. They are generally believed to be slump

Figure 11. Plains-covered terrace on the inner slopes of Sklodowska (arrow). Also note terrace scarps (ts) and central peaks (cp). The small peak on the left is about 4 to 5 km across (after Apollo 15 panoramic camera frame AS-15-9986).

faults that form as pressure is relieved following the forcible rebound uplift created by an impact explosion.

The uppermost terrace scarp reflects to some extent the polygonal nature of the rim crest; this may represent either regional structural control or local control by fracturing events associated with the crater formation. The north-south channeling, however, is thought to be related to the north-south lineaments described by Fielder (1963) and Strom (1965) for the lunar grid. The presence of similar channeling on most large Imbrian and younger farside craters supports this view.

Rim Materials. The ejecta around Sklodowska forms an asymmetrical to bilaterally symmetrical pattern. To the north and south the deposits are fairly extensive. To the east they are less extensive, and to the west they are almost absent. An almost indentical pattern found around the crater Tsiolkovsky is attributed to an oblique impact (Guest and Murray, 1969). Similar ejecta deposits with "zones of exclusion" are found around some Copernican craters. El-Baz (1969), discussing ray-excluded zones, proposed two possible explanations--the effect of local relief and the trajectory of the impacting mass. In the latter case trajecting must be oblique or low angle to cause the asymmetry. There is no evidence to indicate a topographic obstruction west of Sklodowska to account for the relative absence of

ejecta material, and therefore, an oblique angle of trajectory is favored to explain the ejecta distribution.

The ejecta is divided into three morphologic units based on textural changes in the topography. They are: hummocky rim material, radial rim material, and material of the continuous secondary crater field.

The hummocky rim material constitutes the rim proper; that is, the raised portion of the rim that generally extends from the rim crest to the major break in slope. For Sklodowska, the hummocky material includes some of the material beyond the break in slope because of modification of a portion of the radially textured material to resemble the hummocky material.

The hummocky rim material grades outward into the radial rim material, so named because of its characteristic radial and subradial "striations", grooves, and "V" structures (Also called herringbone patterns). A few secondary craters are also present, but they typically take the form of the "V" structures or gouges. "V" structures are V-shaped ridges or craters that are common around many fresh craters, such as Aristarchus on the nearside (Fig. 12), and have been attributed to secondary cratering by Oberbeck and others (1972). Although the "V" structures are poorly preserved around Sklodowska, they are readily identifiable and morphologi-

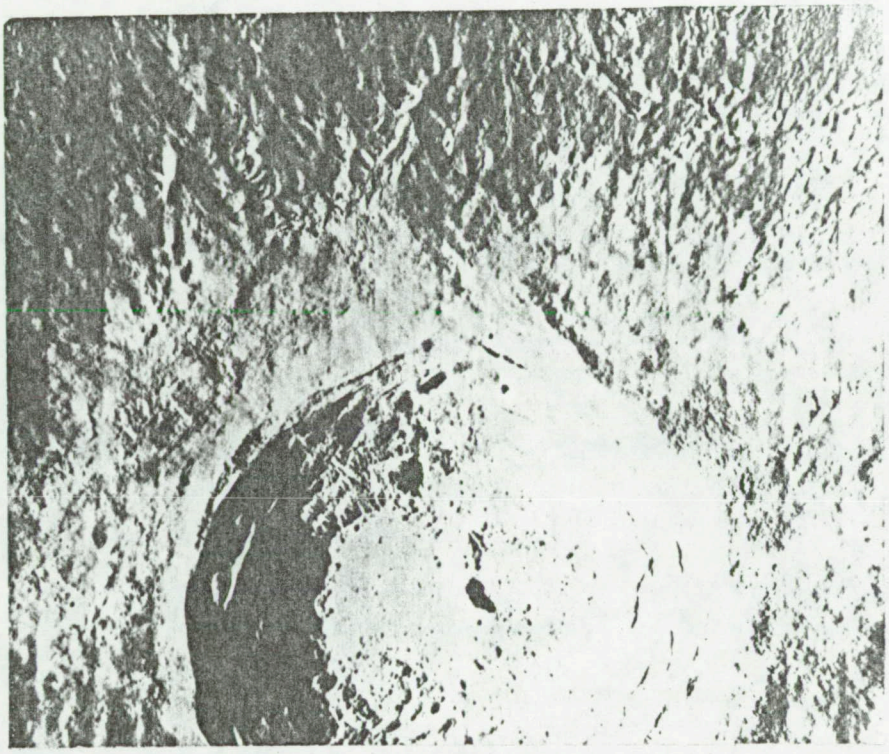

Figure 12. "V" structures around the crater Aristarchus, a Copernican crater on the lunar nearside. Aristarchus is 40 km in diameter (after Lunar Orbiter IV frame 150-H3).

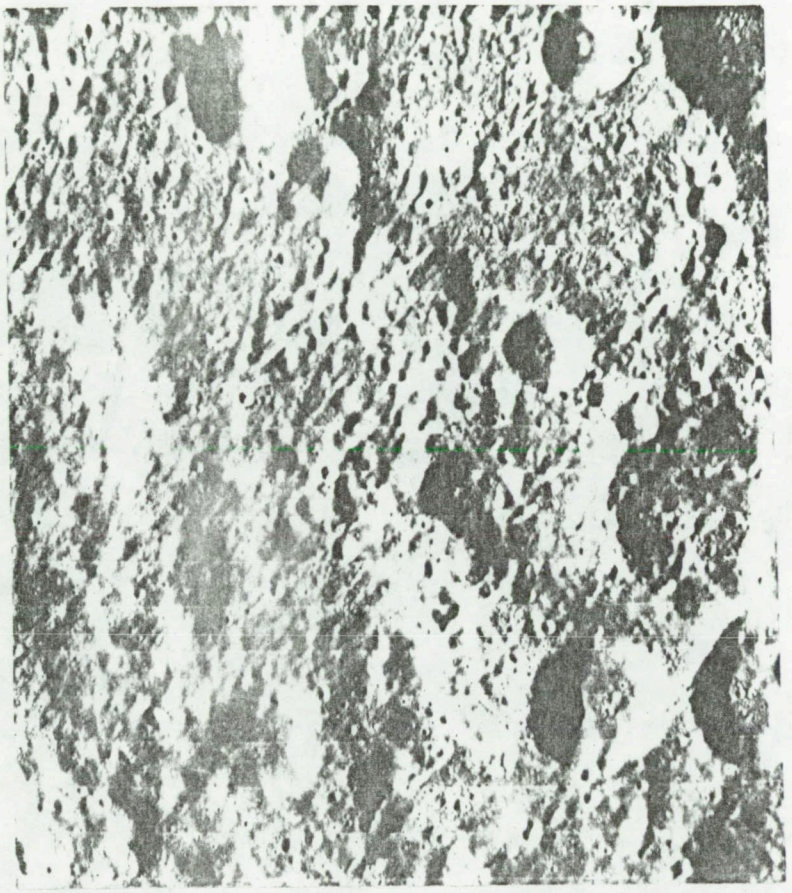

Figure 13. Subdued "V" structures north of Sklodowska. The distance across the photograph is about 115 km (after Lunar Orbiter II frame 196-H3).

cally similar to those around younger craters as can be seen in Figure 13. Lineations or "striations" take the form of narrow ridges and troughs and generally occur in swarms.

Material of the continuous secondary field consists of closely spaced secondary craters and their ejecta material and forms a continuous unit. For Sklodowska, this unit is found only to the south of the crater. Similar secondary craters can be seen to the north, but they are considerably more scattered and do not dominate the surface topography as do their southern counterparts. The craters are all similar in size and shape, generally from 4 to 8 km in diameter and diamond-shaped to elliptical in outline with the elongated axis radial or sub-radial to Sklodowska. The reason for the absence of this unit to the west, east, and north is not known, however, it may be related to an oblique angle of impact, because the absence does not appear to be related to topographic or structural controls.

Other secondary craters, crater chains, and gouges are scatered beyond the continuous ejecta deposit. Some as distant as 400 km from the rim of Sklodowska are believed to be related to the formation of the crater.

The thickness of the ejecta deposit varies in different sectors around Sklodowska, but it consistently thins with increasing distance from the crater rim crest. Several large craters near the rim crest

are almost completely filled with rim material whereas several slightly larger craters at about the same distance are only partially filled. Estimates indicate a thickness for the raised portion of the rim of at least 1000 meters with possible thickness's up to 1500 meters. With increasing distance from the rim crest, the underlying topography becomes less subdued and eventually begins to dominate the surface expression as the covering ejecta thins. The ejecta material becomes discontinuous at about one crater diameter (130 km) although this distance also varies locally. Furrowing of older crater rims is evident where the ejecta no longer completely blankets craters (Fig. 14); generally such conditions occur on crater walls and rim crests facing Sklodowska suggesting erosion by blast ejecta.

All of the materials forming the ejecta deposit appear to have formed contemporaneously or nearly so, supporting a single crater-forming event rather than several events over a period of time. It is entirely possible, however, that impact-induced volcanism may have also played a role in modifying the topography of Sklodowska although no conclusive evidence can be found to support this possibility. Strom and Fielder (1968) have proposed a multiphase development for the nearside crater Tycho. They concluded that considerable intervals of time separate the Tycho-forming event from the event related to some of its rim deposits; they accounted for this by late phase volcanic eruptions. Even if similar eruptions occurred around

Figure 14. Scalloping and furrowing of crater rims and walls by Sklodowska ejecta (arrow). The furrowed crater is 29 km in diameter (after Apollo 15 metric camera frame AS-15-1878).

Sklodowska, subsequent modification would now render them unidentifiable. Regardless of later events, the following evidence supports an impact origin for Sklodowska: 1) tapering thickness of the ejecta blanket with increasing distance from the rim crest; 2) sequence of textural materials similar to those around Copernican craters that are interpreted as impact structures by most moonologist; 3) asymmetrical distribution of the ejecta deposits; 4) presence of "V" structures, secondary craters, crater chains, gouges, and radial grooves; 5) furrowing on older crater walls and rim crests; and 6) age relations suggesting that all ejecta materials and associated features were formed essentially simultaneously.

Materials of Other Selected Craters

Copernican Crater Materials. Although Sklodowska is the dominant feature in the area, there are numerous other craters, especially some of the Copernican system which have equally interesting features. The following discussion concentrates on two Copernican craters, A and B, with somewhat different morphologies. Lists of characteristics of craters in each age classification along with type examples are given in Appendix B.

A total of eighteen Copernican craters ranging in size from 1 km to 25 km in diameter are mapped in this study; smaller rayed craters are abundant in the area but are below the limits of the map

scale. Two craters located southeast of Sklodowska are particularly interesting. The first crater (identified as crater A), about 4 km in diameter, is extremely fresh and has the characteristic ejecta textures of impact craters (Fig. 15). Most of the features associated with Sklodowska's ejecta are present; this includes the hummocky raised rim, radially textured material, "V" structures, and secondary craters and crater chains. In addition, features are much fresher in appearance around crater A, and blocky ejecta flows, braided gouges, boulders, and extensive rays are present. Morphologically it is similar to some of the impact craters discussed by Moore (1972), and is believed to represent a typical small impact crater.

The second crater (identified as crater B) is located approximately 25 km southeast of crater A (Fig. 16). Ray material from crater A is superposed on crater B's rim deposits, and consequently is older than crater A. Crater B has few of the typical Copernican textures and structures. The raised portion of the rim is not hummocky, but rather is relatively smooth with low, closely spaced concentric ridges. To the south and west, this material grades into moderately subdued dune structures, most of which are nearly perpendicular to the direction of ejecta blast (Fig. 17). The dunes are relatively widely space and irregular. Moore observed similar structures around Taal volcano following its eruption in 1965. Ac-

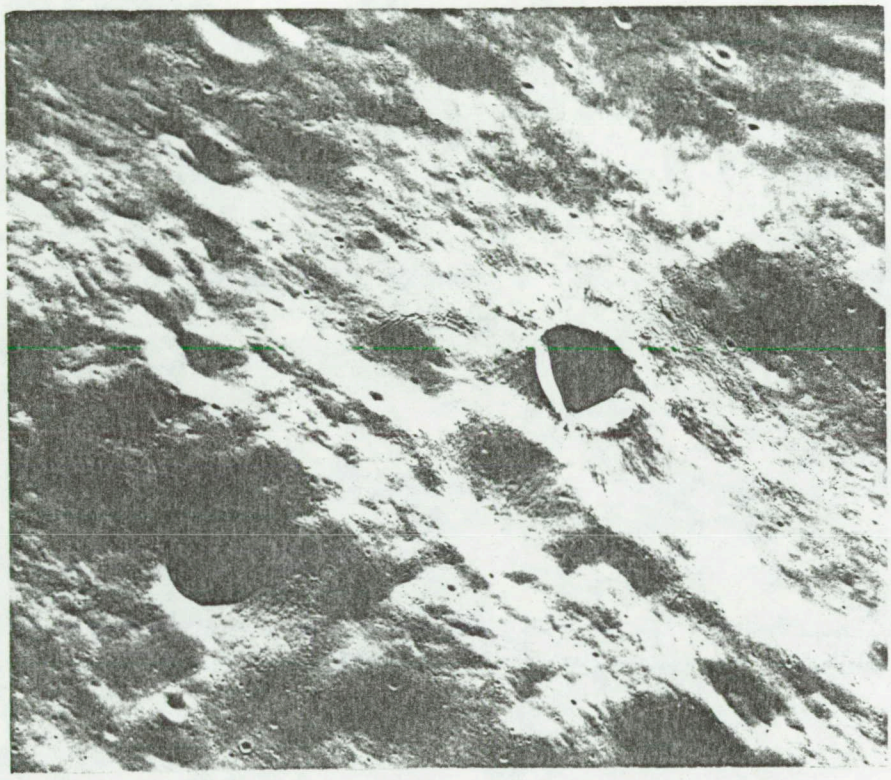

Figure 15. Crater "A" (unofficial name). The crater is 4 km in diameter. Note the bright rays with dark streaks near the crater rim; fresh, sharp features; secondary craters; and striated texture of the rim material (after Apollo 15 Hasselblad frame AS-15-13181).

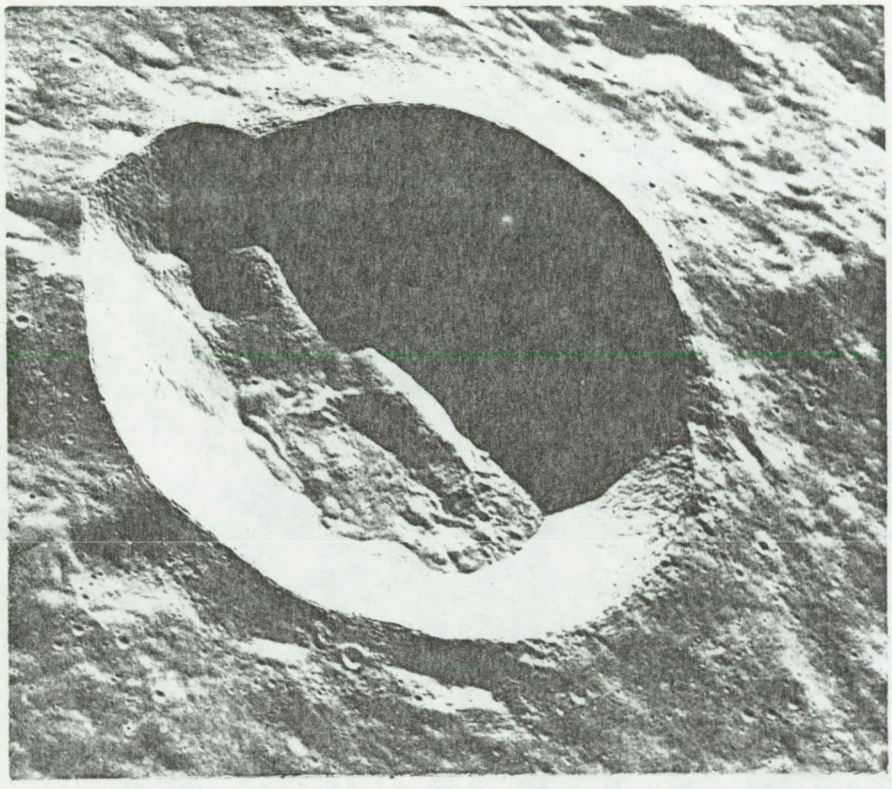

Figure 16. Crater "B" (unofficial name). The crater is 25 km in diameter. Note the large mound on the crater floor; blocks and boulders; lack of bright ray material; and small tension cracks concentric to the rim near the rim crest (after Apollo 15 Hasselblad frame AS-15-13180).

cording to his observations, "in the inner half of the area . . . giant ripple marks or sand dunes are common . . . oriented at right angles to the direction of blast . . ." (1966, p. 959). He also states that "the eruptive clouds followed the contours of the ground, passing up, over, and down the ridges" (loc. cit., p. 959).

The floor of crater B is highly irregular; this is unlike most other Copernican craters in the area which generally have fairly level although sometimes ropey floors. It is characterized by a large, elongated, rounded mound with many small mounds and ridges on the remaining portions of the floor. Large blocky boulders can be seen on the floor material, inner slope surfaces, and on the rim material. Inner terraces are absent, a rather uncommon although not rare occurrence for a crater of this size. In view of the above characteristics, crater B may represent a large caldera that formed by a violent volcanic explosion. However, lacking more conclusive evidence, such as flows or associated cinder cones, an impact origin cannot be ruled out.

Small Imbrian Craters

There is also an anomalous population of Imbrian craters smaller than 8 to 10 km surrounding the ejecta deposits of the large Late Imbrian craters. The relative absence of these small craters on the ejecta deposits suggests one of two possibilities: 1) they are re-

lated to the large craters (i.e., secondary craters); or 2) they pre-date the large craters and are absent due to burial by ejecta material. Although a few of the small craters definitely post-date the large craters, most are believed to be older. Three lines of evidence support this hypothesis: 1) they are typically circular whereas secondary craters of the large craters are mostly elliptical or diamond-shaped with the axis of elongation radial to the parent crater; 2) they normally occur singly or as doublets, rather than in crater chains; and 3) there is a slight decrease in morphologic age of the circular craters with increasing distance from the large craters, indicating less influence from the blanketing material.

The origin of these craters is uncertain, but they may actually be secondary craters of distant basin or large crater-forming events. Orientale is perhaps the most likely source area; however, craters such as Tsiolkovsky may also be considered as potential source areas. Further study of these small craters over large areas on the farside is suggested to provide additional information concerning their origin and possible identification of a source if they are secondary craters.

Plains and Terrae Materials

Stratigraphically, the plains material occupies a higher position than most terra material; however, terra material generally

occurs at higher elevations. Plains material blankets the floors of many large craters and fills many of the topographic lows; terra material is most often found around large pre-Imbrian craters. In a few localities plains material is beginning to develop on the more level areas of the terra.

Nearside plains material has been described as "light plains material", "terra-plains material", and simply "plains material", all indicating similar material. Both an impact and a volcanic origin have been proposed for plains material. Eggleton and Schaber (1972) present a convincing argument supporting the formation of plains material (terra-plains) by basin ejecta. They conclude that ". . . each basin-forming event produced thick plains deposits in a belt peripheral to the continuous ejecta blanket and may have deposited a thinner layer in pools over the entire Moon". Head (1972) adds additional support by examining small scale deposits similar to those discussed by Eggleton and Schaber and concludes that they are impact-associated deposits.

Plains material in the Sklodowska area ranges from Nectarian to Late Imbrian in age. The Imbrian plains material is similar to the terra-plains material described by Eggleton and Schaber, but it is somewhat less cratered and therefore possibly slightly younger. Ejecta deposition is a likely mode of origin; the plains material "softens" much of the older topography and forms "pools" in depres-

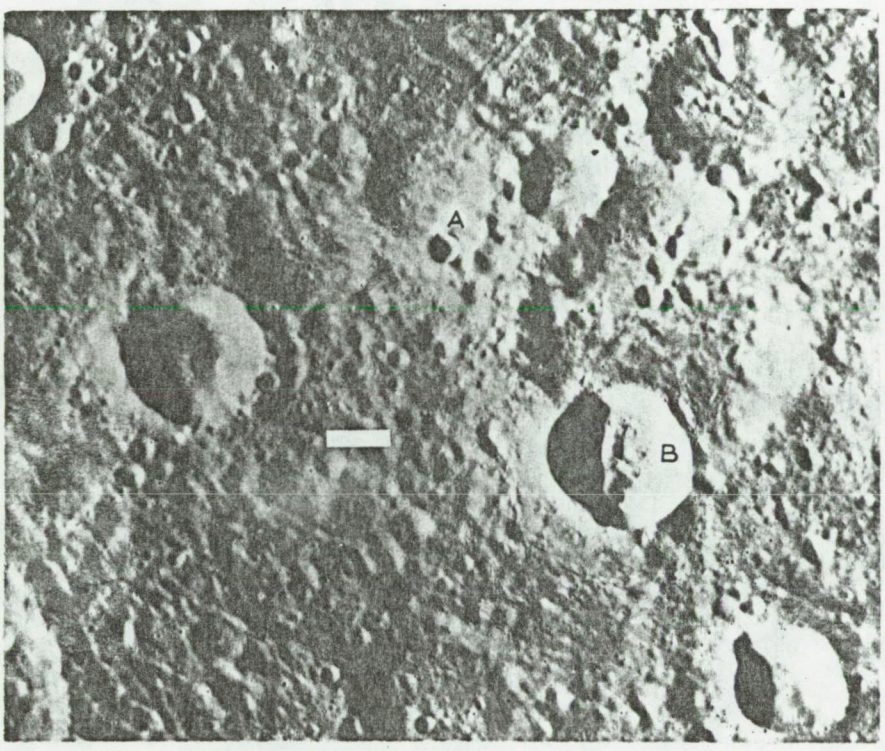

Figure 17. Dune structures to the south and west of crater "B" (arrow). Crater "A" is located about 30 km northwest of "B". Scale bar = 10 km; north is toward the top (after Apollo 15 metric camera frame AS-15-1964).

sions and crater basins. Plains material blankets and partially fills small, older craters, giving them a shallow, bowl-shaped morphology. Small hills and remnant crater rim segments often protrude through the plains material reflecting the former topography.

A highly fluid base surge following a basin- or large crater-forming event could easily account for the deposition of plains material, as Eggleton and Schaber propose. Alternative explanations that plains material is volcanic ash and other fragmental material deposited during an active volcanic stage in lunar history, or that the plains material is a degraded mare surface do not sufficiently account for its occurrence. The fact that the plains material is rather widely and evenly distributed supports an ejecta origin. However, the dark plains unit on the floor of Sklodowska, and perhaps even the light plains unit, may be mare-like material covered with thin ejecta deposits.

Terra material is herein interpreted as sequential accumulations of rim deposits from large ancient craters that have been modified by younger ejecta blanketing and mass wasting processes. Generally terrae units occur adjacent to one or more pre-Imbrian craters (for example, the unit Ntg on the geologic map adjacent to the crater Hilbert). There is often a gradual decrease in elevation of the terra material with increasing distance from the craters. Where pre-Imbrian craters are closely spaced, the terra forms a rugged

intercrater surface with little chnage in average elevation.

Prior to the return of lunar rock samples by the various Apollo missions, terrae units were mostly interpreted as volcanic in origin. However, shocked and brecciated rocks return from the Descartes Region by Apollo 16 indicate that the highlands surface material, i.e. terra material, is mainly of impact origin (Wilshire and others, 1973).

Mass wasting processes undoubtedly play an important role in modifying the appearance of both the plains and terrae materials. Slumps, slope creep, and landslides are all apparent on Apollo 15 Panoramic photographs. These processes are especially active on terrae units because of the rugged topography.

Material mapped as Imbrian-Nectarian terrae material (INt) in the southeast portion of the area resembles some of the near-side terra-plains material although it is more rugged, and is thought to represent a transitional phase between terra and plains material. It is most likely associated with the formation of the multi-ringed basin Milne (see Fig. 1), followed by further modification, especially by secondary cratering, from the Scaliger crater-forming event.

Mare and Associated Material

Mare material is restricted to a small portion of the study area southeast of Sklodowska where an irregular Nectarian crater

and a broad topographic trough have been flooded (Fig. 18). About 4,800 km^2 of surface area have been covered to varying thicknesses. The thickest material partially fills the irregular crater and displays characteristics of terrestrial lava lakes. The material in the trough is somewhat thinner and forms a thin veneer on the older topography in places (Fig. 19). The veneered surface occurs at slightly higher elevations than the main trough filling, indicating that lowering of the mare surface occurred as the lavas drained to the south. The composition of the mare is probably basaltic and similar to near-side mare rocks returned by several Apollo missions. These have been found to be chemically similar to terrestrial basalts (Lunar Sample Preliminary Examination Team, 1969, 1971, 1972). Frontal flow scarps, linear troughs, collapse pits, a fissure and a subsidence bench which are present on the mare are analogous to terrestrial volcanic features.

Frontal scarps on the southern trough (Fig. 19) indicate that the direction of flow was from the north in the general vicinity of a linear fissure 35 km in length. The rim of the fissure is elevated above the surrounding surface and has a slightly higher albedo. Narrow troughs branching from the fissure cross an Eratosthenian terra unit (part of the mare suite) and terminate in small pools of mare material (Fig. 20). The fissure is believed to be the source of

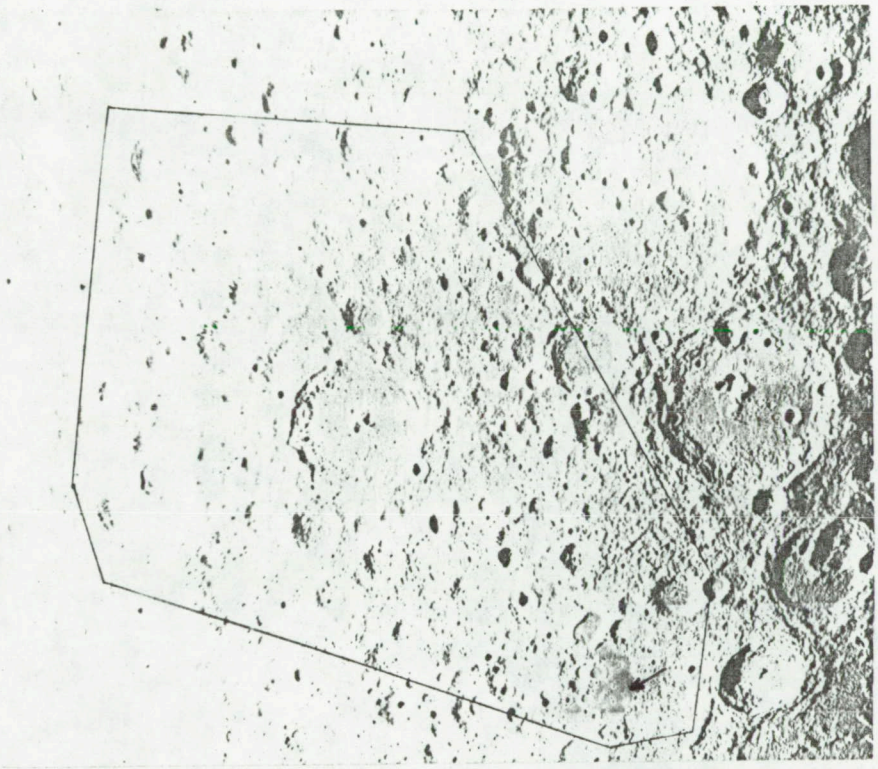

Figure 18. Location of mare material (arrow) to the southeast of Sklodowska (after Lunar Orbiter II frame 196-M).

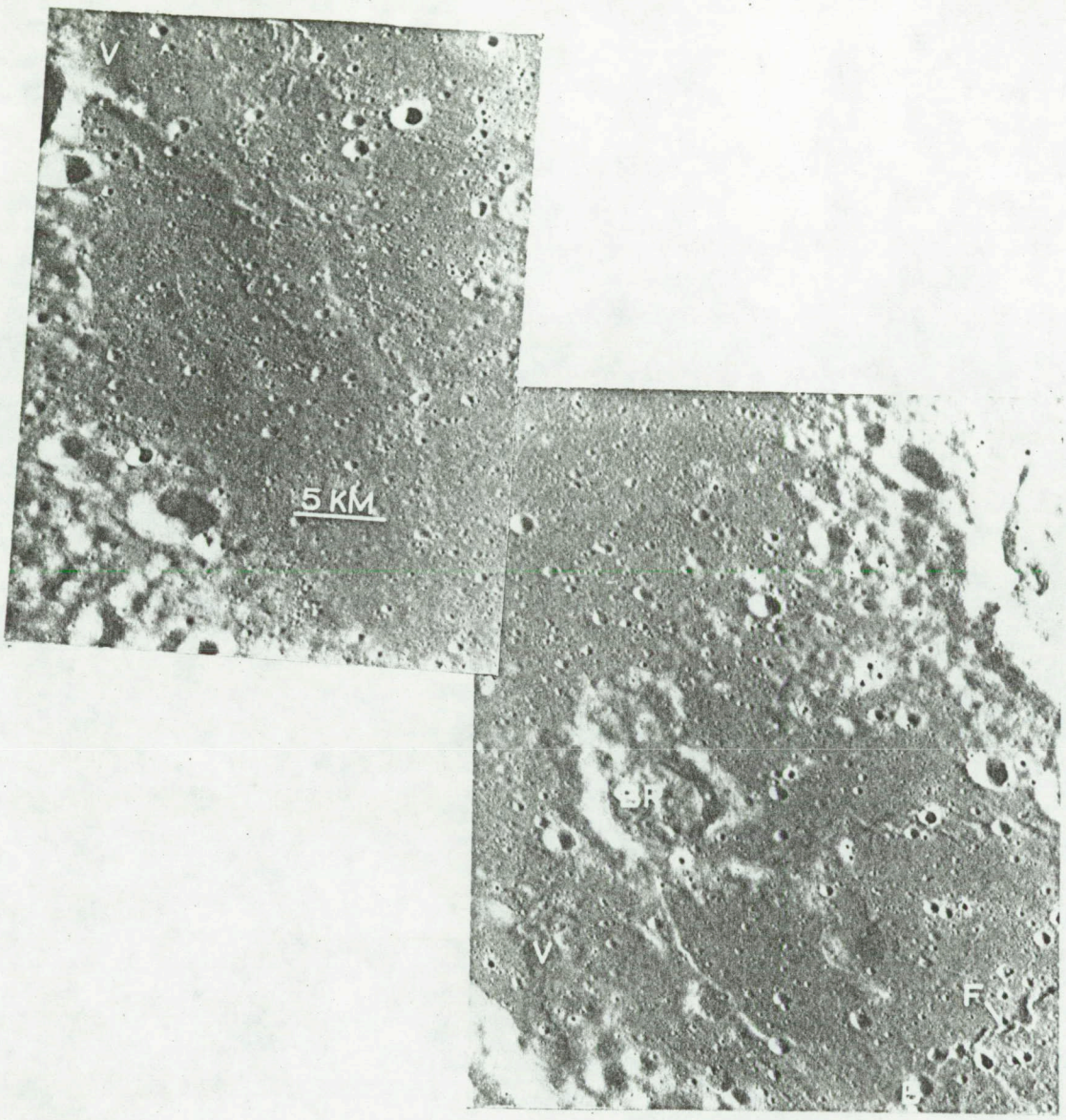

Figure 19. Southern mare trough. Note the veneered topography (v); burried (b) and breached (br) craters; and flow scarps (f). South is toward the top (upper photo after Apollo 15 panoramic camera frame AS-15-9959; lower photo after frame AS-15-9961.

the extruded material with pyroclastic debris forming the raised rim. The troughs are interpreted as collapsed lava tubes through which material was supplied to the small pools. Collapsed lava tubes similar to these are not uncommon in terrestrial volcanic regions (a good analogy is given by Murray, 1971).

Collapse pits (Fig. 20) are evident at several locations as are buried and breached craters (Fig. 19). The collapse pits are rimless and somewhat irregular in form, and resemble terrestrial collapse pits in basalt flows. Buried craters are located by circular depressions formed by differential compaction or draping of the mare basalts in pre-mare craters. Craters which had portionsof their rims above the highest level attained by the mare material are present as breached craters.

A subsidence bench is present around the edge of the material which flooded the irregular Nectarian crater. It varies from 1 to 5 km in width and forms a scarp with an estimated height of 50 to 100 meters. Benches similar to this are common occurrences where pooled lava solidifies on the surface before some of the molten material beneath drains back into the source conduit. A striking example is the bench that formed around the lava lake created by the 1959 eruption of Kilauea Iki volcano (Richter and other, 1970). A comparison of the Kilauea Iki bench and the mare bench is shown in Fig. 21.

The entire mare surface is pitted with small craters; most are less than 1 km in diameter and many are clustered. The clustered craters are generally shallow and bowl-shaped, often slightly elliptical or irregular; they rarely have raised rims. The absence of any large impact craters on the mare suggests that the material is relatively young; crater density also supports this hypothesis. Using Soderblom and Lebofsky's (1973) method of rapid age determination, a D_L value of 135-185 meters was obtained, giving the mare an approximate age of 1.5 to 2.0 X 10^9 years b.p., or Eratosthenian in age. Mare material covering the floor of the crater Tsiolkovsky (a large crater 750 to 800 km East of Sklodowska) is believed to be either Late Imbrian (D. E. Wilhelms, oral comm.) or Eratosthenian (El-Baz and Worden, 1972) in age. Although the mare in this report is higher in albedo than that in Tsiolkovsky, a characteristic generally indicative of older age, it is believed to be considerably younger. The albedo difference may be the result of compositional differences or the result of fine ash deposits on the mare surface causing greater reflectivity.

Two other units are interpreted as part of the mare suite: these are Eratosthenian terra material (Et) and Eratosthenian material of hills and mounds (Ehm). Terra material adjacent to the linear fissure slopes away from the fissure toward the southwest for a

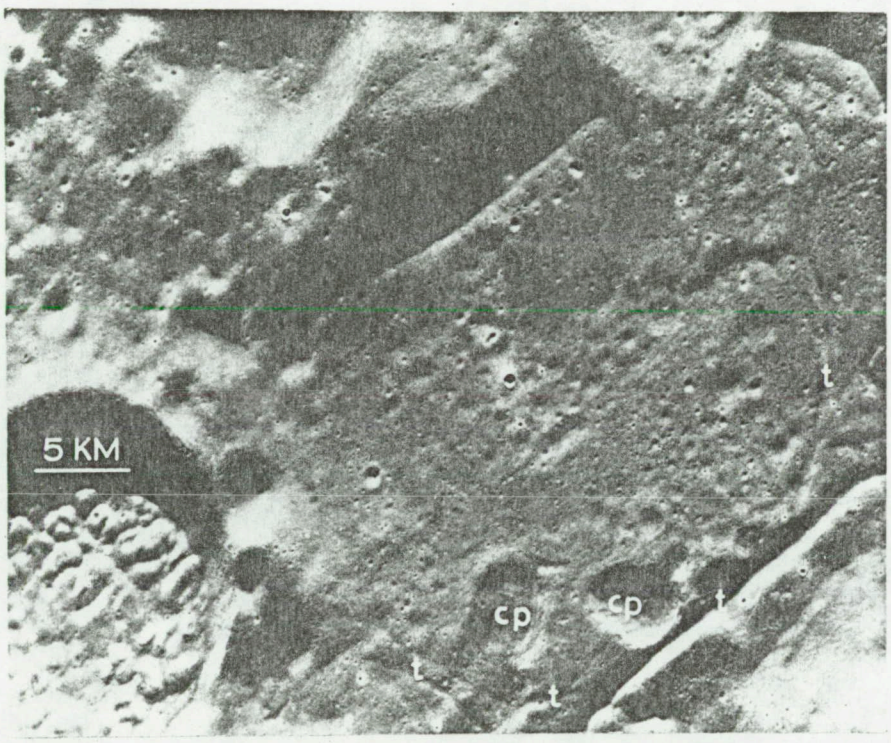

Figure 20. Collapse pits (cp) on volcanic terra material. Note also the smooth pools of mare material and the narrow troughs (t) (after Apollo 15 panoramic camera frame AS-15-9960).

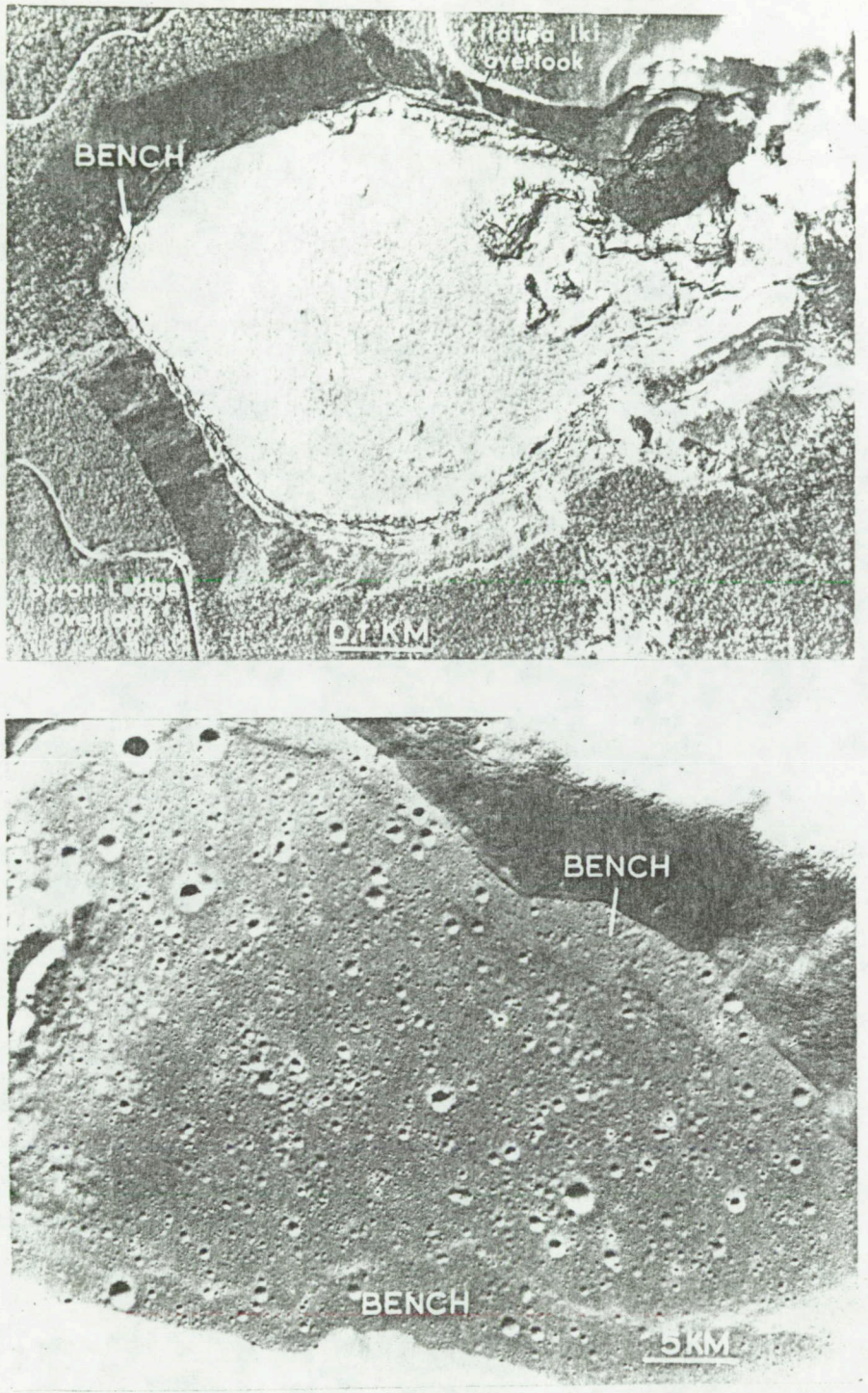

Figure 21. Comparison of Kilauea Iki lava lake (top) and mare lava lake (bottom). Note the subsidence bench around the edge of both lakes (top photo after Richter and others, 1970, p. E11; bottom photo after Apollo 15 panoramic camera frame AS-15-9960).

distance of about 20 km. Its surface is slightly pitted with small craters and has several circular depressions that are interpreted as collapse pits. This material is believed to consist of pyroclastic debris, ash deposits, and perhaps tuff flows expelled from the fissure.

The second type of material forms fairly large rounded hills and mounds on the floor of a nearby crater (lower left corner of Fig. 20). The material has a higher albedo than both the mare and the terra material; this may be the result of steeper slopes or compositional differences. Although no conclusive evidence is present to support a volcanic origin for this material, its location near the mare and its dissimilarity to impact-associated features indicates an endogenic origin, perhaps by upwelling of material from fractures beneath the crater floor. Similar material seen on several Lunar Orbiter photographs is described by Kosofsky and El-Baz (1970, p. 25 and 136) as "bulbous" material.

Lunar volcanic activity is normally associated with basin flooding on a large scale. Extruded material at this site, therefore, is unusual because no basin structure is apparent. The area is marginal to Mare Australe, but is not directly related to any of the mare filling in Australe; however, the possibility that the mare is a late stage eruption site of Australe-related material must be considered.

Two other possibilities also remain: 1) the mare has been extruded at the site of an ancient, completely modified basin; or 2) it is a local extrusion unrelated to any basin structure. Other than the presence of an arcuate ridge near the crater Scaliger and the fact that the area is regionally depressed, there is little evidence to support the hypothesis of an old basin as depicted in Figure 22. A local extrusion unrelated to basin filling seems unlikely, but appears to be a valid hypothesis. Further study of the Australe basin and the mare material flooding much of the basin is necessary to understand any relationship between the mare in the Sklodowska Region and Mare Australe.

Undated Materials

Several types of material have not been assigned an age, even though a maximum age determination is possible. The materials include undulating floor material (fu), hummocky floor material (fh), and landslide material (designated with an arrow to show the direction of movement). In all locales the materials have sufficiently altered the original surface topography to warrant separate map names. The maximum age for any of these materials at any given location is the age of the crater or other material on which it occurs. However, the time required to modify the original topography is unknown. The process is most likely continuous although not

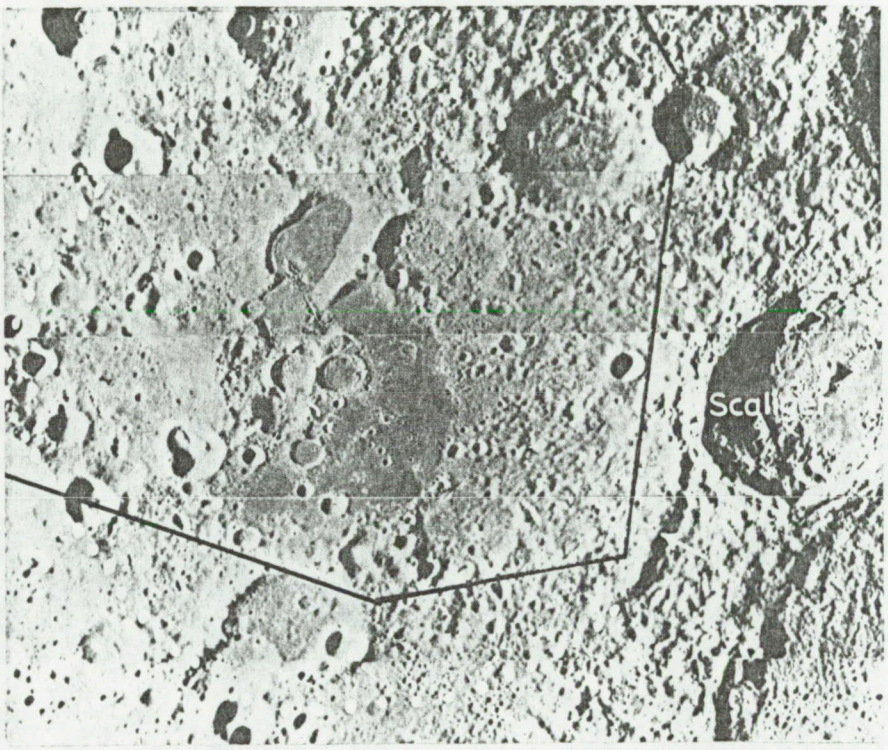

Figure 22. Arcuate ridge near the crater Scaliger (arrow). Possible basin structure outlined by dots has a diameter of 212 km (after Lunar Orbiter II frame 196-M).

necessarily equal in intensity through time (landslide material does not form by this gradual process, but the age of a landslide need be the same as or younger than the material on which it occurs).

Mass wasting processes are thought to be the principal mechanism responsible for the formation of undulating and hummocky floor material. Material on the inner crater slopes apparently moves downslope and accumulates on the crater floor while mixing with other floor material. Blanketing by fine ejecta material also affects the modification process.

Slope creep appears to be one of the more active mass wasting processes and causes the formation of textured slopes (Fig. 23). Trask and Rowan (1967) identify similar slope textures on Lunar Orbiter photographs. They form roughly parallel to obliquely intersecting ridges and furrows and somewhat resemble terrestrial terracettes. Patterned or textured slopes are present on all but the youngest slopes; the greatest development occurs on older slopes.

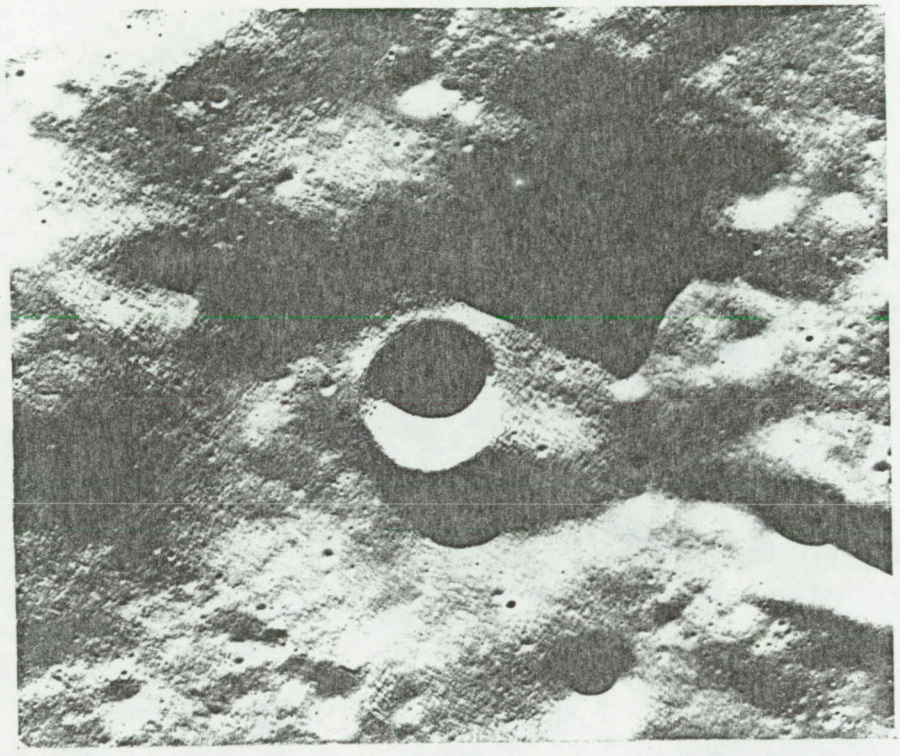

Figure 23. Textured or patterned slopes. Note the absence of textures on more level surfaces. The crater near the center is 3.5 km in diameter (after Apollo 15 panoramic camera frame AS-15-9945).

STRUCTURES AND LINEATIONS

Strom (1964) and Fielder (1963) proposed the existence of a moon-wide structural grid pattern based on the results of independent nearside linear analyses. Their studies showed three general trends of linears, elongated central peaks, and polygonal crater rim sections: northeast, northwest, and north-south. A similar study by Offield (1966) resulted in only one major trend coincident to those of Strom and Fielder, approximately on the north-south axis.

Little evidence exists in the Sklodowska Region that would strongly support a structural grid, although the previously mentioned channeling of the north and south inner crater slopes may be the result of major but subdued structural control. Most lineations are relatively short features usually formed by alternating ridges and grooves on the ejecta deposits surrounding large craters. In this study, most lineations were associated with the craters Sklodowska, Scaliger, Schorr, and Humboldt (refer to Plate 3). Since most of the lineations are radial or sub-radial to these craters, it appears that erosion by ejecta gouging is the primary cause of linears. However, D. J. Scott (pers. comm.) feels that many of the linears are parallel in various segments around the crater and reflect structural control according to a grid system. Similar parallel fracture patterns have been found around Orientale Basin (D. H. Scott, pers. comm.).

A linear scarp north of Sklodowska, well over 150 km in length and approximately 1 km in height, is a prominent structural feature in the region (see Plate 1). Its origin is uncertain, but at least three possibilities may be entertained: 1) the scarp may be related to the outermost Smythii Basin ring; 2) it may represent a remnant terrace scarp, similar to the one in Sklodowska, of an old crater; or 3) it may be a fault scarp with the relative down-dropped block to the west. Some combination of two or more of these possibilities could be considered as a fourth hypothesis.

The southern part of the scarp appears to be definitely related to the Smythii Basin ring, in which case the northern part of the scarp may be a separate feature and the queried section eliminated. This seems to be the most reasonable explanation for the feature although it does not account for the northern part of the scarp. The other two possibilities are doubtful, since the scarp has a relatively fresh appearance that would not be expected for an ancient crater terrace. Also, no remnants of such a crater can be found elsewhere, although the topography has been considerably altered by cratering events. Faulting is also unlikely unless it is related to the Smythii basin-forming event.

CORRELATION OF MORPHOMETRIC PROPERTIES OF CRATERS

Morphometry is the quantitative study of shape and can be used to complement photointerpretation in analyzing lunar craters.

Pike (1973) examined morphometric properties of twenty-five farside craters, including Sklodowska and other craters in the Sklodowska Region (Table 1). When the three morphometric criteria of rim height/crater diameter, rim height/crater depth, and outer-rim width/diameter for these and other craters in the region (Table 2) are plotted on log-log plots (Pike, 1972), the craters are found to follow the linear relationship of nearside normal lunar craters and terrestrial impact and explosion craters, and define a separate field from calderas, volcanic cones, and other volcanic landforms (Figs. 24 to 26).

Pike (loc. cit., p. 43) states that the linear relationship infers that "two or more sets of phenomena within the same general taxonomic group are said to be geometrically similar -- and are inferred to have formed under like physical conditions . . ." The fact that the craters in the Sklodowska Region follow the linear relationship for impact, explosion, and nearside craters suggests that they are also of impact origin. Because most other craters in the region are morphologically similar to those measured, it can be interpreted that most craters in the area are of impact or similar origin.

Name or location	Rim diameter, km	Outer-rim width, km	Floor diameter, km	Inner-rim width, km	Depth, m	Outer-rim height, m	Inner-rim slope, deg	Outer-rim slope, deg	Circularity[a]
In Sklodowska	1.6	0.4	–	0.8	300	95	20.6	13.4	0.90
In Sklodowska	2.8	.5	–	1.4	550	125	21.5	14.0	.88
In Hirayama	3.5	1.0	–	1.7	500	175	16.2	9.9	.84
In Curie	4.3	.9	–	2.1	600	175	15.8	11.0	.64
In Tsiolkovsky	4.9	1.0	–	2.4	950	100	21.3	5.7	.73
In Hilbert	6.0	1.0	–	3.0	950	150	17.6	8.5	.79
In Pasteur[b]	9.9	1.8	2.8	3.6	1100	105	17.2	3.3	.79
In Saha[b]	15.7	3.6	9.0	3.4	880	280	14.7	4.4	.80
In Gagarin	16.0	3.5	10.0	3.0	1350	650	24.2	10.5	.90
In Gagarin	17.0	4.5	6.0	5.5	1700	450	17.2	5.7	.89
In Hilbert	17.0	3.0	5.0	6.0	1800	400	16.7	7.6	.79
On western rim of Gagarin	26.0	6.0	13.0	6.5	2600	725	21.8	6.9	.86
Izsak	33.2	7.7	13.0	10.1	3400	1025	18.6	7.6	.86
Gilbert M	34.0	5.5	18.0	8.0	3100	850	21.2	8.8	.84
Gansky	44.0	12.0	22.0	11.0	3550	950	17.9	4.5	.78
South of Saha	50.5	13.3	24.0	13.3	3640	1380	15.4	5.9	.83
Schorr	53.5	13.0	26.0	13.8	3700	730	15.1	3.2	.77
Ritz	59.0	15.5	24.0	17.5	3750	1800	12.1	6.6	.71
King	71.0	17.0	40.0	15.5	3830	1690	13.9	5.7	.80
Langemak[b]	110.0	17.0	60.0	25.0	4370	880	9.9	3.0	.68
Sklodowska	128.0	18.0	83.0	22.5	4500	1850	11.3	5.9	.78
Curie[b]	158.0	29.0	100.0	29.0	3850	1500	7.5	2.9	.73
Hilbert	178.0	35.0	125.0	26.5	4100	1500	8.8	2.5	.80
Tsiolkovsky	190.0	40.0	140.0	25.0	4700	1750	10.7	2.5	.83
Gagarin[b]	275.0	43.0	200.0	37.5	5375	(3350?)	8.2	(4.5?)	.79

[a]Ratio of areas of circles inscribed and circumscribed on rim-crest outline.
[b]Older appearing craters.

Table 1. Morphometric properties of farside craters (after Pike, 1973). Craters marked with a dot are present in the Sklodowska Region.

Crater Name or Location	Crater Diameter (KM)	Outer-Rim Width (KM)	Rim Height (M)	Crater Depth (M)
1. Sklodowska*	128.0	18.0	1850	4500
2. Brunner	53.6	14.5	1180	2943
3. Schorr*	53.5	13.0	730	3700
4. Curie*	158.0	29.0	1500	3850
5. Backlund	76.5	11.4	1960	2510
6. Perelman	53.4	9.1	1040	1900
7. Ritz*	59.0	15.5	1800	3750
8. "A"	4.7	1.7	275	830
9. "B"	24.3	4.0	830	1810
10. "C"	16.1	3.8	720	1900
11. "D"	10.9	2.9	375	1300
12. "E"	18.8	3.8	545	2180
13. 97°E, 10°S	46.6	8.0	1020	2740
14. 88°E, 18°S	28.8	5.0	375	2240
15. 101°E, 18°S	22.0	4.5	465	1490
16. 101°E, 19°S	24.9	4.5	655	1590

* Measurements from Pike, 1973

Table 2. Morphometric properties for 16 farside craters located in the Sklodowska Region.

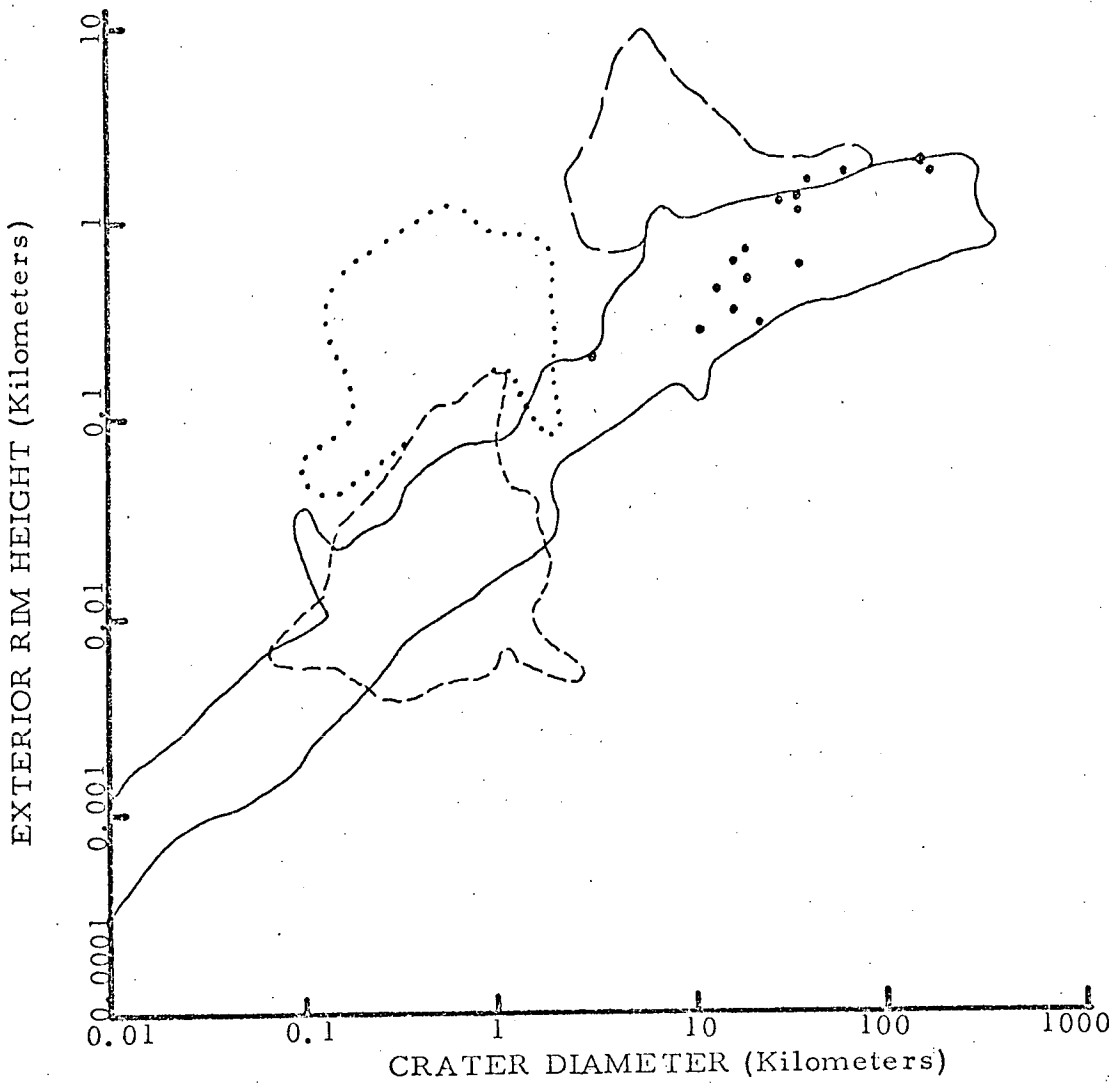

Figure 24. Plot of Exterior Rim Height/Crater Diameter.

Figures 24-26 after Pike (1972). Solid line encloses area for normal lunar craters, experimental explosion craters, and meteorite impact craters; short dashes enclose area of maars and other volcanic explosion craters; dots enclose area of cinder cones and summit craters on lunar domes; long dashes enclose area of terrestrial calderas and volcanic sinks. Large dots are the plots of 16 craters from the Sklodowska area (see Table 2).

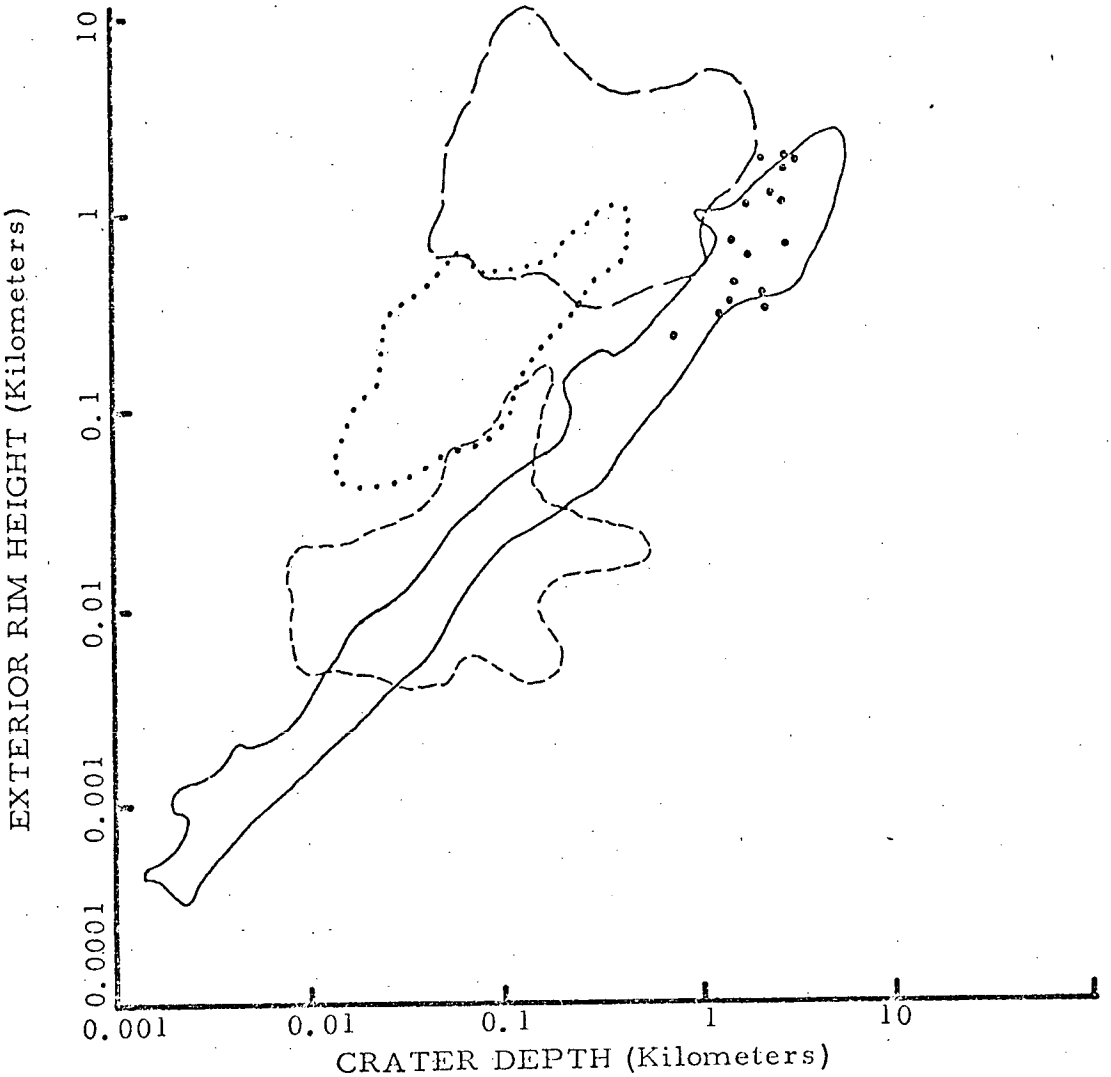

Figure 25. Plot of Exterior Rim Height/Crater Depth.

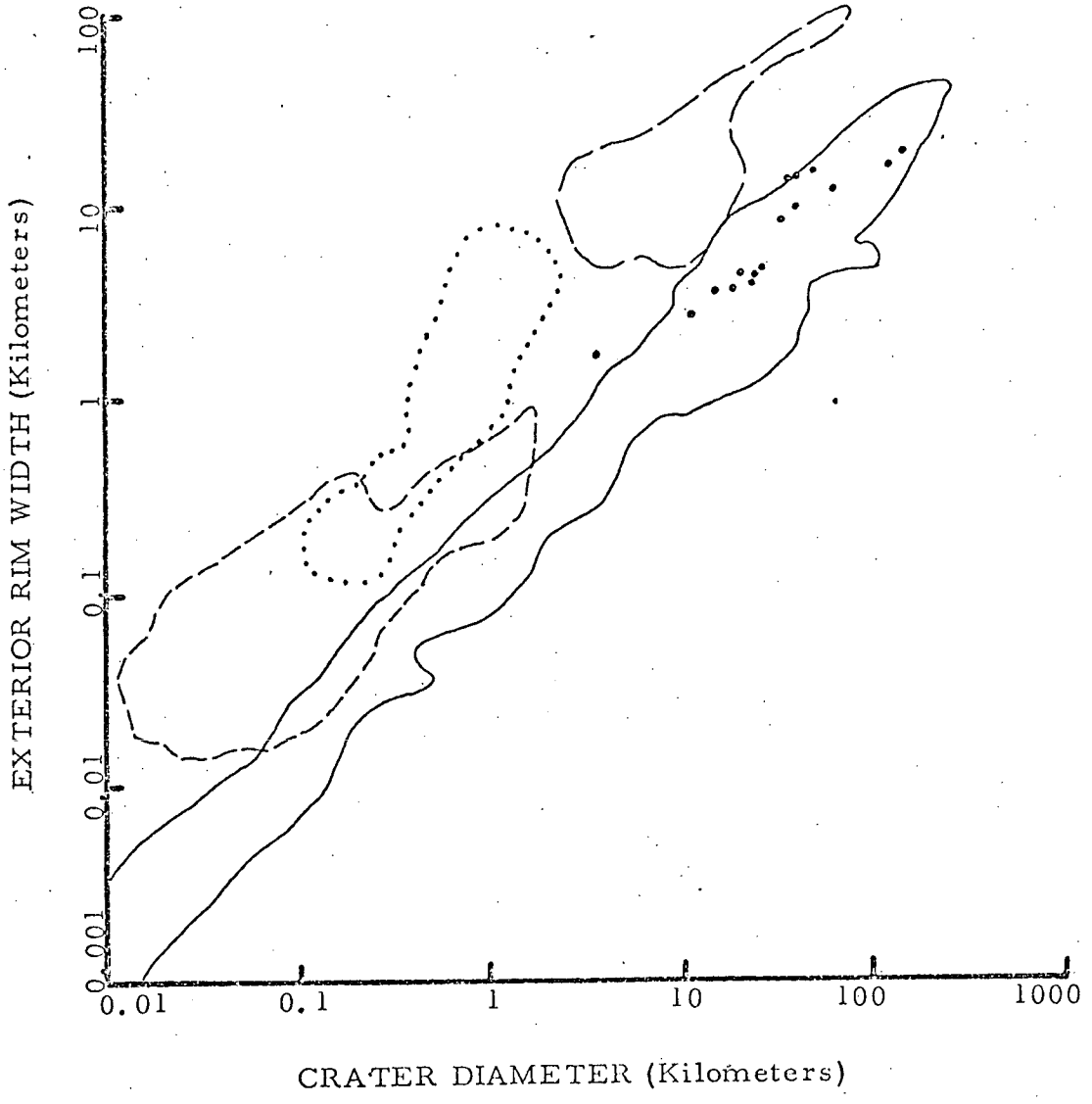

Figure 26. Plot of Exterior Rim Width/Crater Diameter.

COMPARISON OF STATISTICAL RESULTS

Statistical analyses performed are for correlation purposes only, and are not a major aspect of this study. Results are compared to previous works or to interpretations based on visual observations of this study in order to support statements and interpretations, and are not by themselves conclusive evidence confirming or rejecting any hypothesis.

Crater Size/Frequency Determination

Dodd, Salisbury, and Smalley (1963) determined crater size/cumulative frequency relationships for ten areas on the nearside in an attempt to interpret relative age sequences for various units. The following Table lists their calculated values for A and B in the equation: $F = AD^B$, where F is the cumulative number of craters per 10^6 km^2, D is the crater diameter, A is the Y-intercept, and B is the slope of the regression line. Values of A and B calculated for the Sklodowska Region are listed at the bottom of the Table.

As can be seen in the table, values of A and B derived for the Sklodowska Region are similar to those found by Dodd, Salisbury, and Smalley for the nearside Central Crater Province, an old, highly cratered surface. Although the value of B is less for the Sklodowska Region, the two slopes are essentially parallel (Fig. 27);

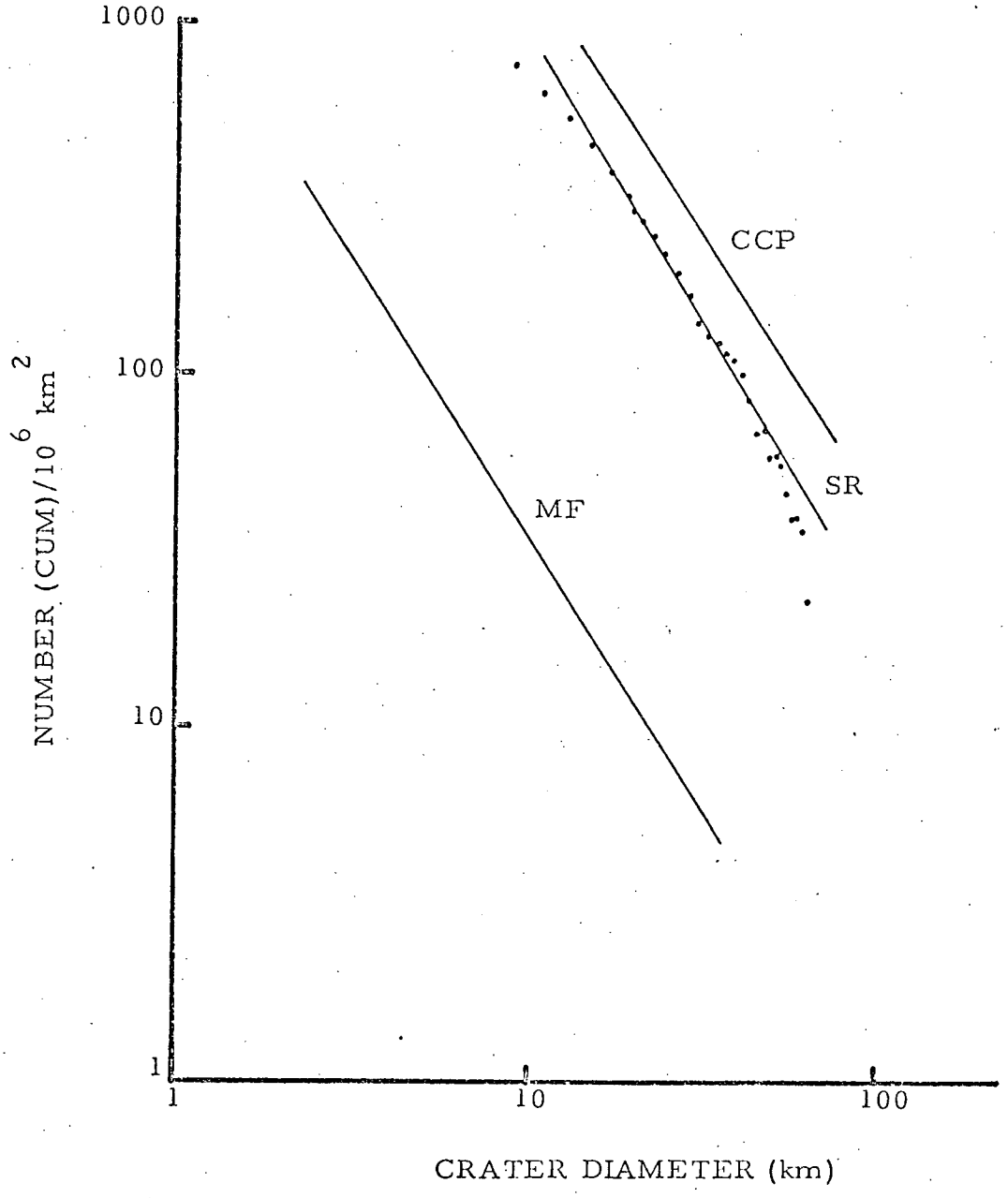

Figure 27. Cumulative crater frequency as a function of crater diameter. Data and computed curve for the Sklodowska Region (SR) are shown as are computed curves, after Dodd, Salisbury and Smalley (1963), for Mare Frigoris (MF) and the Central Crater Province (CCP).

AREA	A	B($\log_{10}$)	R^2
Mare Frigoris	1299.0	-1.545	0.969
Mare Serenitatis	641.7	-1.707	0.977
Light portion	561.6	-1.702	0.959
Dark portion	581.2	-1.535	0.939
Northern Mare Imbrium	1,172.6	-1.776	0.985
Appenninian debris	9,661.8	-2.103	0.989
Central Crater Province	49,687.0	-2.085	0.943
Ptolemaeus	5,072.3	-2.188	0.961
NE of Copernicus	488,317.0	-4.804	0.956
SE of Copernicus	439,110.0	-4.629	0.918
Sklodowska Region	42,490.0	-1.678	0.967

the slightly lower value of A may indicate that the Sklodowska Region is slightly younger than the Central Crater Province. If this age difference is real, it may be the result of rejuvenation of much of the surface in the Sklodowska Region by the deposition of ejecta material from Sklodowska and other Late Imbrian craters in or near the area. Mare Frigoris represents the nearside maria on Figure 27 and demonstrates the use of the frequency/diameter relationship to determine relative ages; that is, the rather large shift of the line for Mare Frigoris to the left indicates that it is considerably younger than either the Central Crater Province or the Sklodowska Region.

Relative Age/Rate of Cratering Determination

Visual observations of the craters in the Sklodowska region agree with Hartmann's conclusions (Hartmann, 1966) that cratering was more intense during the early stages of lunar history than in the

later stages, i.e., prior to basin filling by mare basalts. Basin filling occurred roughly 3.5 billion years b.p., and most mare units are mapped as Imbrian in age (Wilhelms and McCauley, 1971). Therefore it can be reasoned that most craters were formed by 3.5 billion years b.p., or by Middle Imbrian. Assuming this hypothesis is correct, then there should be a noticeable decline in the number of craters in the young relative morphologic age classes.

Three main points have resulted from this aspect of the study: 1) there has been a decline in the rate of cratering through lunar history and most of the craters were formed by a relative morphologic age of 4.0; 2) the overall average size of the craters has decreased through lunar time; and 3) morphologic age can be correlated to stratigraphic age.

All craters larger than 8 km in diameter were given a morphologic age and the number of craters in each of seven relative age classes (see Appendix C) were calculated. Figure 28 shows the percentage of craters greater than 8 km in diameter in each relative morphologic age class, and indicates that the great majority (over 84%) are older than an age of 4.0; that is, most craters had formed by a relative age of 4.0, and the rate of cratering declined sharply after that time. Figures 29 to 31 devide the craters into three size categories and show the tendency for small craters to be rela-

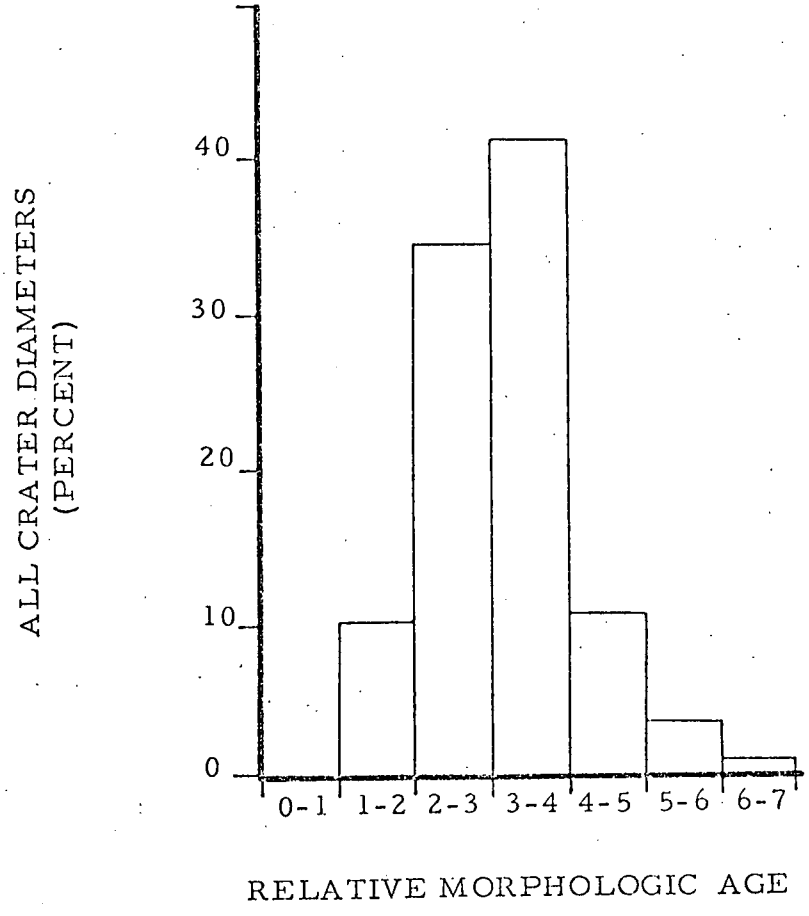

Figure 28. Percentage of craters of all diameters (greater than 8 km) in each relative morphologic age class.

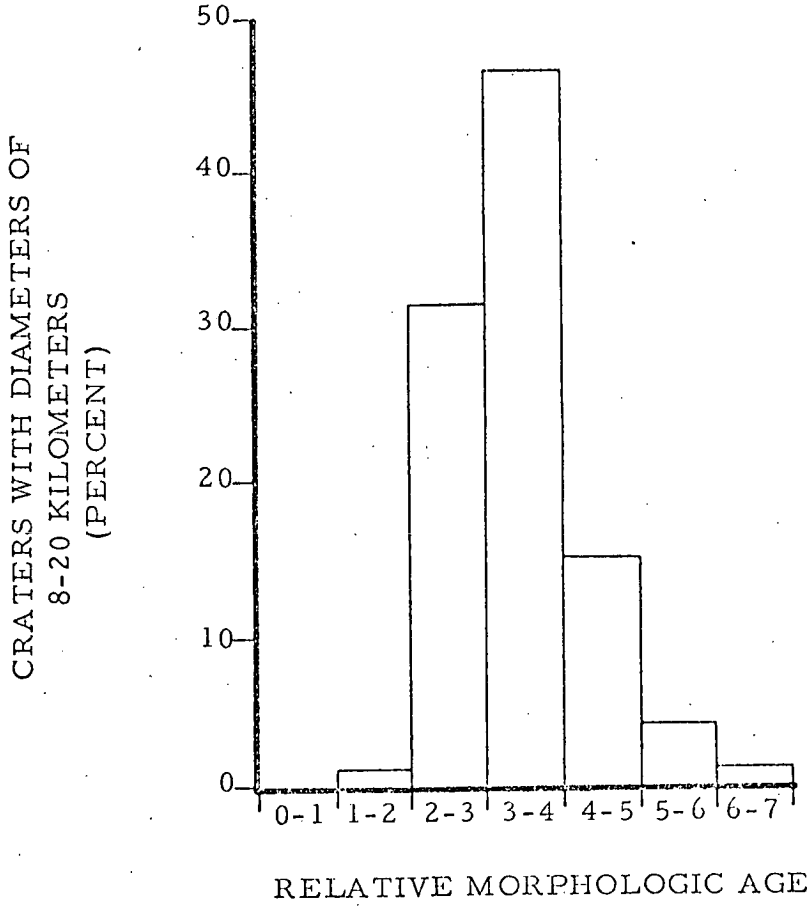

Figure 29. Percentage of craters 8-20 kilometers in diameter in each relative morphologic age class.

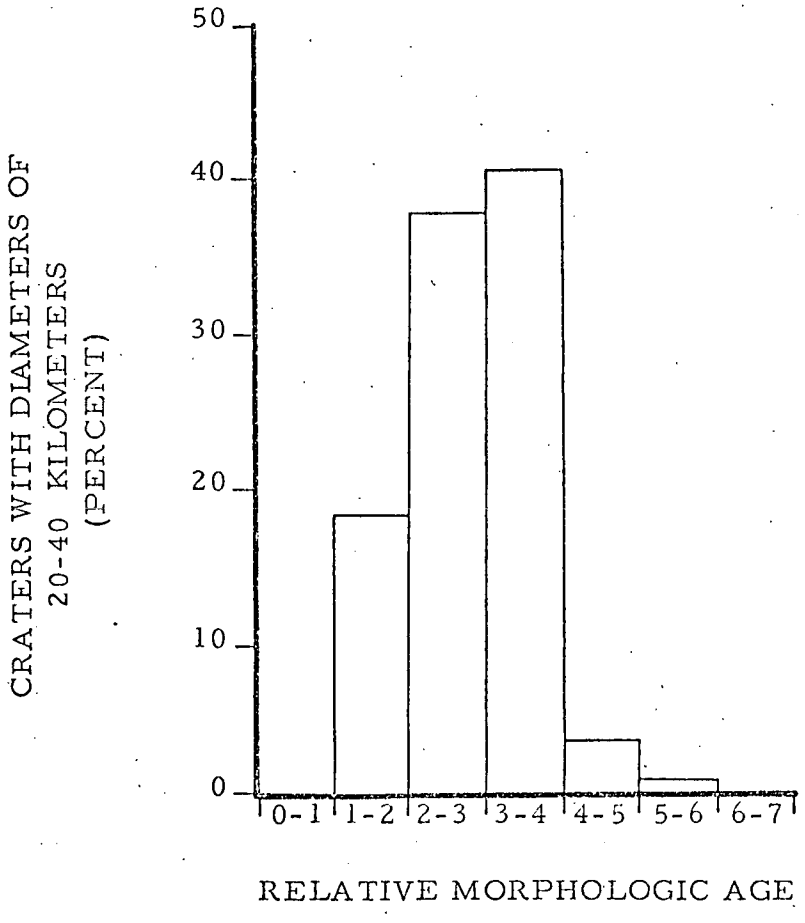

Figure 30. Percentage of craters 20-45 kilometers in diameter in each relative morphologic age class.

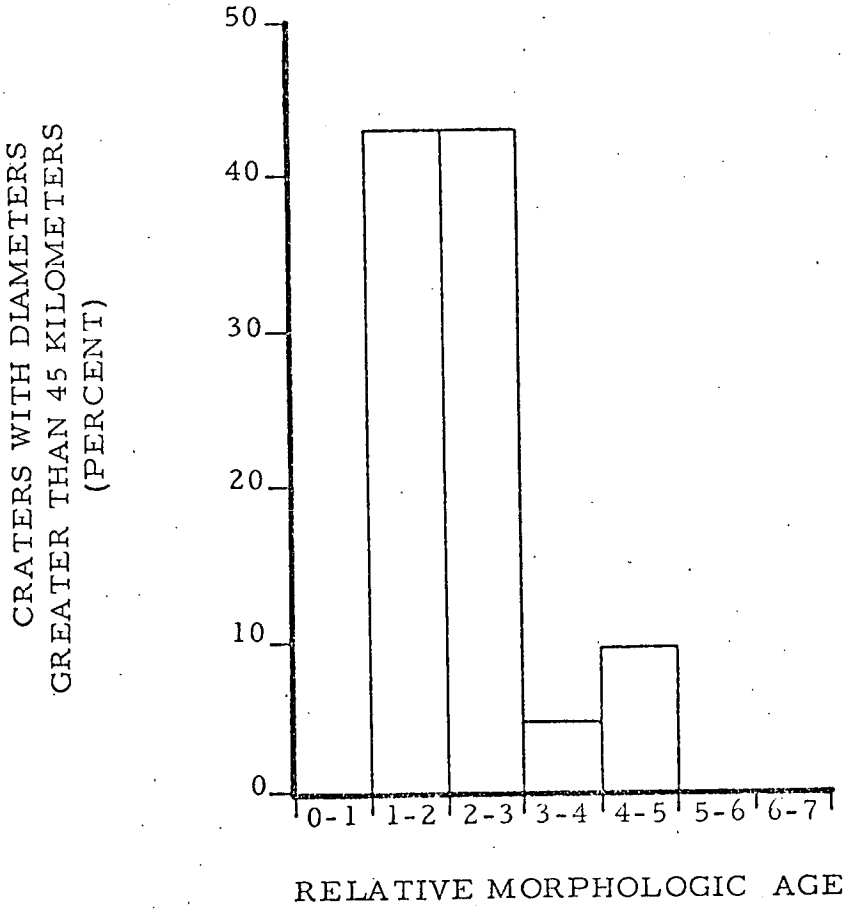

Figure 31. Percentage of scraters greater than 45 kilometers in diameter in each relative morphologic age class.

tively young and the larger craters to be relatively old. Therefore, not only has the rate of cratering declined through time, but also the size of the impacting mass and therefore the crater size decreased.

Baldwin (1974) concludes that the moon accreted from planetesimals, that most of the earliest planetesimals were very small, and that larger planetesimals, such as those that formed the large basins, impacted late in pre-mare time; that is, there was a gradual increase in the average size of the masses impacting on the lunar surface in pre-mare time. These conclusions appear to conflict with the statistical results above; however, Baldwin works with crater sizes below 8 km in diameter as well as those above, and is concerned mainly with pre-mare basins. It is not suggested in this report that large numbers of small craters did not form during pre-mare time, but rather that 1) the original number of craters has been vastly reduced because of destruction by younger events and 2) when considering both pre- and post-mare craters, the larger craters tend to be older than the smaller craters.

The destruction of early-formed craters is also indicated by the decline in crater frequency for the older morphologic ages (0.0 to 3.0), since the frequency should increase if cratering was intense in early lunar time. Although this could be used as evidence against

early intense cratering, Hartmann (1966), and various authors since, have presented convincing evidence in support of early intense cratering.

The morphologic age of craters and the stratigraphic age can be correlated by determining the morphologic age range for craters in each time-stratigraphic division (on the geologic map) as shown in Figure 32. Using this method of correlating morphologic and stratigraphic ages, it can again be estimated that the rate of cratering drastically declined after a morphologic age of 4.0, although several large craters that formed later, such as Sklodowska, Schorr, and Scaliger (ages 4.5, 4.5 and 5.0 respectively), considerably modify the surface topography.

A chi-square test was also performed to test whether the null hypothesis, H_0, stated as "the proportion of craters in each age class is the same for each crater size class", is to be accepted or rejected.

Chi-square is expressed by the following simplified equation:

$$\chi^2 = \sum \frac{(Y - E)^2}{E}$$

where Y is the observed value and E is the expected value. The following chi-square contingency table lists the observed and expected values used to determine chi-square. Expected values are derived by the following equation:

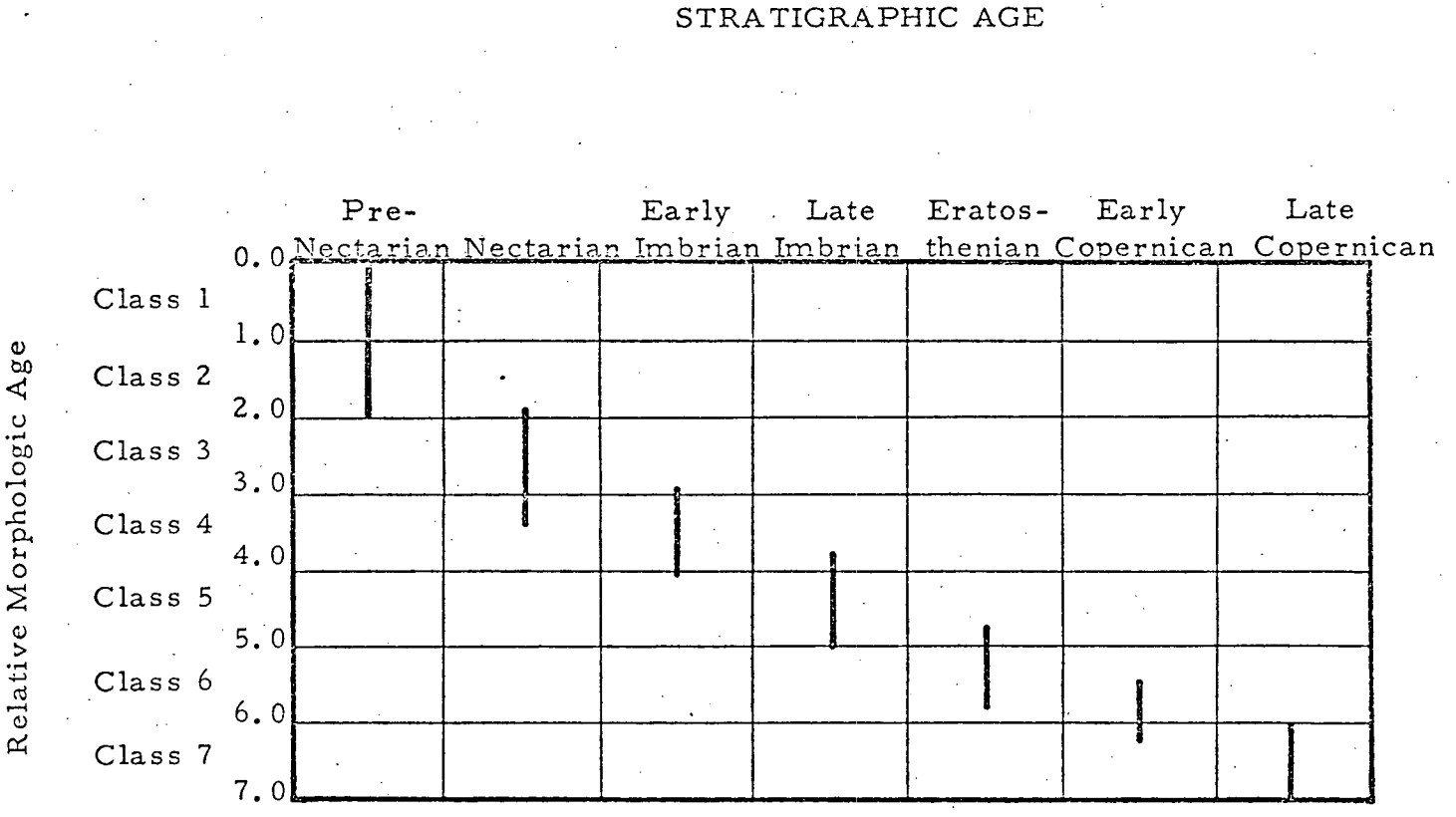

Figure 32. Correlation of relative morphologic ages to stratigraphic ages.

$$E = \frac{RC}{N}$$

where R is the total number of observations in a row, C is the total number of observations in a column, and n is the sample size (= total number of craters = 223). For a complete discussion of the chi-square procedure, the reader is referred to Huntsberger (1967), p. 240-245.

CHI-SQUARE CONTINGENCY TABLE

Crater Size	Relative Morphologic Age						
	Classes 1&2		Class 3		Classes 4 & above		Total
	Y	E	Y	E	Y	E	Y
Rank 1 (8-20 km)	2	13.8	44	47.7	94	78.8	140
Rank 2 (20-45 km)	11	6.1	23	21.1	28	34.8	62
Rank 3 (45 km)	9	2.1	9	7.2	3	11.8	21
TOTAL Y	22		76		125		223

Solving the equation for chi-square with 4 degrees of freedom, a value of 48.56 is obtained. Chi-square at the 1% confidence level and 4 degrees of freedom = 13.28 (Rohlf and Sokal, 1969, p. 165). Therefore, since 48.56 is much greater than 13.28, H_o is rejected and it is determined that the proportion of craters in each relative age class is <u>not</u> the same for each crater size. More specifically, there are fewer young craters for large crater sizes and fewer old

craters for small crater sizes. These results agree with visual observations and with the interpretations of the histograms in Figures 28 and 31.

In a further test of the relative age/crater diameter relationship, a weak but significant negative correlation (-0.45118) was obtained for log age vs. log diameter. This again indicates that there is a tendency for the large craters to be older than the small craters.

GEOLOGIC HISTORY

The geologic history of this region can be reconstructed on the basis of stratigraphic relationships, superposed and subjacent craters, crater morphology, and correlation to previous interpretations, especially those pertaining to continental highlands such as are found in the southern hemisphere of the nearside.

A period of intense cratering during the early stages of lunar history, as recognized by Kuiper (1954) and Hartmann (1965;1966), is evident in the Sklodowska Region. Relatively closely-spaced, large pre-Nectarian craters form the "background" topography. These craters are abundant for diameters between 30 and 150 km. Because of their relative old age and erosion by younger events, pre-Nectarian craters do not display mappable rim deposits.

Nectarian craters are also relatively abundant, although the range in diameter is slightly lower. They are often superposed on pre-Nectarian craters, and their ejecta deposits form plains material on the floors of some large pre-Nectarian craters.

Craters less than 10 km in diameter are absent for pre-Nectarian and Nectarian ages. It is assumed that they were also abundant but have been preferentially destroyed by younger impacts and ejecta blanketing.

Imbrian events were less catastrophic than previous episodes;

early Imbrian craters decrease in abundance and again in size range. Ejecta from these craters added substantial amounts of material to the developing terrae and plains units, and probably caused the destruction of most of the pre-Imbrian craters smaller than 10 km.

Cratering descreased substantially by Late Imbrian as evidenced by the low density of Late Imbrian craters. However, the ejecta deposits of large craters, such as Sklodowska, Scaliger, and Humboldt, caused extensive modification of the former topography. Additional plains units, formed about this same time, are thought to be the result of deposition of material ejected from these large craters in the form of a base surge.

The rate of cratering continued to decline through Eratosthenian and Copernican time. Craters of both ages have caused little modification of the surface except on a local scale. Small, bright haloed Copernican craters dot the surface on all but the steepest slopes where they have been quickly eroded and destroyed by down-slope movement of material.

Extrusion of the mare suite occurred during Middle to Late Eratosthenian along a linear fissure. It is unknown whether the extrusion is related to mare-filling of Mare Australe or whether it is an isolated tectonic-volcanic event.

Slope creep, slumping, and other gravity driven erosion, trans-

portation, and deposition processes were operative throughout lunar history, continually destroying small craters and slowly modifying large craters. Other processes acting to modify and subdue the topography include meteorite and micrometeorite impacts, ejecta deposition (blanketing), seismic shock, and limited volcanic activity.

SUMMARY

The Sklodowska Region has a history similar to other cratered regions of the moon. Statistical and morphologic criteria indicate that most of the surface materials were formed by impact and were later modified by younger impacts and other erosion processes. Volcanism was not an active process in the region except for a small area where a suite of volcanic materials were expelled along a fissure. Regional structural control of lineations is possible, but no conclusive evidence was found to support a lunar grid fracture system. Most lineations appear to be the result of ejecta gouging of the unconsolidated surface material caused by material ejected during large impacts. Mass wasting processes, ejecta blanketing, and meteorite and micrometeorite impacts have continually modified the surface; mass wasting and micrometeorite impact erosion are probably still active.

REFERENCES CITED

Aeronautic Chart and Information Center, 1971, Lunar Planning Chart, 1st ed.: NASA LOC-3.

Alder, J.E.M., and Salisburg, J.W., 1969, Circularity of lunar craters: Icarus, v. 10, p. 37-52.

Baldwin, R.B., 1949, The face of the Moon: Chicago, Univ. Chicago Press, 239 p.

----------, 1963, The measure of the Moon: Chicago, Ill., Univ. Chicago Press, 488 p.

----------, 1964, Lunar crater counts: Astron. Jour., v. 69, no. 5, p. 377-392.

----------, 1974, on the accretion of the earth and moon: Icarus, vol. 23, no. 1, p. 97-107.

Cameron, W.S., and Niksch, M.A., 1972, Data Users' Note, Apollo 15 Lunar Photography: National Space Science Data Center NSSDC 72-07, Greenbelt, Md., 33 p. plus indicies.

Cohen, A.J., 1961, Megashatter cone hypothesis of the origin of lunar volcanoes: Nature, vol. 192, p. 346.

Dodd, R.T., Jr., Salisbury, J.W., and Smalley, V.B., 1963, Crater frequency and the interpretation of lunar history: Icarus, v. 2, no. 5-6, p. 466-480.

Eggleton, R.E., 1965, Geologic map of the Riphaeus Mountains Region of the Moon: U.S. Geol. Survey Misc. Geol. Inv. map I-458.

Eggleton, R.E. and Schaber, G.G., 1972, Cayley Formation interpreted as basin ejecta: Apollo 16 Prelim. Sci. Report, NASA SP-315.

El-Baz, Farouk, 1969, Crater characteristics: Section 2, Analysis of Apollo 8 Pholography and Visual Observations, NASA SP-201, p. 21-29.

----------, 1970 Lunar igneous intrusions, Sci., v. 167, p. 49-50.

----------, 1972, King Crater and its environs: Apollo 16 Prelim. Sci. Rept., NASA, Washington, D.C., p. 29-62 to 29-70.

El-Baz, Farouk and Worden, A.M., 1972, Visual observations from lunar orbit: Apollo 15 Prelim. Sci. Rept., Section 25, Part A, NASA SP-289, p. 25-1 to 25-27.

Erlich, E.N., Gorshkov, G.S., Melekestsev, I.V., and Steinberg, G. S., 1970, The Structure of the lunar crater Tsiolkovsky: Modern Geology, vol. 1, p. 197-201.

Fielder, Gilbert, 1961, Structure of the Moon's surface: New York, Pergamon, 266 p.

----------, 1963, Lunar tectonics: Geol. Soc. London Quart. Jour., v. 119, no. 473, pt. 1, p. 65-69.

----------, 1965, Lunar Geology: London, Butterworth Press, 184 p.

Freeberg, J.H., 1970, Bibliography of the Lunar surface: Washington, D.C., U.S. Dept. of Interior, 344 p.

Guest, J.E., and Murray, J.B., 1969, Nature and Origin of Tsiolkovsky Crater, lunar farside: Planet Space Sci., v. 17, p. 121-141.

Hackman, R.J., and Mason, A.C., 1961, Engineer special study of the surface of the Moon: U.S. Geol. Survey Misc. Geol. Inv. map I-351 (3 maps and expl.).

Hartmann, W.K., 1964, On the distribution of lunar crater diameters: Arizona Univ. Lunar & Planetary Lab. Comm., v. 2, no. 38, p. 197-203.

----------, 1966, Early lunar cratering: Icarus, v. 5, p. 406-418.

----------, 1967, Lunar Crater counts II -- Three lunar surface type-areas: Ariz. Univ. Lunar & Planet. Lab. Comm., v. 6, no. 81, p. 39-41.

----------, 1968, Lunar crater counts III -- Postmare and Archinedian variations: Ariz. Univ. Lunar & Planet. Lab. Comm., v. 7, no. 116, p. 125-129.

Hartmann, W.K., and Yale, G.F., 1968, Lunar Crater counts IV -- Mare Orientale and its basin system: Ariz. Univ. Lunar & Planet. Lab. Comm., v. 7, no. 117, p. 131-137.

Head, J.W., 1972, Small-scale analogs of the Cayley Formation and Descartes Mountains in impact-associated deposits: Sec. 29, Part C, Apollo 16 Prelim. Sci. Reports, NASA SP 315, p. 29-16 to 29-20.

Hixon, S.B., 1968, Topographic and Geologic aspects of a farside lunar crater: Science, v. 159, no. 3813, p. 420-421.

Hodges, Carroll Ann, 1973, Geologic Map of the Langrenus Quadrangle of the Moon: U.S. Geol. Survey Misc. Geol. Inv. map I-739.

Howard, K.A., 1972, Ejecta Blankets of large craters exemplified by King Crater: Apollo 16 Prelim. Sci. Rept., NASA, Washington, D.C., p. 29-70 to 29-77.

Howard, K.A., and Offield, T.W., 1968, Shatter cones at Sierra Madera, Texas: Science, v. 162, no. 3850, p. 261-265.

Huntsberger, D.V., 1967, Elements of statistical inference: Allyn and Bacon, Inc., Boston, Mass., p. 240-245.

Kosofsky, L.J., and El-Baz, Farouk, 1970, The moon as viewed by Lunar Orbiter: Washington, D.C., NASA SP-200, p. 25 and p. 136.

Lunar Sample Preliminary Examination Team, 1969, Preliminary Examination of lunar samples from Apollo 11: Science, v. 165, no. 3899, p. 1211-1227.

Lunar Sample Preliminary Examination Team, 1971, Preliminary Examination of lunar samples from Apollo 15: Science, v. 173, no. 2998, p. 681-693.

Lunar Sample Preliminary Examination Team, 1972, Preliminary Examination of lunar samples: Apollo 15 Prelim. Sci. Rept., NASA SP-289, sec. 6, p. 6-1 to 6-25.

Miyamoto, S., 1968, Morphological study of the lunar crust: Icarus, v. 9, no. 2, p. 373-390.

Moore, H. J., 1972, Ranger and other impact craters photographed by Apollo 16: Apollo 16 Prelim. Sci. Rept., sec. 29, part J, NASA SP-315, p. 29-45 to 29-50.

----------, 1966, The 1965 Eruption of Taal Volcano: Science, v. 151, no. 3713, p. 955-960.

Morris, E. C., and Shoemaker, E. M., 1968, Craters: Part II, Surveyor Project Final Report, JPL-TR-32-1265, p. 65-68.

Murray, J. B., 1971, Sinuous rilles, in Geology and physics of the Moon, G. Fielder, ed.: Elsevier Publishing Company, Amsterdam, p. 27-39.

Mutch, T. A., 1970, Geology of the Moon -- a stratigraphic view: Princton, N. J., Princton Univ. Press, 324 p.

Oberbeck, V. R., Morrison, R. J., and Wedekind, John, 1972, Lunar Secondary Craters: Part K, Apollo 16 Prelim. Sci. Rept., NASA SP-315, p. 29-51 to 29-56.

Offield, T. W., 1966, Structure of the Treisnecker - Hipparchus region, in Astrogeol. Studies Ann. Prog. Rept., July 1965- July 1966, Pt A: U.S. Geol. Survey open-file report, p. 133-154.

Offield, T. W., and Pohn, H. A., 1970, Lunar crater morphology and relative age determination of lunar geologic units, part 2, Application: Geol. Survey Research 1970, U.S.G.S. Prof. paper 700-C, p. C163-C169.

Opik, E. J., 1960, The lunar surface as an impact counter: Monthly Notices Royal Astron. Soc., v. 120, no. 5, p. 404-411.

Palm, Ann, and Strom, R. G., 1963, The craters in the lunar walled plain Ptolemaeus: Planet. Space Sci., v. 11, p. 125-134.

Pike, R. J., 1971a, Genetic implications of the shapes of martian and lunar craters: Icarus, v. 15, p. 384-395.

----------, 1971b, Height-depth ratios of lunar and terrestrial craters: Nature Phys. Sci., v. 234, p. 56-57.

----------, 1972, Geometric Similitude of lunar and terrestrial craters: sec. 15, Proceedings of 24th International Geological Congress (Montreal), p. 41-47.

----------, 1973, Lunar Crater Morphometry: sec. 32, part A, Apollo 17 Prelim. Sci. Rept., NASA SP-330, p. 32-1 to 32-7.

Pohn, H.A., and Offield, T.W., 1970, Lunar crater morphology and relative age determination of lunar geologic units, part 1, classification: Geological Survey Research 1970, U.S.G.S., Prof. Paper 700-C, p. C153-C162.

Quaide, W.L., Gault, D.E., and Schmidt, R.A., 1965, Gravitative effects on lunar impact structures, in Whipple, H.E., ed., Geologic problems in lunar research: New York Academy of Sci. Ann., v. 123, Art. 2, p. 563-572.

Ray, R.G., 1960, Aerial photographs in geologic-interpretation and mapping: U.S. Geol. Survey Prof. Paper 373, p. 50-55.

Richter, D.H., Eaton, J.P., Murata, K.J., Ault, W.U., and Krivoy, H.L., 1970, Chronological narrative of the 1959-60 eruption of Kilauea volcano, Hawaii: U.S.G.S. Prof. Paper 537-E, 73 p.

Rohlf, F.J., and Sokal, R.R., 1969, Statistical tables: W.H. Freeman and Co., San Francisco, p. 165.

Ronca, L.B., 1971, Ages of lunar mare surfaces: Geol. Soc. Amer. Bull., v. 82, p. 1743-1748.

Ronca, L.B., and Salisbury, J.W., 1966, Lunar history as suggested by the circularity of lunar craters: Icarus, v. 5, p. 130-138.

Ross, H.P., 1968, A simplified mathematical model for lunar crater erosion: Jour. Geophys. Research, v. 73, no. 4, p. 1343-1354.

Scott, D.J., 1972, Geologic Map of the Eudoxus Quadrangle of the Moon: U.S. Geol. Survey Misc. Geol. Inv. map I-705.

Scott, D.H., and Pohn, H.A., 1972, Geologic map of the Macrobius Quadrangle of the Moon: U.S. Geol. Survey Misc. Geol. Inv. map I-799

Shoemaker, E.M., and Hackman, R.J., 1962, Stratigraphic basis for a lunar time scale, in Kopal, zdenek, and Mikhailor, Z.K., ed., The Moon -- Intern. Astron. Union Symposium 14, Leningrad 1960 Proc.: New York, Academic Press, p. 289-300.

Smith, E.I., and Sanchez, A.G., 1973, Fresh lunar craters -- morphology as a function of diameter, a possible criterion for crater origin: Modern Geology, v. 4, p. 51-59.

Soderblom, L.A., 1970, A Model for small-impact erosion applied to the lunar surface: Jour. Geophys. Research, v. 75, no. 14, p. 2655-2661.

Soderblom, L.A., and Boyce, J.M., 1972, Relative ages of some near-side and far-side terra plains based on Apollo 16 metric photography: Apollo 16 Prelim. Sci. Rept., Sec. 29, part A, p. 29-3 to 29-6.

Soderblom, L.A., and Lebofsky, L.A., 1972, A technique for rapid determination of relative ages of lunar areas from orbital photography: Jour. Geophys. Res., v. 77, no. 2, p. 279-296.

Spurr, Stephen H., 1948, Aerial photographs in forestry: The Ronald Press Company, New York, p. 98-105.

Steinberg, G.S., 1968, Comparative morphology of lunar craters and rings and some volcanic formations in Kamchatka: Icarus, v. 8, no. 3, p. 387-403.

Strom, R. G., 1964, Analysis of lunar lineaments, I - Tectonic map of the Moon: Ariz. Univ. lunar and planet. Lab. Comm., v. 2 no. 39, p. 205-221.

Strom, R.G., and Fielder, Gilbert, 1968, Multiphase development of the lunar crater Tycho: Nature, v. 217, p. 611-615.

Stuart-Alexander, D.E., and Tabor, R.W., 1972, Geologic map of the Fracastorius Quadrangle of the Moon: U.S. Geol. Survey Misc. Geol. Inv. map I-720.

Trask, N.J., 1971, Geological comparison of mare materials in the lunar equatorial belt, including Apollo 11 and Apollo 12 landing sites: Geol. Survey Res. 1971, U.S. Geol. Survey Prof. Paper 750-D, p. D138-D144.

Trask, N.J., and Rowan, L.C., 1967, Lunar Orbiter photographs -- some fundamental observations: Sci., v. 158, no. 3808, p. 1529-1535.

West, M.N., 1972, Selected volcanic features: Apollo 15 Prelim. Sci. Rept., NASA SP-289, sec. 25, part L, p. 25-81 to 25-83.

Whipple, H.E., ed., 1965, Geologic problems in lunar research: New York Academy of Sciences, Annals, v. 123, art 2, p. 367-1257.

Wilhelms, D.E., 1970, Summary of lunar stratigraphy -- Telescopic observations: U.S. Geol. Sruvey Prof. Paper 599-F, 47 p.

Wilhelms, D.E., and McCauley, J.F., 1971, Geologic map of the near-side of the Moon: U.S.Geol. Survey Misc. Geol. Inv. map I-703.

Wilshire, H.G., and Howard, K.A., 1968, Structural pattern in central uplifts of cryptoexplosion structures as typified by Sierra Madera: Science, v. 162, no. 3850, p. 258-261.

Wilshire, H.G., Stuart-Alexander, D.E., and Jackson, E.D., 1973, Apollo 16 Rocks: Petrology and Classification: JGR, v. 78, no. 14, p. 2379-2392.

Wood, C.A., 1968, Statistics of central peaks in lunar craters: Ariz. Univ. Lunar and Planet. Lab. Comm., v. 7, no. 120, p. 157-160.

APPENDIX A

APPENDIX A

Photographic Data*

Selected photographs from Lunar Orbiter and Apollo missions were used for mapping and interpretive purposes. Plate 4 defines the areas covered by the various types of imagery.

In this appendix, the uses of each type of photograph are discussed followed by an index of frame numbers and other pertinent data.

Lunar Orbiter Photographs

Lunar Orbiter photographic coverage is limited to four images, three high resolution and one medium resolution photographs. The high resolution frames were used to interpret and describe some surface materials. The medium resolution frame was used mainly for geographic orientation and visualization of geologic relationships.

Apollo 15 Photographs

Metric Camera Photographs -- Six flight lines of metric camera sterephotographs were used for construction of the base map, for geologic mapping, and for description and interpretation of geologic units. Forward overlap of the photographs is about 60%; side overlap is about 10-15%. The quality of the frames is excellent with a maximum resolution of about 100-200 meters.

Panoramic Camera Photographs -- Panoramic camera stereophotographs were mainly used to refine descriptions and to check interpretations derived from metric photographs. Extremely fine detail is visible on these images which have a maximum resolution of 2-20 meters. They are also valuable for identifying and interpreting small structures and textures.

70 mm Hasselblad Photographs -- Selected 70 mm Hasselblad frames (negative film) were obtained for illustrative purposes and to assist in the interpretation of certain materials. Maximum resolution is similar to that of the Panoramic photographs.

*Additional information regarding Apollo Mission photographs and photographic instruments is available from the National Space Science Data Center, Greenbelt, Maryland. Further information on Apollo 15 photographs is available in Apollo 15 Lunar Photography Data User's Note (NSSDC, 1972).

METRIC CAMERA PHOTOGRAPHS

All frame numbers preceeded by AS-15-(Rev)-

Frame #	Rev. #	Coordinates of Prin. Pt. Lat.	Long.	Sun Elev. (°) Prin. Pt.	Spacecraft Alt. (km)
1595	38	-13.0	100.3	44.7	118.4
1596		-12.5	99.1	46.0	118.5
1597		-12.0	97.9	47.2	118.5
1598		-11.5	96.7	48.5	118.6
1599		-11.0	95.5	49.7	118.7
1600		-10.5	94.3	51.0	118.8
1601		-10.0	93.1	52.2	118.9
1602		- 9.5	92.0	53.5	118.9
1603		- 9.0	90.8	54.7	118.9
1736	44	-15.3	100.2	38.5	116.8
1737		-14.8	99.0	39.8	116.9
1738		-14.4	97.8	41.0	117.1
1729		-13.9	96.6	42.3	117.2
1740		-13.4	95.4	43.5	117.4
1741		-12.9	94.2	44.8	117.5
1742		-12.4	93.0	46.1	117.6
1743		-12.0	91.8	47.3	117.7
1744		-11.5	90.6	48.6	117.9
1745		-10.9	89.4	49.8	118.0
1868	50	-20.0	105.3	27.3	116.6
1869		-19.6	104.0	28.5	116.7
1870		-19.1	102.8	29.8	116.8
1871		-18.6	101.5	31.0	116.9
1872		-18.1	100.3	32.3	117.0
1873		-17.6	99.1	33.5	117.0
1874		-17.1	97.8	34.8	117.1
1875		-16.6	96.6	36.0	117.2
1876		-16.1	95.4	37.2	117.2
1877		-15.5	94.2	38.5	117.3
1878		-15.0	93.0	39.7	117.4
1879		-14.5	91.9	40.9	117.4
1880		-13.9	90.7	42.2	117.4
1881		-13.4	89.5	43.4	117.5
1960	60	-23.7	96.5	16.8	117.9
1961		-23.2	96.3	18.1	118.0

Frame #	Rev. #	Coordinates of Prin. Pt. Lat.	Long.	Sun Elev. (°) Prin. Pt.	Spacecraft Alt. (km)
1962	60	-22.7	96.1	19.4	118.2
1963		-22.2	95.8	20.6	118.4
1964		-21.7	95.6	21.9	118.5
1965		-21.2	95.4	23.1	118.7
1966		-20.7	95.1	25.4	118.9
1967		-20.2	94.9	26.6	119.0
1968		-19.7	94.7	27.9	119.2
1969		-19.2	93.4	29.2	119.4
1970		-18.7	92.2	30.4	119.6
1971		-18.2	91.0	31.8	119.7
1972		-17.7	89.8	32.9	119.8
1973		-17.2	88.5	34.1	120.0
2354	70	-26.4	109.3	4.7	110.7
2355		-26.2	107.9	5.9	111.0
2356		-25.9	106.6	7.2	111.3
2357		-25.6	105.2	8.4	111.6
2358		-25.3	103.8	9.7	111.8
2359		-25.0	102.4	10.9	112.1
2360		-24.6	101.1	12.2	112.3
2361		-24.3	99.7	13.5	112.6
2625	72	-26.3	106.9	5.1	109.3
2626		-26.0	105.3	6.4	109.6
2627		-25.7	103.8	7.6	109.8
2628		-25.4	102.5	8.9	110.1
2629		-25.2	101.2	10.2	110.3
2630		-24.9	99.9	11.4	110.6
2631		-24.5	98.6	12.6	110.9
2632		-24.2	97.3	13.9	111.2
2633		-23.8	96.0	15.1	111.4
2634		-23.4	94.6	16.4	111.7
2635		-23.0	93.3	17.6	111.9
2636		-22.6	92.0	18.9	112.2
2637		-22.2	90.7	20.1	112.4
2638		-21.8	89.4	21.4	112.6
2639		-21.4	88.1	22.6	112.9
2640		-21.0	86.3	23.8	113.1

PANORAMIC CAMERA PHOTOGRAPHS

Frame # *	Rev. #	Coordinates of Prin. Pt. Lat.	Long.	Sun Elev.(°) Prin. Pt.	Spacecraft Alt. (km)
9942	63	-25.4	110.8	10.5	115.4
9943		-25.3	110.4	9.2	115.5
9944		-25.2	110.1	11.1	115.6
9945		-25.2	109.7	9.8	115.6
9946		-25.1	109.4	11.8	115.7
9947		-25.0	109.0	10.5	115.8
9948		-24.9	108.6	12.5	115.8
9949		-24.8	108.3	11.2	115.9
9950		-24.7	107.9	13.2	115.9
9951		-24.6	107.6	11.8	116.0
9952		-24.5	107.2	13.9	116.1
9953		-24.4	106.9	12.5	116.1
9954		-24.4	106.5	14.5	116.2
9955		-24.3	106.2	13.2	116.3
9956		-24.2	105.8	15.2	116.3
9957		-24.1	105.4	13.8	116.4
9958		-24.0	105.1	15.8	116.4
9959		-23.9	104.7	14.5	116.5
9960		-23.8	104.4	16.5	116.6
9961		-23.7	104.0	15.1	116.6
9962		-23.6	103.7	17.2	116.7
9963		-23.5	103.3	15.8	116.7
9964		-23.4	103.0	17.8	116.8
9965		-23.3	102.6	16.5	116.9
9966		-23.2	102.3	18.5	116.9
9967		-23.1	101.9	17.1	116.9
9968		-23.0	101.6	19.1	117.0
9969		-22.9	101.2	17.8	117.1
9970		-22.8	100.9	19.8	117.1
9971		-22.7	100.6	18.4	117.2
9972		-22.6	100.3	20.3	117.2
9973		-22.5	100.0	18.4	117.3
9974		-22.4	99.7	21.0	117.3
9975		-22.3	99.3	19.6	117.4
9976		-22.2	99.0	21.6	117.4
9977		-22.1	98.7	20.2	117.5
9978		-22.0	98.4	22.2	117.5
9979		-21.9	98.1	20.8	117.6
9980		-21.8	97.8	22.8	117.6

Frame # *	Rev. #	Coordinates of Prin. Pt. Lat.	Long.	Sun Elev. (°) Prin. Pt.	Spacecraft Alt. (km)
9981	63	-21.7	97.5	21.4	117.7
9982		-21.6	97.1	23.4	117.8
9983		-21.4	96.8	22.0	117.8
9984		-21.4	96.5	24.0	117.8
9985		-21.3	96.2	22.6	117.9
9986		-21.1	95.9	24.6	117.9
9987		-21.0	95.6	23.2	118.0
9988		-20.9	95.2	25.3	118.0
9989		-20.8	94.9	23.9	118.1
9990		-20.7	94.6	25.9	118.1
9991		-20.6	94.3	24.4	118.2
9992		-20.5	94.0	26.4	118.2
9993		-20.4	93.7	25.0	118.3
9994		-20.3	93.4	27.0	118.3
9995		-20.2	93.2	25.6	118.3
9996		-20.1	92.8	27.6	118.4
9997		-19.9	92.5	26.2	118.4
9998		-19.8	92.2	28.3	118.5
9999		-19.7	91.8	26.9	118.5
0000		-19.6	91.6	28.9	118.6
0001		-19.5	91.2	27.5	118.6
0002		-19.4	90.9	29.5	118.7
0003		-19.2	90.6	28.1	118.7
0004		-19.1	90.3	30.1	118.7
0005		-19.0	90.0	28.7	118.8
0006		-18.9	89.7	30.7	118.8
0007		-18.8	89.4	29.3	118.9
0008		-18.6	89.1	31.4	118.9
0009		-18.5	88.8	29.9	119.0
0010		-18.4	88.5	31.9	119.0
9675	38	-14.4	103.4	42.2	118.1
9676		-14.3	103.1	40.7	118.1
9677		-14.2	102.9	42.8	118.2
9678		-14.0	102.6	41.3	118.2
9679		-13.9	102.3	43.4	118.2
9680		-13.8	102.0	41.9	118.2
9681		-13.6	101.8	43.9	118.3
9682		-13.5	101.5	42.5	118.3
9683		-13.4	101.3	44.5	118.3
9684		-13.3	101.0	43.1	118.3
9685		-13.2	100.7	45.1	118.4

Frame # *	Rev. #	Coordinates of Prin. Pt. Lat.	Long.	Sun Elev. (°) Prin. Pt.	Spacecraft Alt. (km)
9686	38	-13.1	100.5	43.6	118.4
9687		-13.0	100.2	45.6	118.4
9688		-12.9	99.9	44.2	118.4
9689		-12.8	99.6	46.3	118.4
9690		-12.6	99.3	44.9	118.5
9691		-12.5	99.0	46.9	118.5
9692		-12.4	98.7	45.5	118.5
9693		-12.3	98.5	47.5	118.5
9694		-12.2	98.1	46.1	118.5
9695		-12.0	97.9	48.1	118.6
9696		-11.9	97.6	46.7	118.6
9697		-11.8	97.2	48.7	118.6
9698		-11.6	96.9	47.4	118.6
9699		-11.5	96.6	49.4	118.6
9700		-11.4	96.3	48.0	118.7
9701		-11.3	96.1	50.0	118.7
9702		-11.2	95.8	48.6	118.7
9703		-11.1	95.5	50.5	118.7
9704		-10.9	95.2	49.2	118.7
9705		-10.8	95.0	51.1	118.7
9706		-10.7	94.7	49.7	118.7
9707		-10.6	94.5	51.6	118.8
9708		-10.5	94.2	50.3	118.8
9709		-10.4	94.0	52.2	118.8
9710		-10.2	93.7	50.8	118.8
9711		-10.1	93.4	52.8	118.8
9712		-10.0	93.0	51.5	118.8
9713		- 9.8	92.7	53.5	118.8
9714		- 9.7	92.4	52.1	118.8
9715		- 9.6	92.2	54.1	118.9
9716		- 9.5	91.9	52.7	118.9
9717		- 9.3	91.6	54.7	118.9
9718		- 9.2	91.3	53.4	118.9
9719		- 9.1	91.0	55.4	118.9
9720		- 8.9	90.7	54.0	118.9

*All frame numbers are preceeded by "AS-15-".

LUNAR ORBITER PHOTOGRAPHS

Frame #	L. O. Mission	Coordinates of Prin. Pt. Lat.	Long.	Spacecraft Alt. (km)
II-196-M	II	-89	100.5	1519.0
II-196-H1	II	-	-	-
II-196-H2	II	-	-	-
II-196-H3	II	-	-	-

70 MM HASSELBLAD PHOTOGRAPHS

Frame #	Data Available from NSSDC
AS-15-13180	x
AS-15-13181	x
AS-15-13182	x
AS-15-13183	x
AS-15-13184	x
AS-15-13185	x
AS-15-13186	x
AS-15-13187	x
AS-15-13188	x
AS-15-13189	x
AS-15-13190	x
AS-15-13191	x
AS-15-13192	x
AS-15-13193	x

APPENDIX B

APPENDIX B

Description of Lunar Materials

In this appendix, a general description of the characteristics of the materials in each age category is given. Following the general description, characteristics of each unit are listed along with interpretations of the materials comprising each unit. Some similar units in the same age category are described together to avoid unnecessary repetition. This section serves as an expanded legend to accompany the Geologic Map (Plate 1). Description is from youngest to oldest; that is, down the map legend.

Materials of the Copernican System

Craters and their associated deposits are the only materials mapped as Copernican. Copernican craters are subdivided into two relative age groups, Cc_1 and Cc_2, oldest to youngest respectively. This division is based on the presence or absence or ray material around otherwise fresh, distinct craters possessing other typically Copernican features.

Copernican craters are characterized by sharp rim crests, steep inner slopes with high albedo, raised rims, usually bright ray systems (around Cc_2 craters), and an ejecta deposit that grades from hummocky texture near the rim crest to a radially grooved texture. Ejecta dunes, blocky boulders, V structures, and secondary crater

fields are also associated with most Copernican craters. These youthful features are retained because there has not been sufficient time for the erosive processes to cause substantial modification.

Both early and late Copernican materials are similar except that early Copernican materials are very slightly subdued and lack bright ray material.

Type crater for Early Copernican: crater designated as crater "C"
Type crater for Late Copernican: crater designated as crater "D"

Mapped subdivision

Bright ray material
Characteristics: high albedo plumous streaks around fresh craters; at high resolution, rays often consist of many small secondary craters; seldom has relief except near the crater rim crest; often asymmetrical distribution.
Interpretation: impact ejecta material and bright walls of small secondary and tertiary craters; where asymmetrically deposited, probably due to oblique impact.

Cc_2
Cc_1

Crater material, undivided
Characteristics: craters less than 3-5 km in diameter; further separation not practical at map scale; bright craters, some with rays; includes rim, wall, and floor material.
Interpretation: small impact craters, either primary or secondary; high albedo suggests exposure of fresh rock.

For larger craters, the following subdivisions are mapped.

Ccf_2
Ccf_1

Crater floor material
Characteristics: generally level surface, smooth to ropey texture on metric camera photographs; small hills and mounds evident on panoramic and hasselblad photographs; blocks and boulders common, especially in association with mounds; floors lower than terrain surrounding crater; often low to moderate albedo.
Interpretation: probably original unmodified floor material;

possibly some impact-generated melts; irregularities and boulders may represent fall-back or localized impact-induced volcanism.

Crater wall material

Ccw_2
Ccw_1

Characteristics: very high albedo; steep slopes; boulders common; smooth and unchanneled.
Interpretation: freshly exposed rock and rock fragments forming talus slopes as the result of a youthful impact.

Crater rim material, undivided

Ccr_2
Ccr_1

Characteristics: mapped around small craters whose deposits are not extensive or are not divisible at the map scale; includes all continuous ejecta material.

Where possible, subdivided into:

Crater rim material, hummocky texture

Crh_2
Crh_1

Characteristics: finely textured hummocks; hummock size dependent on crater size; boulders common near rim crest; finely lineated.

And:

Crater rim material, radial texture

Crr_2
Crr_1

Characteristics: distal to hummocky material; strongly lineated, lineations often ropey; small satellitic craters, crater chains, and V structures present, mostly radial to the crater.
Interpretation: both hummocky and radial material impact ejecta deposits; some satellitic craters occur on radial material; some of radial lineations may be caused by boulder and rock flows; with the lineations parallel to the direction of flow; most of these features visible only on panoramic and hasselblad photographs.

MATERIALS OF THE ERATOSTHENIAN SYSTEM

Eratosthenian craters are physically similar to Copernican craters except that they are slightly subdued and do not have well developed rim textures (none of the craters in the research area are

large enough to display rim textures normally present around large Eratosthenian craters). They are characterized by relatively steep, bright walls, flat floors, and slightly subdues rim crests. Rim deposits are commonly speckled by very small, bright-haloed Copernican craters.

The mare material is similar to nearside maria in both appearance and albedo. The entire suite of materials is believed to be Eratosthenian in age.

Type crater for Eratosthenian: crater designated as crater "E"

Ec

Crater material, undivided
Characteristics: craters less than 6-8 km in diameter; includes floor, wall, and rim materials.
Interpretation: small impact craters, either primary or secondary.

For larger craters, the following subdivisions are mapped.

Ecf

Crater floor material
Characteristics: flat to hummocky texture; generally not as hummocky as Copernican floor material; albedo similar to that of rim deposits; blocks and boulders less abundant than on Copernican floor material.
Interpretation: mostly original floor material; some modification by younger impacts and ejecta deposition; irregularities may represent fall-back or localized volcanism.

Ecw

Crater wall material
Characteristics: fairly high albedo; steep slopes; faintly streaked with darker material; smooth and unchanneled.
Interpretation: bedrock (?) and rock fragments continually being exposed causing high albedo; streaks the result of stabilizing talus slopes.

Crater rim material, undivided
Characteristics: rim crests slightly subdued and slightly

Ecr

rounded; rays lacking; faint remains of hummocky and radial textures around larger craters, absent around small craters.

Interpretation: impact ejecta deposits, slightly modified by small Copernican impacts.

Mare material

Characteristics: low albedo; level surface; pitted by small (less than 2 km diameter), shallow, bowl-shaped craters; clustering of shallow craters common; craters often rimless; largest superposed crater about 4 km in diameter; pre-existing craters breached or buried; fresh superposed craters extremely blocky, often with central mound of blocks on floor; pressure ridges, rimless pits, lobate scarps, and a subsidence bench present on mare material.

Em

Interpretation: extrusive flows, probably basaltic in composition; scarps are flow-fronts; pits appear to be collapse features; bowl-shaped craters, especially those in clusters, may be volcanic in origin; a mare bench several kilometers wide, probably formed as molten material drained back into the source vent and the solidified crust subsided; a linear structure with a raised rim appears to be the source of the extruded material and is interpreted as a fissure.

Terra material, undivided

Characteristics: higher albedo than mare material; gently rolling or undulating surface; crossed by narrow linear troughs; few craters preserved except for small Copernican craters; several large collapse pits present, partially associated with the narrow troughs; surface slopes gently away from the fissure toward the southwest.

Et

Interpretation: pyroclastic debris and ash deposits extruded from the fissure; possibly some flows intermixed; small craters rapidly destroyed by down-slope movement of material; linear troughs interpreted as collapsed lava tubes that connect the fissure with small pools of mare material; collapse along some of the tubes formed the pits.

Material of hills and mounds

Characteristics: slightly higher albedo than terra material; characterized by many low, rounded mounds and hills; completely fills the floor of a 12-15 km crater located near the mare; very few superposed craters; no summit craters or flow features present.

Ehm

Interpretation: related to the volcanic activity that extruded the mare material and the terra material; possibly formed by upwelling of material through fractures beneath the crater; composition probably more feldspathic than mare; lack of craters caused by rapid destruction by mass wasting processes.

MATERIALS OF THE ERATOSTHENIAN SYSTEM OR THE IMBRIAN SYSTEM

Several craters are superposed on Imbrian materials that do not have the normal Eratosthenian characteristics; basically they are more subdued than typical Eratosthenian craters. This age designation is used for craters that could be either Late Imbrian or Early Eratosthenian in age.

No type crater is given.

Crater material, undivided
Characteristics: craters less than 8 km in diameter; subdued and rounded rim crests; rim deposits indistinguishable from surrounding material.
Interpretation: some may be secondary craters of Late Imbrian craters; other may be primary impacts.

For larger craters, the following subdivisions are mapped.

Crater wall material
Characteristics: lower albedo than younger craters; shallower than corresponding craters of younger ages; some have dark streaks developing.
Interpretation: slopes becoming less steep and beginning to stabilize; dark streaks probably talus slopes.

Crater rim material, undivided
Characteristics: youthful textures absent; rim crests rounded and subdued; ejecta deposits not detectible beyond the raised portion of the rim.
Interpretation: subdued impact ejecta material.

EIfp

Floor material, pitted
Characteristics: level surface, highly pitted with small (< 1km diameter) craters; craters moderately subdued.
Interpretation: possibly a remnant plains unit preserved by presence of two crater peaks; or could be a group of young secondary craters.

MATERIALS OF THE IMBRIAN SYSTEM

Two ages of Imbrian craters are mapped in the Sklodowska Region based on morphologic differences. Early Imbrian craters are considerably more subdued than Late Imbrian craters, and do not retain the rim textures present on younger ejecta deposits.

Large Late Imbrian craters are moderately subdued but usually retain the raised rim and most of the rim textures. Terraces are common in large craters although they are moderately coalesced. Small Imbrian craters exhibit greater modification than the large craters.

In addition to crater materials, plains and terra-like material are also present. Plains material is typically level or nearly so; terra-like material (hilly and pitted material) is more rugged. Plains material normally occurs as depression-filling material, while hilly material comprises the higher, elevated material.

Type crater for Early Imbrian: the crater Brunner
Type crater for Late Imbrian: the crater Sklodowska

Ic

Crater material, undivided
Characteristics: craters less than 6-8 km in diameter; most are circular in plan view; occur mainly on pre-Imbrian terrae units surrounding Late Imbrian ejecta deposits of Sklodowska, Scaliger, and Humboldt; raised rims are

subdued or absent; not differentiated into Early and Late Imbrian ages.

Interpretation: may be primary, but are believed to be distant secondaries, possibly ejected during the Orientale basin-forming event; most are believed to be older than the Late Imbrian craters mentioned above.

For larger craters, and where applicable, the following subdivisions are mapped.

Crater peak material

Icp_2
Icp_1

Characteristics: range from small conical hills to high, steep-sloped irregular peaks; sometimes elongated; generally occur near the center of the crater; steep slopes have high albedo; moderately to highly subdued and rounded.

Interpretation: central uplift of rock material as the result of impact; probably brecciated; shatter cone structures may be present; a few peaks may be volcanic cones.

Crater wall material

Icw_2
Icw_1

Characteristics: dark vertical streaks developing on unterraced crater walls; terraces in larger craters moderately to highly coalesced; albedo intermediate except on steep slopes; some radial channeling present on smaller craters; terrace benches sometimes capped by plains material.

Interpretation: stabilizing slopes (talus) cause dark vertical streaks; terraces form by slump-faulting of rim segments; coalescence caused by mass wasting processes; moderate modification by fine ejecta blanketing from younger impacts.

Crater rim material, undivided

Icr_2
Icr_1

Characteristics: undifferentiated rim material of craters lacking or too small to map separate textural units on the ejecta deposits; Early Imbrian rim crests rounded and subdued; raised rim low to absent for small craters.

Where possible, subdivided into:

Crater rim material, hummocky texture

Irh_2

Characteristics: subdued hummocks; low crater density; local radial lineations; mantles and significantly modifies the former topography; forms gradational contact with radially textured unit.

And:

Crater rim material, radial texture

Irr_2

Characteristics: low radial ridges and grooves producing a striated appearance; "V" structures locally present; some secondary craters present; all structures moderately subdued; lineations mostly radial and subradial to craters.

And:

Material of the continuous secondary crater field

Isf_2

Characteristics: closely spaced, elongated, 5 to 10 km diameter secondary craters; axis of elongation radial or subradial to Sklodowska and Humboldt and Scaliger; completely modifies the former topography; trough-like crater chains sometimes formed.

Interpretation: rim material and material of the continuous secondary crater field formed as the result of impact explosion; material thins from hummocky to radial material because of loss of transport energy of base surge; continuous secondary craters separate fraction from base surge material, but deposited contemporaneously; materials mainly subdued by mass wasting and ejecta blanketing; radial textures result mainly from eject gouging, although some may be surface expression of fractures related either to the impact event or the lunar grid.

Secondary crater material

Isc

Characteristics: discontinuous craters and crater chains; individual craters mostly 2-8 km in diameter; slightly less elongated than craters in the continuous secondary crater field; rounded rim crests; seldom exhibit raised rims; all are subdued.

Interpretation: secondary craters to large Late Imbrian craters, especially Sklodowska, Scaliger, and Humboldt; considerably modified by ejecta blanketing and mass wasting.

Plains material, undivided

Ip

Characteristics: level, moderately pitted material; moderate albedo; generally forms in basins and depressions; craters on the surface often shallow and bowl-shaped; few ghost craters.

Interpretation: sequential deposits of fine ejecta meterial dispersed during large crater-forming impacts; probably semi-fluid when deposited; blanketing of pre-existing craters to

form shallow craters; some modification by younger secondary craters and fine ejecta; most of the deposits probably formed during Early and Middle Imbrian.

Ipl

Plains material, light

Characteristics: similar to undivided plains material only slightly less cratered; moderate albedo; fairly level surface; main occurrence is on floor of Sklodowska.

Interpretation: formed by same process as undivided plains material only is younger; may have formed during Sklodowska crater-forming event.

Ipd

Plains material, dark

Characteristics: lower albedo than other plains material; lower crater density; relatively smooth, level surface; forms pools around margin of floor of Sklodowska, with minor occurrences elsewhere.

Interpretation: either younger plains material formed by process mentioned above, or localized extrusion of mare-like material that has since been partially modified; probably formed at a later time than Sklodowska.

Ihp

Hilly and pitted material

Characteristics: small, often conical hills and mounds; pitted by many small craters, many of which may be secondary craters; forms rugged portion of Sklodowska's floor.

Interpretation: may be original floor material that has been modified by secondary cratering, ejecta blanketing, and mass wasting; possibly some volcanic material.

MATERIALS OF THE IMBRIAN SYSTEM OR THE NECTARIAN SYSTEM

These materials consist of terrae and plains units which cannot accurately be classified into either system, but which have certain characteristics of both. Generally these materials occur in or around large Nectarian craters that have been somewhat modified by Imbrian ejecta material.

No type crater is given.

INp

Plains material, undivided
Characteristics: level to slightly hummocky surface; moderately pitted by small, subdued craters; albedo similar to Imbrian plains material or slightly lower.
Interpretation: mainly formed by Early Imbrian crater and basin ejecta deposition; hummocky surfaces caused by severe erosion of small craters.

INt

Terra material, undivided
Characteristics: nearly level, highly pitted to hilly, rugged material; subdued and rounded features.
Interpretation: gradational between plains and older more rugged terrae materials; mostly modified rim deposits of Nectarian craters; some may be modified plains material.

MATERIALS OF THE NECTARIAN SYSTEM

The Nectarian System consists of those materials younger than the Nectaris Basin, located on the eastern limb of the nearside. Few if any effects of the Nectaris basin-forming event are evident in the research area making it necessary to use morphologic criteria to assign relative ages to pre-Imbrian materials.

Nectarian craters are highly subdued with rounded rim crests and no separable rim units. Terraces, where present, are coalesced into subdued, hummocky masses. Rim crests and rim deposits are frequently interrupted by large craters and numerous small craters. Walls on smaller craters are generally channeled and sometimes hummocky.

Terrae materials show greater evidence of mass wasting than younger units. Textured patterns are visible on all slopes on high resolution photographs. Plains material of Nectarian age is consi-

derably more subdued than Imbrian plains material and mainly occurs as floor covering material in pre-Nectarian craters. The reliability of a Nectarian age for this plains material is questionable because of an anomalously low crater density. Several explanations may be advanced to account for this: 1) the material is actually much younger than mapped; 2) the material has considerably fewer secondary craters; 3) other plains units have a higher than normal crater density because of secondary cratering from nearby crater-forming impacts; 4) the material has been highly eroded and subdued by mass wasting processes and ejecta blanketing. The morphology of the material as seen on Apollo 15 photographs and the presence of superposed craters of Imbrian age do not support a younger age for the plains material. Therefore, a combination of the three remaining explanations is favored.

Type crater for Nectarian: the crater Backlund

Crater peak material

Ncp

Characteristics: highly eroded and rounded; may be single or multiple

Interpretation: same as Imbrian crater peak material; highly modified by mass wasting.

Crater wall material

Ncw

Characteristics: terraces almost totally coalesced, with a few scarps still visible; walls channeled and hummocky; floor and wall material have gradational contact; relatively low interior slope angle.

Interpretation: highly modified terraces and slope material; slopes probably stabilized except for steepest portions.

Ncr

Crater rim material, undivided

Characteristics: rim crests rounded, highly subdued; rim slightly raised, coarsely hummocky; interrupted by other large craters; outer rim deposits modified beyond recognition.

Interpretation: old impact ejecta deposits substantially modified by younger material; hummocky texture caused by degradation of small craters rather than by ejecta deposition.

Np

Plains material, undivided

Characteristics: level on broad scale but hummocky on small scale; hummocks caused by degradation of small Imbrian craters; crater density generally low; occurs mainly as floor-covering material in pre-Nectarian craters; albedo lower than Imbrian plains material.

Interpretation: essentially material deposited following large Nectarian crater-forming events; probably thinly blanketed with younger material.

Nt

Terra material, undivided

Characteristics: undulating to hilly material; a few Nectarian and younger craters superposed; small craters highly degraded; often adjacent to Inp or Int units.

Interpretation: modified rim deposits of Nectarian craters and some pre-Nectarian craters; probably little difference between this unit and INt, except this material has a greater contribution of Nectarian age material.

Ntg

Terra material, grooved

Characteristics: forms an extensive unit adjacent to the SW rim of the crater Hilbert; long grooves or gouges and shorter lineations radial to Hilbert; rugged, hilly texture; many 3-8 km diameter craters of Imbrian age.

Interpretation: thick ejecta deposit, possibly an ejecta flow, formed during the Hilbert crater-forming event; large gouges interpreted as secondary impacts of Hilbert; may be some volcanic cones on this unit, although if present, they are highly subdued.

Ntd

Terra dome material

Characteristics: 5-7 km diameter positive relief features; form several isolated "islands" in plains material; possibly should be called "massifs".

Interpretation: either remnant crater segments or peaks, or igneous dome structures (intrusive or extrusive).

MATERIALS OF THE NECTARIAN SYSTEM OR OF PRE-NECTARIAN AGE

Some terrae materials cannot be accurately dated because of their similarity in morphology to both Nectarian and pre-Nectarian terrae materials and their location near craters of both these ages.

No type crater is given.

NpNt

Terra material, undivided

Characteristics: generally rugged surface; many secondary craters from large Imbrian craters; usually located near Nectarian and pre-Nectarian craters.

Interpretation: modified rim deposits with large contributions of material from both Nectarian and pre-Nectarian craters; probably blanketed by younger material; small craters highly subdued by mass wasting processes.

MATERIALS OF PRE-NECTARIAN AGE

Pre-Nectarian craters are highly to completely subdued and do not have distinct units. Rim crests are completely rounded so that no crestline can be accurately located. Wall and rim materials are Hummocky and generally interrupted by several large craters. The oldest craters are barely discernible, visible only as large, shallow depressions.

Terra material is rugged and occurs mainly around large pre-Nectarian craters. All materials are highly subdued and modified by

erosion processes.

Type crater for pre-Nectarian: the crater Curie

pNc

Crater material, undivided
Characteristics: includes wall and rim material; completely subdued; original rim textures absent; rim crests rounded; rim and walls coarsely hummocky; generally interrupted by several large craters of younger age; smaller craters barely recognizable; little rim material mappable.
Interpretation: highly degraded impact craters; rim deposits modified to terra material; hummocky rim and walls caused by mass wasting processes.

pNcp

Crater peak material
Characteristics: usually low, rounded hills; highly subdued.
Interpretation: highly eroded peaks originally formed by impact or volcanism.

pNt

Terra material, undivided
Characteristics: similar to Nt and NpNt except somewhat more rugged; occurs in elevated terrain around large pre-Nectarian craters; generally has one or more Nectarian crater superposed; highly subdued positive and negative relief forms.
Interpretation: modified rim deposits; maincontribution of material from pre-Nectarian craters; mass wasting processes active and small craters quickly eroded causing hummocky, hilly surface.

UNDATED MATERIALS

Undated material is characterized by undulating to hummocky topography. It is restricted to the floors of Imbrian and older craters where erosion processes have significantly modified the original floor material. Undualting material has a smooth surface texture; hummocky material has a coarse texture of low hills and hummocks.

Landslide material is also undated.

The rational for classifying these units as "undated" is given in the body of the text.

Undulating floor material

Characteristics: gently rolling, undulating surface; low crater density.

Interpretation: modified floor material, consisting mainly of material eroded from the interior slopes of craters; some contribution of material by ejecta blanketing.

Hummocky floor material

Characteristics: hilly, hummocky surface; low crater density; hills low and rounded.

Interpretation: slump material and other material eroded from the crater slopes; floor may have been hilly originally; some ejecta blanketing.

Landslide material

Characteristics: irregular masses, sometimes with lobate base; generally an irregular section missing from the slope above the mass.

Interpretation: landslide and slump material formed on unstable slopes.

APPENDIX C

TABLE 1: LIST OF MOON CRATER DATA.

NUMBER	COORDINATE X	COORDINATE Y	RIM	DIAM	AGE
1	0	0	4.800	28.800	2.000
2	0	0	28.800	40.300	2.000
3	0	0	41.200	15.800	3.400
4	0	0	65.100	15.300	4.300
5	0	0	70.900	17.200	2.900
6	0	0	93.400	19.100	3.600
7	0	0	95.000	11.500	3.500
8	0	0	107.200	9.000	3.100
9	0	0	96.000	13.400	3.800
10	0	0	113.000	13.100	3.600
11	0	0	134.100	14.500	2.900
12	0	0	134.200	12.600	2.100
13	0	0	130.500	14.500	3.800
14	0	0	153.900	46.500	2.800
15	0	0	153.200	15.000	3.300
16	0	0	148.900	24.100	3.200
17	0	0	154.600	22.300	3.700
18	0	0	180.600	30.500	2.800
19	0	0	201.300	10.700	4.400
20	0	0	213.000	9.700	5.000
21	0	0	141.000	10.700	3.200
22	0	0	115.100	8.200	3.300
23	0	0	26.800	19.200	4.000
24	0	0	34.600	35.600	2.500
25	0	0	46.000	28.700	2.700
26	0	0	66.100	32.600	2.000
27	0	0	70.000	10.500	4.200
28	0	0	100.700	12.400	3.000
29	0	0	90.000	18.200	3.500
30	0	0	76.500	22.000	3.600
31	0	0	60.000	14.300	3.000
32	0	0	74.600	28.800	2.100
33	0	0	98.500	33.400	1.800
34	0	0	99.500	24.900	3.600
35	0	0	95.800	42.100	1.800
36	0	0	117.600	26.800	3.600
37	0	0	138.900	20.100	4.300
38	0	0	149.800	62.300	2.100
39	0	0	171.500	76.500	2.500
40	0	0	207.700	12.400	2.800
41	0	0	235.400	11.000	4.800
42	0	0	57.500	95.900	3.000
43	0	0	136.000	8.200	3.700
44	0	0	0.0	16.100	6.000
45	0	0	44.800	12.200	2.800
46	0	0	4.000	10.700	2.700
47	0	0	44.900	25.200	3.800
48	0	0	52.500	24.400	3.200
49	0	0	72.300	21.400	3.100
50	0	0	78.000	12.700	2.900

NUMBER	COORDINATE X	COORDINATE Y	RIM	DIAM	AGE
51	C	0	97.400	16.200	4.300
52	C	0	102.100	52.400	2.100
53	C	0	105.800	24.300	5.900
54	C	0	112.800	28.200	3.400
55	0	0	162.100	19.400	4.300
55	0	0	162.100	19.400	4.500
56	0	0	166.000	9.200	4.800
57	C	0	157.500	8.200	5.000
58	C	0	139.000	9.200	3.100
59	0	0	162.100	17.000	3.500
60	C	0	164.100	37.900	3.200
61	C	0	192.300	13.100	3.000
62	C	C	207.000	8.700	4.700
63	0	0	208.500	17.000	2.800
64	C	0	260.200	15.200	3.500
65	C	0	270.700	15.600	3.300
66	0	0	241.900	27.100	3.300
67	C	0	248.600	27.200	2.500
68	C	0	268.000	25.200	2.500
69	C	0	270.000	9.200	4.800
70	0	0	251.700	9.200	4.400
71	0	0	284.900	26.600	1.800
72	0	0	286.100	53.400	2.900
73	C	0	309.300	8.000	4.200
74	C	0	305.100	27.100	3.000
75	C	0	319.600	13.100	4.000
76	C	0	345.400	11.700	5.500
77	C	0	10.700	61.400	1.100
78	C	0	13.700	22.400	3.300
79	0	0	24.400	21.900	3.200
80	C	0	49.800	8.000	3.400
81	C	0	57.600	9.300	3.300
82	C	0	49.700	11.200	3.000
83	0	0	55.600	42.000	3.000
84	C	C	86.700	9.200	3.500
85	0	0	92.600	55.000	2.000
86	0	0	125.600	11.900	3.500
87	0	0	101.100	21.900	2.100
88	0	0	104.200	34.600	3.000
89	0	0	121.000	15.500	3.200
90	C	0	135.000	11.800	3.200
91	C	0	139.900	40.100	3.000
92	C	0	151.700	19.200	3.300
93	C	0	150.200	61.400	1.400
94	0	0	158.500	14.000	2.900
95	C	C	181.300	38.200	3.000
96	0	0	178.500	15.800	3.100
97	C	0	193.100	14.000	3.300
98	0	0	192.700	13.100	4.800
99	C	C	203.300	15.500	3.500
100	0	0	205.800	13.600	3.800

NUMBER	COORDINATE X	COORDINATE Y	RIM	DIAM	AGE
101	C	0	214.100	11.300	4.500
102	C	0	201.300	75.300	2.000
103	C	0	237.600	13.100	4.500
104	0	0	261.900	20.800	3.900
105	C	0	263.900	19.400	3.000
106	C	0	286.500	11.700	4.000
107	0	0	197.100	24.900	3.400
108	0	C	192.400	17.300	3.000
109	0	0	31.300	8.000	2.700
110	C	0	21.100	47.500	2.800
111	0	0	57.800	22.400	2.600
112	0	0	76.400	8.300	2.800
113	0	0	84.200	9.800	2.900
114	C	0	67.500	13.300	2.800
115	0	0	57.700	143.100	1.700
116	C	0	154.100	11.000	3.100
117	0	0	127.500	22.100	3.500
118	C	0	139.400	8.000	3.500
119	C	0	167.000	11.500	3.500
120	C	0	127.500	12.200	5.200
121	C	0	154.100	11.000	3.800
122	C	0	156.600	16.100	3.500
123	0	0	161.000	23.600	2.800
124	0	0	184.200	27.600	1.500
125	C	0	207.700	38.800	1.700
126	C	0	182.200	16.100	3.000
127	0	0	170.400	18.400	3.500
128	C	0	171.100	8.500	3.800
129	0	0	225.500	9.700	6.200
130	C	0	33.200	19.100	3.400
131	0	0	53.800	13.200	3.300
132	C	0	67.400	23.400	3.500
133	0	0	109.700	15.700	2.800
134	C	0	122.600	12.900	4.300
135	0	0	90.300	60.100	2.000
136	0	0	99.100	55.400	4.500
137	C	0	138.200	13.700	3.200
138	0	0	148.100	10.900	3.200
139	0	0	148.000	62.100	2.800
140	0	0	160.800	28.800	4.300
141	C	0	178.700	59.000	2.000
142	C	0	178.200	27.000	3.400
143	C	0	162.900	46.200	1.300
144	0	0	167.800	9.900	3.800
145	0	0	171.600	37.300	1.500
146	0	0	201.400	13.500	3.400
147	C	0	228.100	15.500	3.300
148	C	0	219.600	16.200	2.600
149	C	0	209.100	8.000	3.100
150	0	0	212.900	14.700	3.200
151	0	0	209.000	15.700	3.300

NUMBER	COORDINATE X	COORDINATE Y	RIM	DIAM	AGE
152	C	0	211.000	11.500	3.000
153	C	0	233.700	13.900	3.200
154	C	0	232.100	18.100	3.200
155	C	0	253.400	18.500	3.400
156	C	0	269.200	10.200	3.300
157	0	0	5.300	10.900	6.300
158	C	0	39.900	11.500	3.900
159	C	0	50.900	60.900	1.500
160	C	0	53.800	43.700	2.300
161	C	0	84.600	28.400	3.500
162	C	0	111.500	9.600	4.600
163	C	0	113.300	18.300	3.900
164	C	0	120.100	25.000	3.600
165	C	0	134.600	9.500	3.900
166	0	0	123.100	12.500	2.800
167	C	0	120.200	17.300	3.100
168	0	0	139.300	10.600	2.400
169	0	0	148.100	11.500	3.400
170	0	0	142.300	8.200	2.600
171	C	0	145.200	31.800	3.000
172	C	0	157.600	9.100	2.900
173	C	0	164.200	14.400	2.600
174	C	0	177.200	16.300	2.500
175	C	0	172.500	22.200	3.800
176	0	0	181.900	16.400	2.700
177	C	0	188.300	16.800	3.500
178	C	0	194.200	18.800	5.300
179	C	0	89.500	9.100	2.800
180	C	0	192.300	28.800	3.000
181	C	0	213.800	13.900	5.200
182	C	0	215.900	53.600	3.800
183	C	0	225.400	12.100	3.200
184	0	0	235.100	8.200	3.100
185	0	0	271.900	16.600	3.500
186	C	0	268.000	40.000	1.700
187	C	0	287.500	14.600	2.500
188	0	0	286.100	18.000	3.100
189	C	0	324.500	8.500	2.900
190	0	0	4.800	14.400	3.000
191	C	0	11.000	50.000	2.800
192	C	0	46.100	28.800	2.700
193	C	0	72.100	19.200	4.000
194	0	0	76.900	20.200	2.200
195	C	0	92.300	20.400	2.000
196	0	0	104.000	8.300	2.500
197	C	0	119.500	14.100	3.000
198	0	0	119.200	14.100	4.400
199	0	0	130.400	9.700	2.500
200	C	0	163.400	10.700	2.400
201	C	0	169.500	11.600	2.800
202	C	0	172.400	8.300	4.500

NUMBER	COORDINATE X	COORDINATE Y	RIM	DIAM	AGE
203	C	0	176.100	10.200	2.600
204	C	0	180.800	14.600	2.000
205	C	0	192.400	11.600	2.800
206	C	0	185.100	38.800	2.100
207	C	0	178.500	8.900	4.200
208	C	0	178.500	21.400	3.100
209	C	0	199.000	26.200	2.500
210	C	0	200.200	10.400	6.000
211	C	0	211.500	31.100	4.000
212	C	0	221.200	10.400	2.500
213	C	0	232.000	13.600	3.800
214	C	0	228.400	40.900	3.600
215	C	0	243.400	9.500	2.600
216	C	0	247.500	11.600	3.000
217	C	0	249.600	13.600	2.000
218	C	0	267.100	42.400	2.500
219	C	0	280.300	17.000	4.000
220	C	0	305.900	28.200	3.000
221	C	0	319.000	17.500	4.300
222	C	0	186.200	42.500	3.600
223	C	0	0.0	128.000	4.500

TABLE 2: STATISTICS FOR MCCN CRATER DATA SHOWN IN TABLE 1.

OF SAMPLES = 224

VARIABLE	MEAN	STANDARD DEV.	VARIANCE	SKEWNESS	KURTOSIS
RIM	150.7451	76.9520	5921.6055	0.11	-0.60
DIAM	22.5290	18.3223	335.7073	3.03	13.08
AGE	3.2625	0.9171	0.8410	0.61	0.95

** VM/370 VERSION 02 LEVEL 00 ************************ CLASS A *** DEV 00E ******************************** 11/04/74 *** 11:50:09 **

USERID ORIGIN	CMSBATCH CMSBATCH
DISTRIBUTION CODE	KAUFFREQ
SPOOL FILE NAME TYPE	CMSBATCH PRINTER
CREATION DATE	11/04/74 11:49:06
SPOOL FILE ID	0351
RECORD COUNT	0184

```
            VV          VV    MM          MM
             VV        VV     MMM        MMM
              VV      VV      MMMM      MMMM
               VV    VV       MM MM    MM MM
   3333333333     777777777777MMMM  C0000000
  333333333333    77777777777  MM  000000000
  33       VV33   77VV     77      00MM      00
             V33     VV   77M      00MM      C0
              33      VV 77MM      00MM      00
          3333VV   VV   77 MM      00MM      00
          3333 VVVV     77 MM      00MM      00
                33 VV   77 MM      00MM      00
                33      77         00        00
  33            33      77         00        00
  333333333333          77          C000000000
   3333333333           77           CCCCC000

 CCCCCCCCC   MM         MM  SSSSSSSSSS  BBBBBBBBBBB    AAAAAAAAAA   TTTTTTTTTTTT   CCCCCCCCCC   HH        HH
CCCCCCCCCCC  MMM       MMM SSSSSSSSSSSS BBBBBBBBBBBB  AAAAAAAAAAAA  TTTTTTTTTTTT  CCCCCCCCCCCC  HH        HH
CC        CC MMMM     MMMM SS        SS BB        BB  AA        AA       TT       CC        CC  HH        HH
CC           MM MM   MM MM SS           BB        BB  AA        AA       TT       CC            HH        HH
CC           MM  MMMM  MM  SSS          BB       BB   AA        AA       TT       CC            HH        HH
CC           MM   MM   MM   SSSSSSSSS   BBBBBBBBBB    AAAAAAAAAAAA       TT       CC            HHHHHHHHHHHH
CC           MM        MM     SSSSSSSSS BBBBBBBBBB    AAAAAAAAAAAA       TT       CC            HHHHHHHHHHHH
CC           MM        MM          SSS  BB       BB   AA        AA       TT       CC            HH        HH
CC           MM        MM           SS  BB        BB  AA        AA       TT       CC            HH        HH
CC        CC MM        MM  SS       SS  BB        BB  AA        AA       TT       CC        CC  HH        HH
CCCCCCCCCCC  MM        MM  SSSSSSSSSSSS BBBBBBBBBBBB  AA        AA       TT       CCCCCCCCCCC   HH        HH
 CCCCCCCCC   MM        MM   SSSSSSSSS   BBBBBBBBBBB   AA        AA       TT        CCCCCCCCC    HH        HH

KK        KK   AAAAAAAAAA  UU        UU FFFFFFFFFFFF FFFFFFFFFFFF RRRRRRRRRRR  EEEEEEEEEEEE   CCCCCCCCCC
KK       KK   AAAAAAAAAAAA UU        UU FFFFFFFFFFFF FFFFFFFFFFFF RRRRRRRRRRRR EEEEEEEEEEEE  CCCCCCCCCCCC
KK      KK    AA        AA UU        UU FF           FF           RR        RR EE            QQ        QQ
KK     KK     AA        AA UU        UU FF           FF           RR        RR EE            CC        CQ
KK    KK      AA        AA UU        UU FF           FF           RR        RR EE            QQ        QQ
KKKKKKK       AAAAAAAAAAAA UU        UU FFFFFFFF     FFFFFFFF     RRRRRRRRRRRR EEEEEEEE      CQ        QQ
KKKKKKK       AAAAAAAAAAAA UU        UU FFFFFFFF     FFFFFFFF     RRRRRRRRRRR  EEEEEEEE      CQ        CQ
KK    KK      AA        AA UU        UU FF           FF           RR    RR     EE            QQ    QC  QQ
KK     KK     AA        AA UU        UU FF           FF           RR     RR    EE            CQ     CQ QQ
KK      KK    AA        AA UU        UU FF           FF           RR      RR   EE            QQ      CQQQ
KK       KK   AA        AA UUUUUUUUUUUU FF           FF           RR       RR  EEEEEEEEEEEE  CCCCCCCCCCQQ
KK        KK  AA        AA  UUUUUUUUUU  FF           FF           RR        RR EEEEEEEEEEEE   CCCCCCCC QQ
```

128

```
FORTRAN IV G1  RELEASE 2.0            MAIN            DATE = 74308        11/49/03        PAGE 0001

0001                  DIMENSION KOUNT(3,7),ICOUNT(7)
0002                  DO 3 J=1,7
0003                  DO 2 I=1,3
0004                2 KOUNT(I,J)=0
0005                3 ICOUNT(J)=0
0006                6 READ(5,1,END=7)DIAM,AGE
0007                1 FORMAT(17X,F5.1,2X,F4.1)
0008                  IF (DIAM .LE. 20)I=1
0009                  IF ((DIAM .GT. 20).AND.(DIAM .LE. 45)) I=2
0010                  IF (DIAM .GT. 45) I=3
0011                  DO 4 J=1,7
0012                  A=J
0013                   B=J-1
0014                  IF ((AGE .GT. B) .AND. (AGE .LE. A)) GO TO 5
0015                  GO TO 4
0016                5 KOUNT(I,J)=KOUNT(I,J)+1
0017                  ICOUNT(J)=ICOUNT(J)+1
0018                4 CONTINUE
0019                  GO TO 6
0020                7 DO 8 I=1,3
0021                  SUM=0.0
0022                  DO 9 J=1,7
0023                9 SUM=KOUNT(I,J)+SUM
0024                  DO 10 J=1,7
0025                  F=KOUNT(I,J)/SUM
0026                  F=F*100.
0027               10 WRITE(6,11)J,KOUNT(I,J),F,I
0028               11 FORMAT(1X,'CLASS ',I1,5X,'F= ',I3,5X,'% F = ',F5.2,5X,'RANK= ',I1)
0029                8 WRITE(6,12)
0030               12 FORMAT(//)
0031                  SUM=0.0
0032                  DO 13 I=1,7
0033               13 SUM=ICOUNT(I)+SUM
0034                  DO 14 I=1,7
0035                  F=100.*(ICOUNT(I)/SUM)
0036               14 WRITE(6,15)I,ICOUNT(I),F
0037               15 FORMAT(1X,'CLASS ',I1,5X,'F= ',I3,5X,'% F = ',F5.2,5X,'ALL DIAMETE
                     1RS')
0038                  WRITE(6,16)
0039               16 FORMAT(/1X,'RANK 1 CONTAINS DIAMETERS FROM 0-20.0'/1X,'RANK 2 CONT
                     1AINS DIAMETERS FROM 20.1-45'/1X,'RANK 3 CONTAINS DIAMETERS EXCEEDI
                     2NG 45')
0040                  STOP
0041                  END
```

```
      *OPTIONS IN EFFECT*   NOTERM,NOID,EBCDIC,SOURCE,NOLIST,NODECK,LOAD,NOMAP,NOTEST
      *OPTIONS IN EFFECT*   NAME = MAIN     , LINECNT =       50
      *STATISTICS*     SOURCE STATEMENTS =       41,PROGRAM SIZE =     1722
      *STATISTICS*   NO DIAGNOSTICS GENERATED
 CLASS 1      F=   0      % F =  0.0       RANK= 1
 CLASS 2      F=   2      % F =  1.43      RANK= 1
 CLASS 3      F=  44      % F = 31.43      RANK= 1
 CLASS 4      F=  65      % F = 46.43      RANK= 1
 CLASS 5      F=  21      % F = 15.00      RANK= 1
 CLASS 6      F=   6      % F =  4.29      RANK= 1
 CLASS 7      F=   2      % F =  1.43      RANK= 1


 CLASS 1      F=   0      % F =  0.0       RANK= 2
 CLASS 2      F=  11      % F = 17.74      RANK= 2
 CLASS 3      F=  23      % F = 37.10      RANK= 2
 CLASS 4      F=  25      % F = 40.32      RANK= 2
 CLASS 5      F=   2      % F =  3.23      RANK= 2
 CLASS 6      F=   1      % F =  1.61      RANK= 2
 CLASS 7      F=   0      % F =  0.0       RANK= 2


 CLASS 1      F=   0      % F =  0.0       RANK= 3
 CLASS 2      F=   9      % F = 42.86      RANK= 3
 CLASS 3      F=   9      % F = 42.86      RANK= 3
 CLASS 4      F=   1      % F =  4.76      RANK= 3
 CLASS 5      F=   2      % F =  9.52      RANK= 3
 CLASS 6      F=   0      % F =  0.0       RANK= 3
 CLASS 7      F=   0      % F =  0.0       RANK= 3


 CLASS 1      F=   0      % F =  0.0       ALL DIAMETERS
 CLASS 2      F=  22      % F =  9.87      ALL DIAMETERS
 CLASS 3      F=  76      % F = 34.08      ALL DIAMETERS
 CLASS 4      F=  91      % F = 40.81      ALL DIAMETERS
 CLASS 5      F=  25      % F = 11.21      ALL DIAMETERS
 CLASS 6      F=   7      % F =  3.14      ALL DIAMETERS
 CLASS 7      F=   2      % F =  0.90      ALL DIAMETERS

 RANK 1 CONTAINS DIAMETERS FROM 0-20.0
 RANK 2 CONTAINS DIAMETERS FROM 20.1-45
 RANK 3 CONTAINS DIAMETERS EXCEEDING 45
```

```
RUN NAME        RELATICN OF CRATOR FREQUENCY AND DIAMETER OF CRATOR.
FILE NAME       CURR, CRATOR FREQUENCY AND DIAMETER
VARIABLE LIST   DIAM,CUMFREQ
INPUT FORMAT    FIXED(F5.0,1X,F7.3)
```

ACCORDING TO YOUR INPUT FORMAT, VARIABLES ARE TO BE READ AS FOLLOWS

VARIABLE	FORMAT	RECORD	COLUMNS
DIAM	F 5. 0	1	1- 5
CUMFREQ	F 7. 3	1	7- 13

THE INPUT FORMAT PROVIDES FOR 2 VARIABLES. 2 WILL BE READ
IT PROVIDES FOR 1 RECORDS ('CARDS') PER CASE. A MAXIMUM OF 13 'COLUMNS' ARE USED ON A RECORD.

```
# OF CASES      28
INPUT MEDIUM    CARD
VAR LABELS      DIAM,DIAMETER OF CRATORS IN KM/
                CUMFREQ,GREATER THAN CUMULATIVE FREQUENCY
COMPUTE         LOGDIAM=LG10(DIAM)
COMPUTE         LOGCUM=LG10(CUMFREQ)
PRINT FORMATS   DIAM,CUMFREQ (3)/LOGDIAM,LOGCUM (5)
REGRESSION      VARIABLES=LOGDIAM,LOGCUM/
                REGRESSION=LOGCUM WITH LOGDIAM (1)/
                REGRESSION=LOGDIAM WITH LOGCUM (1)
STATISTICS      ALL
READ INPUT DATA
```

FILE CORR (CREATION DATE = 12/05/74) CRATOR FREQUENCY AND DIAMETER

VARIABLE	MEAN	STANDARD DEV	CASES
LOGDIAM	1.5010	0.2394	28
LOGCUM	2.1091	0.4085	28

FILE CORR (CREATION DATE = 12/05/74) CRATOR FREQUENCY AND DIAMETER

CORRELATION COEFFICIENTS

A VALUE OF 99.00000 IS PRINTED
IF A COEFFICIENT CANNOT BE COMPUTED.

	LOGDIAM	LOGCUM
LOGDIAM	1.00000	-0.98334
LOGCUM	-0.98334	1.00000

FILE CORR (CREATION DATE = 12/05/74) CRATOR FREQUENCY AND DIAMETER

* MULTIPLE REGRESSION * * * * * * * * * * * * * VARIABLE LIST 1
REGRESSION LIST 1

DEPENDENT VARIABLE.. LOGCUM

VARIABLE(S) ENTERED ON STEP NUMBER 1.. LOGDIAM

MULTIPLE R	0.98334	ANALYSIS OF VARIANCE	DF	SUM OF SQUARES	MEAN SQUARE	F
R SQUARE	0.96697	REGRESSION	1.	4.35720	4.35720	761.09561
STANDARD ERROR	0.07566	RESIDUAL	26.	0.14885	0.00572	

---------- VARIABLES IN THE EQUATION ----------

VARIABLE	B	BETA	STD ERROR B	F
LOGDIAM	-1.67821	-0.98334	0.06083	761.096
(CONSTANT)	4.62817			

---------- VARIABLES NOT IN THE EQUATION ----------

VARIABLE	BETA IN	PARTIAL	TOLERANCE	F

MAXIMUM STEP REACHED

FILE CCRR (CREATION DATE = 12/05/74) CRATOR FREQUENCY AND DIAMETER

* MULTIPLE REGRESSION * * * * * * * * * * * * * VARIABLE LIST 1
REGRESSION LIST 1

DEPENDENT VARIABLE.. LOGCUM

SUMMARY TABLE

VARIABLE	MULTIPLE R	R SQUARE	RSQ CHANGE	SIMPLE R	B	BETA
LOGDIAM	0.98334	0.96697	0.96697	-0.98334	-1.67821	-0.98334
(CONSTANT)					4.62817	

FILE CORR (CREATION DATE = 12/05/74) CRATER FREQUENCY AND DIAMETER

* MULTIPLE REGRESSION * * * * * * * * * * * * * VARIABLE LIST 1
REGRESSION LIST 2

DEPENDENT VARIABLE.. LOGDIAM

VARIABLE(S) ENTERED ON STEP NUMBER 1.. LOGCUM

MULTIPLE R	0.98334	ANALYSIS OF VARIANCE	DF	SUM OF SQUARES	MEAN SQUARE	F
R SQUARE	0.96697	REGRESSION	1.	1.49598	1.49598	761.09561
STANDARD ERROR	0.04433	RESIDUAL	26.	0.05110	0.00197	

VARIABLES IN THE EQUATION

VARIABLE	B	BETA	STD ERROR B	F
LOGCUM	-0.57619	-0.98334	0.02089	761.096
(CONSTANT)	2.71628			

VARIABLES NOT IN THE EQUATION

VARIABLE	BETA IN	PARTIAL	TOLERANCE	F

MAXIMUM STEP REACHED

FILE CORR (CREATION DATE = 12/05/74) CRATER FREQUENCY AND DIAMETER

* MULTIPLE REGRESSION * * * * * * * * * * * * * * VARIABLE LIST 1
REGRESSION LIST 2

DEPENDENT VARIABLE.. LCGDIAM

SUMMARY TABLE

VARIABLE	MULTIPLE R	R SQUARE	RSQ CHANGE	SIMPLE R	B	BETA
LCGCUM	0.98334	0.96697	0.96697	-0.98334	-0.57619	-0.98334
(CONSTANT)					2.71628	

```
RUN NAME        BASIC STATISTICS FOR MOON DATA,KAUFFMAN,223 SAMPLES.
FILE NAME       MOON,RIM, DIAMETER AND AGE OF CRATOR
VARIABLE LIST   NUMBER,RIM,DIAM,AGE
INPUT FORMAT    FIXED(T77,A4,T11,3F6.1)
```

ACCORDING TO YOUR INPUT FORMAT, VARIABLES ARE TO BE READ AS FOLLOWS

VARIABLE	FORMAT	RECORD	COLUMNS
NUMBER	A 4	1	77- 80
RIM	F 6. 1	1	11- 16
DIAM	F 6. 1	1	17- 22
AGE	F 6. 1	1	23- 28

THE INPUT FORMAT PROVIDES FOR 4 VARIABLES. 4 WILL BE READ
IT PROVIDES FOR 1 RECORDS ('CARDS') PER CASE. A MAXIMUM OF 28 'COLUMNS' ARE USED ON A RECORD.

```
PRINT FORMATS   NUMBER (A)/RIM TO AGE (1)
# OF CASES      223
INPUT MEDIUM    CARD
VAR LABELS      RIM,DISTANCE FROM MAJOR CRATOR, IN KM/
                DIAM,DIAMETER OF CRATOR IN KM/
                AGE,AGE OF CRATOR
COMPUTE         LOGRIM=LG10(RIM)
COMPUTE         LOGDIAM=LG10(DIAM)
COMPUTE         LOGAGE=LG10(AGE)
CODEBOOK        RIM TO LOGAGE
OPTIONS         1
STATISTICS      ALL
READ INPUT DATA
```

FILE MOON (CREATION DATE = 12/05/74) RIM, DIAMETER AND AGE OF CRATOR

VARIABLE DIAM DIAMETER OF CRATOR IN KM

VALUE LABEL	VALUE	ABSOLUTE FREQUENCY	RELATIVE FREQUENCY (PERCENT)	ADJUSTED FREQUENCY (PERCENT)	CUMULATIVE ADJ FREQ (PERCENT)
	8.0	5	2.2	2.2	2.2
	8.2	5	2.2	2.2	4.5
	8.3	3	1.3	1.3	5.8
	8.5	2	0.9	0.9	6.7
	8.7	1	0.4	0.4	7.2
	8.9	1	0.4	0.4	7.6
	9.0	1	0.4	0.4	8.1
	9.1	2	0.9	0.9	9.0
	9.2	5	2.2	2.2	11.2
	9.3	1	0.4	0.4	11.7
	9.5	2	0.9	0.9	12.6
	9.6	1	0.4	0.4	13.0
	9.7	3	1.3	1.3	14.3
	9.8	2	0.9	0.9	15.2
	10.2	2	0.9	0.9	16.1
	10.4	2	0.9	0.9	17.0
	10.5	1	0.4	0.4	17.5
	10.6	1	0.4	0.4	17.9
	10.7	4	1.8	1.8	19.7
	10.8	1	0.4	0.4	20.2
	10.9	1	0.4	0.4	20.6
	11.0	3	1.3	1.3	22.0
	11.2	1	0.4	0.4	22.4
	11.3	1	0.4	0.4	22.9

11.5	5	2.2	2.2	25.1
11.6	3	1.3	1.3	26.5
11.7	2	0.9	0.9	27.4
11.8	1	0.4	0.4	27.8
11.9	1	0.4	0.4	28.3
12.1	1	0.4	0.4	28.7
12.2	2	0.9	0.9	29.6
12.4	2	0.9	0.9	30.5
12.5	1	0.4	0.4	30.9
12.6	1	0.4	0.4	31.4
12.7	1	0.4	0.4	31.8
12.8	1	0.4	0.4	32.3
13.1	5	2.2	2.2	34.5
13.2	1	0.4	0.4	35.0
13.3	1	0.4	0.4	35.4
13.4	1	0.4	0.4	35.9
13.5	1	0.4	0.4	36.3
13.6	3	1.3	1.3	37.7
13.7	1	0.4	0.4	38.1
13.9	2	0.9	0.9	39.0
14.0	2	0.9	0.9	39.9
14.1	2	0.9	0.9	40.8
14.3	1	0.4	0.4	41.3
14.4	2	0.9	0.9	42.2
14.5	2	0.9	0.9	43.0
14.6	2	0.9	0.9	43.9
14.7	1	0.4	0.4	44.4

15.0	1	0.4	0.4	44.8
15.2	1	0.4	0.4	45.3
15.3	1	0.4	0.4	45.7
15.5	3	1.3	1.3	47.1
15.6	1	0.4	0.4	47.5
15.7	2	0.9	0.9	48.4
15.8	2	0.9	0.9	49.3
16.1	3	1.3	1.3	50.7
16.2	2	0.9	0.9	51.6
16.3	1	0.4	0.4	52.0
16.4	1	0.4	0.4	52.5
16.6	1	0.4	0.4	52.9
16.8	1	0.4	0.4	53.4
17.0	3	1.3	1.3	54.7
17.2	1	0.4	0.4	55.2
17.3	2	0.9	0.9	56.1
17.5	1	0.4	0.4	56.5
18.0	1	0.4	0.4	57.0
18.1	1	0.4	0.4	57.4
18.2	1	0.4	0.4	57.8
18.3	1	0.4	0.4	58.3
18.4	1	0.4	0.4	58.7
18.5	1	0.4	0.4	59.2
18.8	1	0.4	0.4	59.6
19.1	2	0.9	0.9	60.5
19.2	3	1.3	1.3	61.9
19.4	2	0.9	0.9	62.8

20.1	1	0.4	0.4	63.2
20.2	1	0.4	0.4	63.7
20.4	1	0.4	0.4	64.1
20.8	1	0.4	0.4	64.6
21.4	2	0.9	0.9	65.5
21.5	1	0.4	0.4	65.9
21.9	1	0.4	0.4	66.4
22.0	1	0.4	0.4	66.8
22.1	1	0.4	0.4	67.3
22.2	1	0.4	0.4	67.7
22.3	1	0.4	0.4	68.2
22.4	2	0.9	0.9	69.1
23.0	1	0.4	0.4	69.5
23.4	1	0.4	0.4	70.0
24.1	1	0.4	0.4	70.4
24.3	1	0.4	0.4	70.9
24.4	1	0.4	0.4	71.3
24.9	2	0.9	0.9	72.2
25.0	1	0.4	0.4	72.6
25.2	2	0.9	0.9	73.5
26.2	1	0.4	0.4	74.0
26.6	1	0.4	0.4	74.4
26.8	1	0.4	0.4	74.9
27.0	1	0.4	0.4	75.3
27.1	2	0.9	0.9	76.2
27.2	1	0.4	0.4	76.7
27.6	1	0.4	0.4	77.1

28.2	2	0.9	0.9	78.0
28.4	1	0.4	0.4	78.5
28.7	1	0.4	0.4	78.9
28.8	5	2.2	2.2	81.2
30.5	1	0.4	0.4	81.6
31.1	1	0.4	0.4	82.1
31.8	1	0.4	0.4	82.5
32.6	1	0.4	0.4	83.0
33.4	1	0.4	0.4	83.4
34.6	1	0.4	0.4	83.9
35.6	1	0.4	0.4	84.3
37.3	1	0.4	0.4	84.8
37.9	1	0.4	0.4	85.2
38.2	1	0.4	0.4	85.7
38.8	2	0.9	0.9	86.5
40.0	1	0.4	0.4	87.0
40.1	1	0.4	0.4	87.4
40.3	1	0.4	0.4	87.9
40.9	1	0.4	0.4	88.3
42.0	1	0.4	0.4	88.8
42.1	1	0.4	0.4	89.2
42.4	1	0.4	0.4	89.7
42.5	1	0.4	0.4	90.1
43.7	1	0.4	0.4	90.6
46.2	1	0.4	0.4	91.0
46.5	1	0.4	0.4	91.5
47.5	1	0.4	0.4	91.9

50.0	1	0.4	0.4	92.4
52.4	1	0.4	0.4	92.8
53.4	1	0.4	0.4	93.3
53.6	1	0.4	0.4	93.7
55.0	1	0.4	0.4	94.2
55.4	1	0.4	0.4	94.6
59.0	1	0.4	0.4	95.1
60.1	1	0.4	0.4	95.5
60.9	1	0.4	0.4	96.0
61.4	2	0.9	0.9	96.9
62.1	1	0.4	0.4	97.3
62.3	1	0.4	0.4	97.8
75.3	1	0.4	0.4	98.2
76.5	1	0.4	0.4	98.7
95.9	1	0.4	0.4	99.1
128.0	1	0.4	0.4	99.6
143.1	1	0.4	0.4	100.0
TOTAL	223	100.0	100.0	100.0

STATISTICS..

MEAN	22.543	STD ERROR	1.230	MEDIAN	16.050
MODE	28.800	STD DEV	18.362	VARIANCE	337.175
KURTOSIS	13.146	SKEWNESS	3.039	RANGE	135.100
MINIMUM	8.000	MAXIMUM	143.100		

VALID OBSERVATIONS - 223
MISSING OBSERVATIONS - 0

FILE MCCN (CREATION DATE = 12/05/74) RIM, DIAMETER AND AGE OF CRATOR

VARIABLE AGE AGE OF CRATOR

VALUE LABEL	VALUE	ABSOLUTE FREQUENCY	RELATIVE FREQUENCY (PERCENT)	ADJUSTED FREQUENCY (PERCENT)	CUMULATIVE ADJ FREQ (PERCENT)
	1.1	1	0.4	0.4	0.4
	1.3	1	0.4	0.4	0.9
	1.4	1	0.4	0.4	1.3
	1.5	3	1.3	1.3	2.7
	1.7	3	1.3	1.3	4.0
	1.8	3	1.3	1.3	5.4
	2.0	10	4.5	4.5	9.9
	2.1	6	2.7	2.7	12.6
	2.2	1	0.4	0.4	13.0
	2.3	1	0.4	0.4	13.5
	2.4	1	0.4	0.4	13.9
	2.5	11	4.9	4.9	18.8
	2.6	6	2.7	2.7	21.5
	2.7	5	2.2	2.2	23.8
	2.8	18	8.1	8.1	31.8
	2.9	7	3.1	3.1	35.0
	3.0	20	9.0	9.0	43.9
	3.1	10	4.5	4.5	48.4
	3.2	13	5.8	5.8	54.3
	3.3	12	5.4	5.4	59.6
	3.4	9	4.0	4.0	63.7
	3.5	16	7.2	7.2	70.9
	3.6	8	3.6	3.6	74.4
	3.7	2	0.9	0.9	75.3

3.8	11	4.9	4.9	80.3
3.9	3	1.3	1.3	81.6
4.0	7	3.1	3.1	84.8
4.2	3	1.3	1.3	86.1
4.3	6	2.7	2.7	88.8
4.4	3	1.3	1.3	90.1
4.5	5	2.2	2.2	92.4
4.6	1	0.4	0.4	92.8
4.7	1	0.4	0.4	93.3
4.8	4	1.8	1.8	95.1
5.0	2	0.9	0.9	96.0
5.2	2	0.9	0.9	96.9
5.3	1	0.4	0.4	97.3
5.5	1	0.4	0.4	97.8
5.9	1	0.4	0.4	98.2
6.0	2	0.9	0.9	99.1
6.2	1	0.4	0.4	99.6
6.3	1	0.4	0.4	100.0
TOTAL	223	100.0	100.0	100.0

STATISTICS..

MEAN	3.257	STD ERROR	0.061	MEDIAN	3.177
MODE	3.000	STD DEV	0.915	VARIANCE	0.838
KURTOSIS	1.032	SKEWNESS	0.623	RANGE	5.200
MINIMUM	1.100	MAXIMUM	6.300		

VALID OBSERVATIONS - 223
MISSING OBSERVATIONS - 0

FILE MOON (CREATION DATE = 12/05/74) RIM, DIAMETER AND AGE OF CRATOR

CORRELATION COEFFICIENTS..

	LOGRIM	LOGDIAM	LOGAGE
LOGRIM	1.00000	-0.19976	0.04707
LOGDIAM	-0.19976	1.00000	-0.45076
LOGAGE	0.04707	-0.45076	1.00000

DETERMINANT = 0.76317691(0.763176920 00)

PLATE 2

CONSTRUCTED BASE MAP

Reduced from original scale of
1:800,000 to 1:2,000,000

Symbols do not all conform to
United States Geological Survey
standards and are not the same as
those on the geologic map (Plate 1)

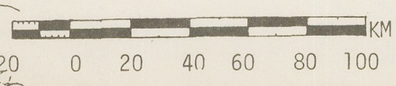

PLATE 3

LINEATION MAP

Reduced from original scale of 1:800,000
to 1:2,000,000

Craters and features outlined and labeled
are believed to be the sources of the
majority of linears

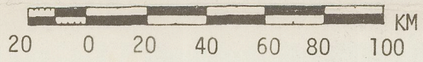

PLATE 4

PLATE 4a

APOLLO 15

MAPPING CAMERA PHOTOGRAPHS

STRIP #	REV #	FRAME #
I	38	AS-15-1595 to 1603
II	44	-1736 to 1745
III	63	-1868 to 1881
IV	60	-1960 to 1973
V	70	-2354 to 2361
VI	72	-2625 to 2640

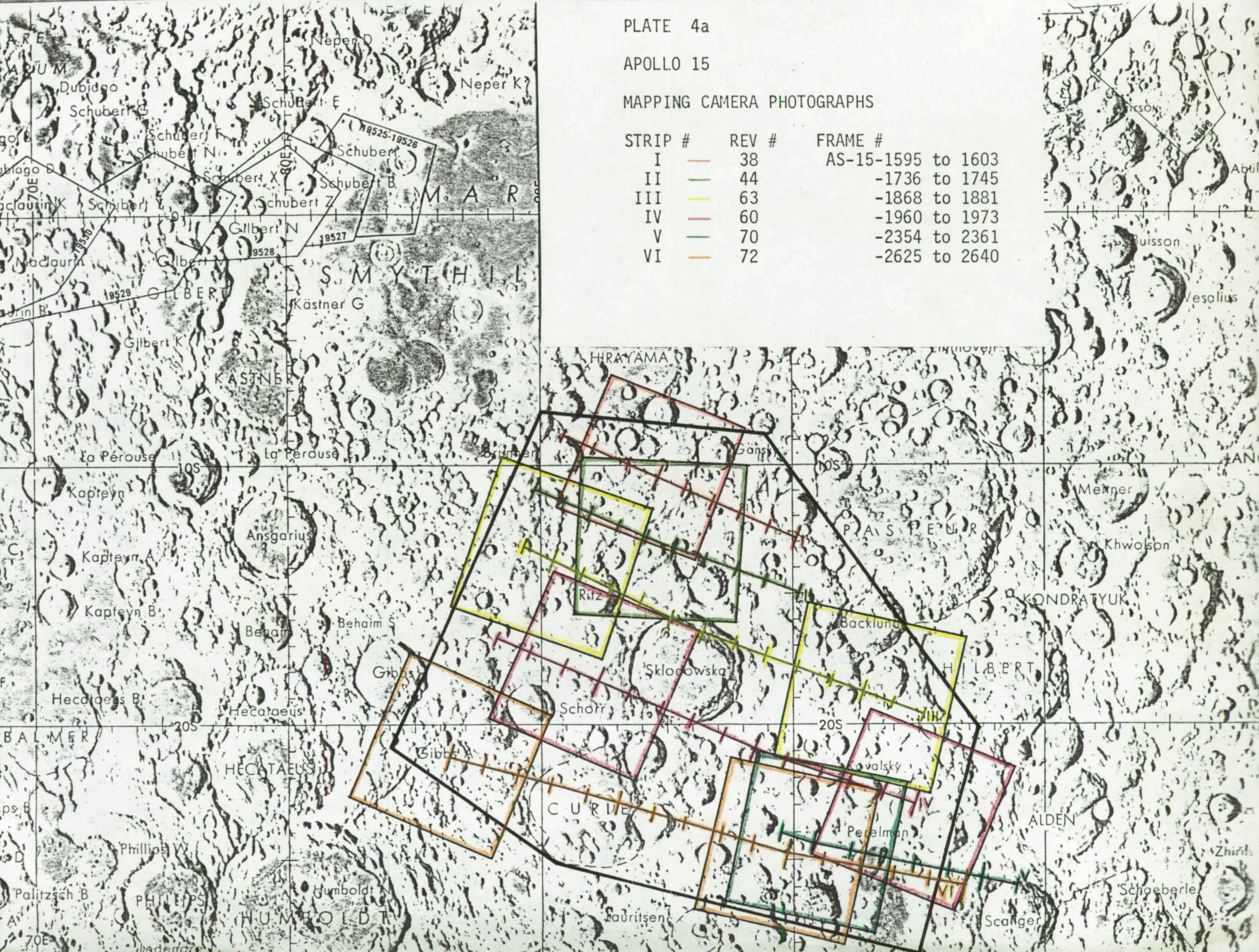

PLATE 4b

APOLLO 15

PANORAMIC CAMERA PHOTOGRAPHS

STRIP #		REV #	FRAME #
I	(yellow)	38	AS-15-9675 to 9720
II	(green)	63	-9942 to 9989

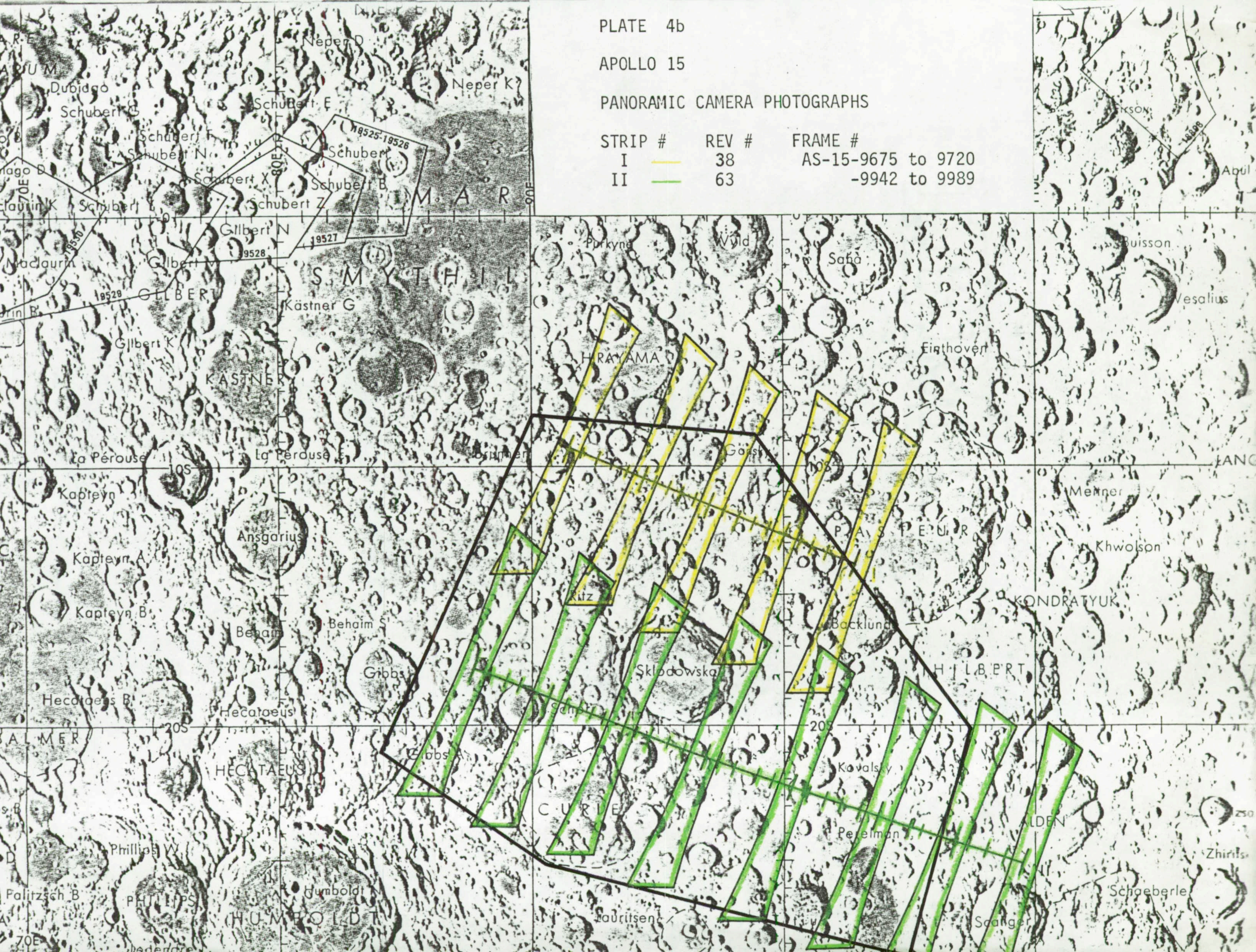

PLATE 4c

APOLLO 15

HASSELBLAD PHOTOGRAPHS (70mm)

FRAME # AS-15-13181 to 13193

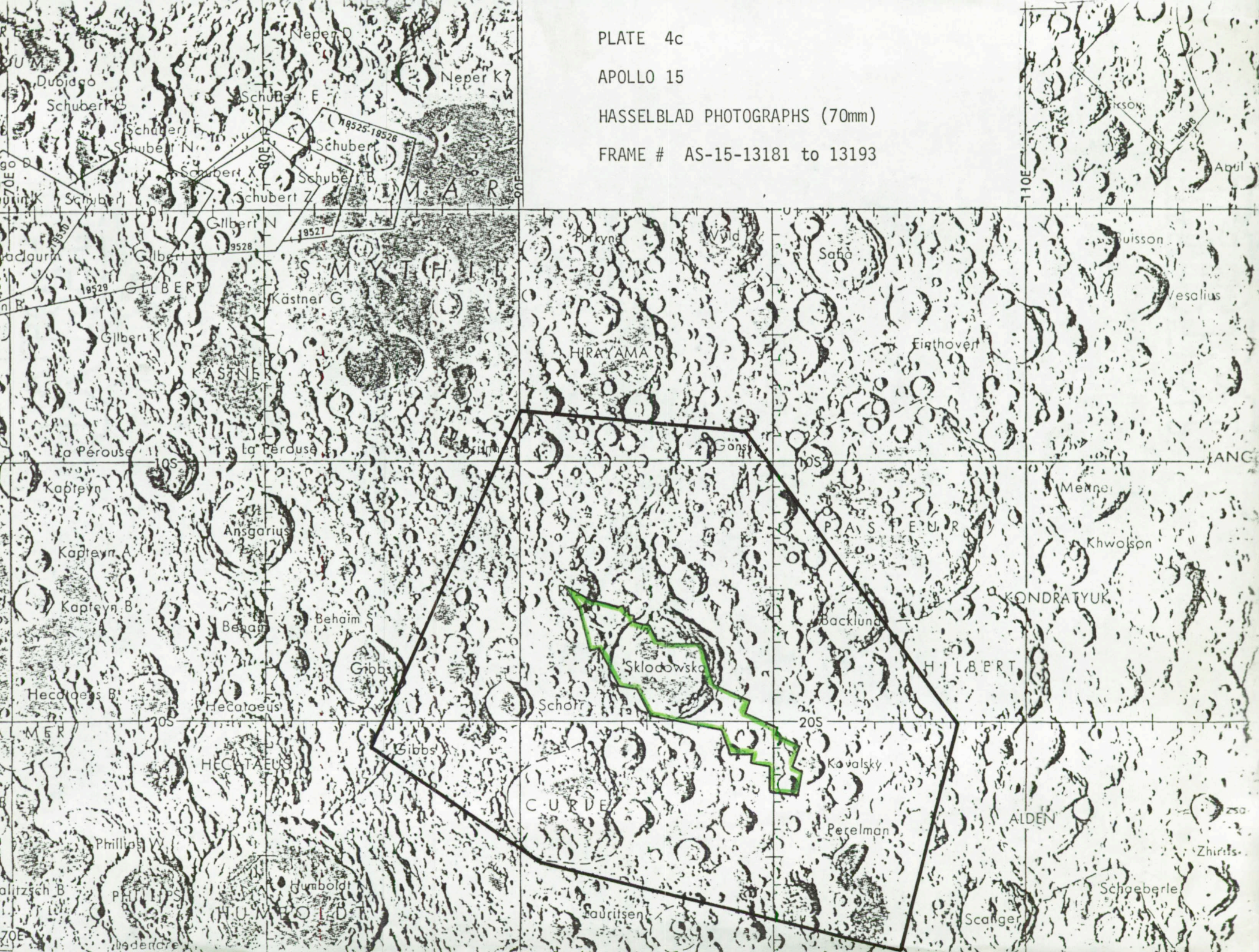

PLATE 4d

LUNAR ORBITER PHOTOGRAPHS

LUNAR ORBITER II

FRAME # 196-H1
-H2
-H3